DOI: 10.1655/HERPMONOGRAPHS-D-19-00008.1

Herpetological Monographs, 34, 2020, 1–38
© 2020 by The Herpetologists' League, Inc.

Systematic Revision of the Rare Bromeligenous Genus *Crossodactylodes* Cochran 1938 (Anura: Leptodactylidae: Paratelmatobiinae)

Marcus Thadeu T. Santos[1,2,10], Rafael F. Magalhães[2,3], Rodrigo B. Ferreira[4], Stenio E. Vittorazzi[5], Iuri R. Dias[6], Felipe S. F. Leite[7], Luciana B. Lourenço[8], Fabrício R. Santos[2], Célio F. B. Haddad[1,9], and Paulo C. A. Garcia[2]

[1] Programa de Pós-graduação em Zoologia, Instituto de Biociências, Universidade Estadual Paulista (UNESP), Caixa Postal 199, 13506-900, Rio Claro, SP, Brazil
[2] Programa de Pós-graduação em Zoologia, Instituto de Ciências Biológicas, Departamento de Zoologia, Universidade Federal de Minas Gerais, 31270-901, Belo Horizonte, MG, Brazil
[3] Departamento de Ciências Naturais, Universidade Federal de São João del-Rei, 36301-160, São João del-Rei, MG, Brazil
[4] Projeto Bromeligenous, Instituto Marcos Daniel, 29090-160, Vitória, ES, Brazil
[5] Departamento de Ciências Biológicas, Universidade do Estado de Mato Grosso, 78300-000, Tangará da Serra, MT, Brazil
[6] Departamento de Ciências Biológicas, Universidade Estadual de Santa Cruz, 45662-900, Ilhéus, BA, Brazil
[7] Sagarana Lab, Instituto de Ciências Biológicas e da Saúde, Universidade Federal de Viçosa, Campus Florestal, 35690-000, Florestal, MG, Brazil
[8] Departamento de Biologia Estrutural e Funcional, Instituto de Biologia, Universidade Estadual de Campinas, 13083-863, Campinas, SP, Brazil
[9] Universidade Estadual Paulista (UNESP), Instituto de Biociências, Departamento de Biodiversidade e Centro de Aquicultura (CAUNESP), Caixa Postal 199, 13506-900, Rio Claro, SP, Brazil

Abstract: *Crossodactylodes* is a poorly known genus of small-sized bromeligenous frogs, endemic to Brazil. They have a patchy distribution across the mountains of the Atlantic Forest and the "campo rupestre" ecosystem. To better resolve their evolutionary relationships, we performed phylogenetic analyses using a multigene DNA matrix and representative sampling within the genus. We then evaluated the evolution of phenotypical and natural history traits with the inferred phylogeny. We recovered *Crossodactylodes* as monophyletic, diagnosed by seven putative synapomorphies in morphological and natural history characters. Evidence supports some morphological synapomorphies as adaptations to the bromeligenous habit. We found high genetic distances among closely distributed lineages within *C. bokermanni* and *C. izecksohni*. Some of these lineages might represent undescribed cryptic species. We provide detailed accounts for each species including data on their geographic range, conservation, and natural history. All species of *Crossodactylodes* occur in highly threatened environments, are restricted to very small geographic ranges, and probably have limited dispersal capacity due to their small body size and dependence on bromeliads. These factors emphasize the need for habitat protection to safeguard species viability.

Key words: Atlantic Forest; Campo rupestre; Character evolution; Endemism; Molecular phylogenetics; Taxonomic revision

The Brazilian anuran fauna is the richest in the world, with more than 1090 species within 105 genera and 20 families (Segalla et al. 2019). This is likely still an underestimation, given that 262 new species were described between 2004 and 2016 (Tapley et al. 2018). The Atlantic Forest contributes greatly to this number, harboring 625 species, most of which are endemic to the domain (Rossa-Feres et al. 2017). This high richness and endemism within the Atlantic Forest might be due to the wide latitudinal range, variable climatic gradient, presence of distinct ecoregions, high topographical complexity, and intense sampling effort (Vasconcelos et al. 2014; Rodríguez et al. 2015; Oliveira et al. 2016). Even with high sampling efforts along the Atlantic Forest, several new species of anurans are still described every year (e.g., Bornschein et al. 2015; Forlani et al. 2017; Taucce et al. 2018; Carvalho et al. 2019). Factors such as the many remote and still-unsampled areas, limited geographical range, and low abundance of some species, cryptic habits, and the difficulty to differentiate some species from related congeners can explain the high rate of new descriptions (Pimm et al. 2014; Costello et al. 2015).

Although the description of new species is an important step to overcome knowledge gaps on biodiversity, decreasing the Linnean shortfall (see Hortal et al. 2015), this is only a small fraction of the biological complexity of the organisms and their interaction networks. Beyond the recognition of species, there are shortfalls related to the geographic distributions, evolution, and biotic interactions (i.e., Wallacean, Darwinian, and Eltonian shortfalls, respectively; Hortal et al. 2015). Overcoming these shortfalls is especially important for species that are rare, geographically constrained, and habitat-specialized because they are more prone to be threatened (Pimm et al. 2014; Toledo et al. 2014). In the Brazilian Atlantic Forest, a high proportion of the anuran species have these characteristics (Haddad et al. 2013; Villalobos et al. 2013; Toledo et al. 2014). Therefore, comprehensive studies addressing these taxa are crucial for a better understanding of their life history traits and an accurate evaluation of their conservation status.

Among the endemic and habitat-specialized anurans of Atlantic Forest, the leptodactylid genus *Crossodactylodes* Cochran 1938 clearly illustrates the aforementioned biological shortfalls. It currently comprises five bromeligenous species (i.e., life cycle in some way dependent on bromeliads; Peixoto 1995): *C. pintoi* Cochran 1938; *C. bokermanni* Peixoto 1983 "1982"; *C. izecksohni* Peixoto 1983 "1982"; *C. septentrionalis* Teixeira, Recoder, Amaro, Damasceno, Cassimiro, and Rodrigues 2013; and *C. itambe* Barata, Santos, Leite, and Garcia 2013. Four species inhabit montane regions of Atlantic Forest across the Brazilian states of Bahia, Espírito Santo, and Rio de Janeiro (Cochran 1938; Peixoto 1983; Teixeira et al. 2013). A single species inhabits a transitional zone between Atlantic Forest and Cerrado in the "campo rupestre" ecosystem (rupestrian grasslands; Silveira

---

[10] Correspondence: email, mthadeusantos@gmail.com

et al. 2016) of the Espinhaço Mountain Range in the state of Minas Gerais, Brazil (Barata et al. 2013). All species are narrow-range endemics, mostly known from only the type locality (Frost 2019). The recent species discoveries after more than 3 decades without new descriptions (i.e., *C. itambe* and *C. septentrionalis*; Barata et al. 2013 and Teixeira et al. 2013, respectively), as well as the record of the genus in an unexpected environment (i.e., campo rupestre; Barata et al. 2013), could indicate that the richness and geographic range of *Crossodactylodes* are underestimated. The small body size, the strict association to bromeliads, the occurrence in remote areas, and the lack of knowledge on vocalization (Barata et al. 2013; Teixeira et al. 2013) hamper further study of the genus and location of unknown populations.

Taxonomic studies on *Crossodactylodes* began with Cochran (1938), who proposed it to allocate *C. pintoi* based on distinct morphological traits compared to other genera of Leptodactylidae Werner 1896. Originally, Cochran (1938) briefly diagnosed the species. Decades later, Cochran (1955) complemented the description and suggested that *Crossodactylodes* is closely related to the genus *Crossodactylus* Duméril and Bibron 1841 (Hylodidae) based on the presence of spines on the inner surface of the first finger set in a round mass, similarity of the tooth development, and bilobed appearance of toe when dried.

Lynch (1971) provided a more complete diagnosis of *Crossodactylodes*, mainly based on characters of skull osteology. Lynch's diagnosis differs from that of Cochran (1955) due to Y-shaped terminal phalanges (T-shaped in Cochran 1955) and an absent tympanum (hidden in Cochran 1955). Lynch (1971) suggested that *Crossodactylodes* is closely related to *Cycloramphus* Tschudi 1838 and *Zachaenus* Cope 1866 due to similarity in the architecture of the temporal region and size of the roofing bones. Therefore, Lynch (1971) placed *Crossodactylodes* into the Grypiscini tribe of Leptodactylidae. Lynch (1971) also mentioned the oviposition of a few large eggs attached to bromeliads for *Crossodactylodes*.

Following Lynch's work, Heyer (1975) proposed an informal unit named "grypiscines" to allocate *Crossodactylodes*, *Cycloramphus*, *Zachaenus*, *Craspedoglossa* Müller 1922 (later synonymized to *Cycloramphus*), *Crossodactylus*, *Hylodes* Fitzinger 1826, *Megaelosia* Miranda-Ribeiro 1923, *Thoropa* Cope 1865, *Paratelmatobius* Lutz and Carvalho 1958, and *Scythrophrys* Lynch 1971. Dubois (2005) made minor adjustments and formalized the arrangement proposed by Heyer (1975) including *Crossodactylodes* in Leptodactylidae, subfamily Cycloramphinae, along with *Cycloramphus*, *Zachaenus*, *Rupirana* Heyer 1999, *Paratelmatobius*, *Scythrophrys*, and *Thoropa*. The genera *Crossodactylus*, *Hylodes*, and *Megaelosia* were transferred to the subfamily Hylodinae (Dubois 2005).

The first molecular phylogenetic studies with extensive taxonomic sampling on amphibians resulted in substantial modifications on the anuran classification (Frost et al. 2006; Pyron and Wiens 2011). However, these studies did not include *Crossodactylodes* in the analyses. Thus, Frost et al. (2006) classified the genus in the tribe Cycloramphini, family Cycloramphidae, based on the phylogenetic placement found for its putative relatives according to Lynch (1971), while Pyron and Wiens (2011) left *Crossodactylodes* as an incertae sedis genus within Hyloidea. Fouquet et al. (2013) were the first authors to include *Crossodactylodes* in an extensive molecular phylogenetic analysis and the genus was unambiguously grouped with *Rupirana*, *Paratelmatobius*, and *Scythrophrys* within Leptodactylidae. For this clade, Fouquet et al. (2013) proposed the new subfamily Crossodactylodinae, which is a junior synonym of Paratelmatobiinae Ohler and Dubois 2012 (Dubois 2013). Further, Teixeira et al. (2013) provided the first phylogenetic arrangement within *Crossodactylodes* and included the three formally recognized species for which tissue samples were available (*C. bokermanni*, *C. izecksohni*, and *C. septentrionalis*).

Although there are recent contributions on phylogenetic relationships of *Crossodactylodes* (Fouquet et al. 2013; Teixeira et al. 2013), the phylogenetic placement of *C. itambe* remains unknown. This information has implications for the diversification pattern of the genus, as it is the only species that occurs in the campo rupestre. Moreover, the knowledge about behavior, geographical distribution, and evolution of morphological characters is limited for the genus. The diagnosis of *Crossodactylodes* was based solely on its type species (*C. pintoi*; Cochran 1938, 1955; Lynch 1971), and the morphological variation within the genus is poorly understood because the earliest species descriptions (*C. pintoi*, *C. bokermanni*, and *C. izecksohni*) are hardly comparable to the more recent ones (*C. septentrionalis* and *C. itambe*). In addition, *C. septentrionalis* was described based solely on one female specimen (Teixeira et al. 2013) and thus some morphological characters observed in males, which are commonly used in the taxonomy of the genus, have not been evaluated for this species.

In this study, we provide phylogenetic analyses of a matrix composed of mitochondrial (mtDNA) and nuclear (nDNA) gene fragments, including for the first time specimens of *Crossodactylodes itambe* and increasing the sampling within *C. bokermanni*, *C. izecksohni*, and *C. septentrionalis*. We also evaluate the evolution of several phenotypic and natural history traits and provide a systematic revision of *Crossodactylodes*, with updated diagnoses for the genus, comparing it with the other genera of Paratelmatobiinae. We redescribe *C. pintoi*, *C. bokermanni*, and *C. izecksohni* to enhance comparisons and offer the first assessment of male morphological characters for *C. septentrionalis*. Lastly, we provide detailed accounts for each species including data on geographic range, natural history, and conservation. Our main goal is to afford an extensive taxonomic framework for *Crossodactylodes*, which can benefit future species descriptions and contribute to the overcoming of Wallacean, Darwinian, and Eltonian shortfalls regarding these poorly known bromeligenous anurans.

MATERIALS AND METHODS

Phylogenetics and Character Evolution

Taxon and genetic sampling.—As an ingroup, we included specimens of four of the five species of *Crossodactylodes*. The missing species, *C. pintoi*, is known only from its type series and has not been recorded since 1909 (Peixoto and Carvalho-e-Silva 2004). We included for the first time specimens of *C. itambe* and increased the sampling within *C. septentrionalis*, *C. bokermanni*, and *C. izecksohni*. For the last two species, we included specimens from localities not included in previous analyses (Fouquet et al. 2013; Teixeira et al. 2013). Outgroups were selected based on the results of Pyron and Wiens (2011), Fouquet et al. (2013), Teixeira et al. (2013), and Pyron (2014). We broadly sampled the other Paratelmatobiinae genera, with three of the seven species of *Paratelmatobius* (*P. cardosoi* Pombal and Haddad 1999, *P. gaigeae* [Cochran 1938], and *P. poecilogaster* Giaretta and Castanho 1990) and three specimens for each of the two monotypic genera *Scythrophrys* and *Rupirana*. We also sampled genera of the other two subfamilies of Leptodactylidae: *Pleurodema* Tschudi 1838 and *Physalaemus* Fitzinger 1826 for Leiuperinae and *Adenomera* Steindachner 1867 and *Leptodactylus* Fitzinger 1826 for Leptodactylinae. We used an allophrynid, *Allophryne ruthveni* Gaige 1926, to root the trees due to its close relationship with Leptodactylidae (Pyron and Wiens 2011; Pyron 2014).

Our matrix included sequences for six genes. Noncoding mtDNA gene sequences produced for this study include gene fragments of the heavy strand transcription unit 1 (H1: 12S and 16S rRNA genes, plus the intervening tRNA valine gene). Protein-coding mtDNA gene sequences included fragments of cytochrome oxidase subunit I (COI), and cytochrome b (cytb). The nDNA protein-coding gene sequences included fragments of proopiomelanocortin A (POMC), recombination-activating protein 1 (RAG-1), and tyrosinase (Tyr). Our sampling was complemented with GenBank sequences. GenBank accession numbers are listed in Appendix I.

DNA amplification and sequencing.—We extracted genomic DNA from ethanol-preserved tissues using standard phenol-chloroform extraction protocols (Sambrook and Russel 2001). For all the amplifications, the polymerase chain reaction program included an initial denaturing step of 60 s at 94°C followed by 35 cycles of amplification (94°C for 30 s; variable annealing temperatures and times, Appendix II; and 72°C for 60 s for extension), with a final extension step at 72°C for 7 min. Amplifications were performed in a 15-μL volume reaction containing: 20 ng of genomic DNA, 1× buffer, 2.5 mM $MgCl_2$, 1.25 μM each primer, 3 mM dNTPs, 0.72 μg bovine serum albumin, and 0.625 U Platinum Taq DNA polymerase (Thermo Fisher Scientific). Primers are listed in Appendix II. The amplification products were cleaned using polyethylene glycol 20% protocol with modifications (Sambrook and Russel 2001; Santos et al. 2015) and sequenced using fluorescent dye-labelled terminators (ABI Prism BigDye™ Terminators v1.1 cycle sequencing kit; Applied Biosystems) with an ABI 3130XL (Applied Biosystems). All sequences were made in both directions to check for potential errors and confirm heterozygous nucleotide position. Chromatograms obtained from the automated sequencer were read and assembled using the sequence editing software SeqScape (v2.6, Thermo Fisher Scientific Inc.).

Phylogenetic analyses and genetic distance.—We performed a multiple sequence alignment for each fragment with MAFFT v7.394 (Katoh and Standley 2013) using the MAFFT online service (Katoh et al. 2019). We used the G-INS-i algorithm and default transition/transversion cost ratio and gap opening penalty, with minor adjustments by eye for H1. For the Bayesian analysis, we selected the optimal partition scheme and nucleotide substitution models for each data block in PartitionFinder v2.1.1 (Lanfear et al. 2017) under the linked model of branch lengths and greedy search algorithm. For this, we defined 18 a priori partitions, including the 12S rRNA, the tRNA valine, the 16S rRNA genes, and the first, second, and third codon positions of COI, cytb, POMC, RAG-1, and Tyr separately. The analysis was repeated to check congruence in results and the best model was selected through Bayesian Information Criterion (BIC). We performed the Bayesian phylogenetic inference analysis using MrBayes v3.2.6. (Ronquist et al. 2012) implemented in online CIPRES Science gateway portal (Miller et al. 2010). For this analysis, we made two parallel runs, using eight chains (seven heated and one cold) with 5×10^7 generations each. The runs were summarized in a 50% majority rule consensus tree after a discarded burn-in of 25% first trees. Convergence and minimal effective sample sizes (ESS $>$ 200) of all parameters were verified in Tracer v1.6 (Rambaut et al. 2014).

For the most-parsimonious trees reconstruction we used TNT v1.5 (Goloboff and Catalano 2016), applying equal weights to all transformations and considering gaps as a fifth state. Searches were conducted using the traditional search option consisting of 1000 random addition sequences followed by tree bisection and reconnection swapping and holding a maximum of 100 trees each step. The optimal trees obtained were submitted to an additional round of tree bisection and reconnection swapping. Parsimony jackknife absolute frequencies (Farris et al. 1996) were estimated using a traditional search, with 1000 resampling iterations.

For comparative purposes, we estimated mtDNA uncorrected *p*-distances inside and between the monophyletic and geographically structured lineages found in the phylogenetic reconstructions. For this we used concatenated mtDNA fragments and each of the fragments separately (COI, cytb, and H1). We also computed the distances for the 16S rRNA gene fragment limited by the primers 16SAR and 16SBR (Palumbi et al. 1991), which is commonly used for genetic distances calculations in anurans (Fouquet et al. 2007). The distances were estimated in MEGA v7.0 (Kumar et al. 2016). This analysis was made to highlight putative cryptic species or deep conspecific lineages within *Crossodactylodes*.

Character evolution analysis.—We assembled a discrete matrix composed of 30 morphological and natural history characters (Appendices III, IV) using Mesquite v3.2 (Maddison and Maddison 2017). Then, we optimized unambiguous characters in a simplified tree of the Paratelmatobiinae clade derived from our previous analyses using WinClada v1.00.08 (Nixon 2002). This simplification was made by collapsing multiple individuals from a single species or lineage into a single branch. In this case, variation in characters within each branch was treated as a multistate character. This analysis was made to show putative synapomorphies of each node emphasizing *Crossodactylodes*. Data were obtained through direct examination of specimens (see Referred specimens sections and Appendix V) or from literature in the absence of primary data. All characters were equally weighted without any ordering. We also included the morphometric character foot length, which is represented by the ratio foot length:snout–vent length (SVL; Appendices III, IV). This character was optimized as a continuous character. For this, we reconstructed ancestral states using the Trace Character History and Reconstruct

Ancestral States modules from Mesquite v3.2 (Maddison and Maddison 2017) under a squared-change parsimony model. We obtained the measurements for other Paratelmatobiinae from literature when individual values were available or through direct examination when only the means were provided in the literature (Appendix V).

Phylogenetic placement of *Crossodactylodes pintoi*.—We also used the discrete matrix, supplemented with the DNA sequences matrix, to perform a total evidence analysis in TNT v1.5 (Goloboff and Catalano 2016). This analysis was made to provide a phylogenetic placement for *C. pintoi*, for which DNA sequences were unavailable. For this, we used a single terminal per species or lineage and rooted the analysis in *Rupirana cardosoi*. The optimal trees and parsimony jackknife absolute frequencies (1000 resampling iterations) were obtained using implicit enumeration.

Taxonomic Analyses

All collected specimens were euthanized in 5% lidocaine solution, fixed in 10% commercial grade formalin, and preserved in 70% ethanol. All geographic coordinates are in the system datum WGS84. Museum acronyms follow Sabaj (2016), except by MZUESC, which stands for Museu de Zoologia of the Universidade Estadual de Santa Cruz, Ilhéus, Bahia, Brazil. We examined types of all species of *Crossodactylodes*. For comparative purposes, we examined representatives of each genus of Paratelmatobiinae (Appendix V).

We analyzed external qualitative and morphometric characters. Terminology for external qualitative characters follows Duellman (1970), Heyer et al. (1990), and Duellman and Lehr (2009). To the nearest 0.1 mm with a digital caliper under a stereomicroscope, we measured SVL (from the tip of snout to the posterior margin of the vent), head length (from the tip of snout to the angle of the jaw), head width (between the angles of the jaws), arm length (from the anterior insertion of the arm to the elbow), arm width (greatest width), forearm length (from the elbow to the proximal edge of the inner metacarpal tubercle), forearm width (greatest width), hand length (from the proximal edge of the inner metacarpal tubercle to the tip of the third finger), thigh length (from the posterior margin of the vent to the outer edge of the knee), tibia length (from the outer edge of the knee to the outer edge of the heel), tarsal length (from the outer edge of the heel to the inner metatarsal tubercle), foot length (from the proximal edge of the inner metatarsal tubercle to the tip of the fourth toe). We used ImageTool v3.0 (Wilcox et al. 1996) to take measurements to the nearest 0.1 mm for eye diameter (between the anterior and posterior margins of the eye), interorbital distance (between the anterior margins of the eyes), eye–nostril distance (from the anterior corner of the eye to the posterior margin of the nostril), nostril–snout distance (from the posterior margin of the nostril to the tip of snout), internarial distance (between the inner margins of the nostrils), third finger disc diameter (greatest horizontal distance between the outer edges of the third finger disk), and fourth toe disc diameter (greatest horizontal distance between the outer edges of the fourth toe disk). For details of this method, see Barata et al. (2013). For one specimen of *C. pintoi* (MCZ 25707), we only measured SVL from a scaled photograph. All measurements were taken by MTTS.

Descriptions of coloration in life are based on field observations and photographs. Sex was determined by observation of gonads or secondary sexual characters (arm and forearm hypertrophy and nuptial pads on males). Variations are based on adult specimens. To verify the presence of tympanic annulus concealed by the skin and internal vocal sac, we made dissections in the skin on the lateral side of the head and on the gular region of some specimens (*Crossodactylodes bokermanni*: UFMG 13769, 14198; *C. itambe*: UFMG 14031, 14037; *C. izecksohni*: UFMG 14174, 14178, 14182, 14219). To verify the size of the zygomatic process of squamosal, and if a columella was present in *C. itambe*, we cleared and double-stained two specimens (UFMG 14033, 14034) with alizarin red and alcian blue following the protocol of Taylor and Van Dyke (1985). Due to the poor preservation of coloration in the specimens of *C. pintoi*, we did not consider characters related to color pattern in its diagnosis and comparisons with congeners. Terminology for egg morphology and ovipositional mode follow Altig and McDiarmid (2007).

For *Crossodactylodes pintoi*, *C. bokermanni*, and *C. izecksohni* we provided redescriptions of the holotypes because the original descriptions were hardly comparable to the more-recent descriptions. For *C. septentrionalis* and *C. itambe*, we provided new diagnoses, comparisons, and additional information on morphological variation.

Conservation Accounts

We provided relevant data on geographic distribution, habitat, and potential threats for the species of *Crossodactylodes* following the suggestion of Tapley et al. (2018). For this, we calculated the extent of occurrence for the species known from more than two occurrence points (*C. bokermanni* and C. *izecksohni*). First, we generated minimum convex polygons using ArcGis (v10.0, ESRI Inc., Redlands, CA), following the International Union for Conservation of Nature (IUCN 2019) guidelines. Then, we calculated: (1) the area above 700 m elevation within the extent of occurrence, as the lower elevation limit known for these species is approximately 800 m; (2) the area of forest remnants within the extent of occurrence which is above this elevational limit, as these species occur only in forested areas; and (3) the percentage of protected areas present in the extent of occurrence. Spatial data on the protected areas were obtained from Instituto Chico Mendes de Conservação da Biodiversidade (ICMBio 2017); forest remnants data were obtained from SOS Mata Atlântica and Instituto Nacional de Pesquisas Espaciais (2018); and elevation shapefile was obtained from the Topodata project (Valeriano and Rossetti 2012). For species known only for localities in the same grid size of 2 km (i.e., a cell area of 4 km^2), the area of occupancy was considered equivalent to this cell, as recommended by the IUCN (2019). We then provided conservation assessments for each species of *Crossodactylodes*, applying the IUCN (2019) criteria.

Results

Phylogenetics and Character Evolution Analyses

Our final alignment comprised 5351 characters, with 23% of missing data, mainly in H1. The BIC in Partition Finder selected six subsets as the best partition scheme, BIC =

61,899.638: SYM + I + G for COI and cytb first positions; HKY + I for COI and cytb second positions; GTR + G for COI and cytb third positions; GTR + I + G for 12S rRNA, 16S rRNA, and tRNA valine genes; and two independent partitions of HKY + G for first and second positions and for third positions of nDNA fragments (POMC, RAG-1, and Tyr).

The Bayesian and parsimony phylogenetic inference analyses result in the same general topology, varying only on internal relationships among terminals within species or at intraspecific lineage level (Fig. 1). The parsimony analysis resulted in 45 trees with 5780 steps (strict consensus in Fig. S1). The analyses recovered *Crossodactylodes* as an unambiguously supported monophyletic group (100% Bayesian posterior probability and parsimony jackknife; Fig 1), diagnosed by seven putative synapomorphies in morphological and natural history characters (see genus diagnosis section; Fig. 2; Appendices III, IV). *Paratelmatobius* is strongly supported as the sister taxon of *Crossodactylodes* (99% Bayesian posterior probability; 97% parsimony jackknife; Fig. 1) and the clade containing these genera is diagnosed by one putative morphological synapomorphy (absence of tarsal fold; Fig. 2; Appendices III, IV). Within the other Paratelmatobiinae, *Scythrophrys* was unambiguously supported as the sister taxon of *Crossodactylodes* plus *Paratelmatobius* (100% Bayesian posterior probability and parsimony jackknife) and *Rupirana* was recovered as the earliest diverging genus (Fig. 1). The clade which shows *Rupirana* as the sister taxon of the other Paratelmatobiinae is unambiguously supported in the Bayesian analysis (100% posterior probability) but poorly supported in the parsimony analysis (46% jackknife frequency). Within the remaining outgroups, the two genera representing the subfamily Leptodactylinae (*Adenomera* and *Leptodactylus*) form the sister taxon of Paratelmatobiinae (Fig. 1).

Within *Crossodactylodes*, both analyses recovered *C. bokermanni* as the sister taxon of the remaining species (Fig. 1). The clade composed by *C. izecksohni*, *C. itambe*, and *C. septentrionalis* is diagnosed by three putative morphological synapomorphies (absence of vocal slit, absence of dorsolateral fold, and skin texture of males coarsely granular; Fig. 2; Appendices III, IV). In this clade, *C. izecksohni* (diagnosed by one putative morphological autapomorphy: iris coloration in life yellowish with dark brown reticulations, interrupted by a brown horizontal bar at the pupil level) is recovered as the sister taxon of *C. itambe* plus *C. septentrionalis* (Figs. 1, 2; Appendices III, IV). The clade containing these two species is diagnosed by one putative morphological synapomorphy (zygomatic process of squamosal bone long, passing the anterior margin of the optic foramen; Fig. 2; Appendices III, IV). Moreover, *C. itambe* is diagnosed by two putative morphological autapomorphies (presence of an anterior projection in medial region of the upper lip and iris coloration in life uniformly black or brownish black; Fig. 2; Appendices III, IV) while *C. septentrionalis* is supported by one putative autapomorphy (disc of Finger I acute, i.e., no apparent disc; Fig. 2; Appendices III, IV). The total evidence analysis resulted in three trees with 3052 steps (strict consensus in Fig. S2) and recovered *C. pintoi* in a clade together with *C. itambe*, *C. septentrionalis*, and *C. izecksohni* (97% jackknife frequency). However, the relationships among terminals within this clade were not fully resolved.

The uncorrected p-distances among recognized species of *Crossodactylodes* vary from 7.8% to 11.4% for the concatenated mtDNA fragments and from 3.2% to 7.9% for the 16S rRNA fragment (Table 1). For COI, cytb, and H1 the distances vary from 11.3% to 17.3%, 11.2% to 16.0%, and 5.2% to 9.2%, respectively (Appendices VI, VII).

Within *Crossodactylodes bokermanni*, the analyses recovered three well-supported clades, exclusives of different localities in the state of Espírito Santo: a lineage from Estação Biológica de Santa Lúcia, municipality of Santa Teresa (Lineage A); a lineage from Parque Estadual do Forno Grande, municipality of Castelo (Lineage B); and a lineage from Penha district, municipality of Santa Teresa, vicinities of the type locality (Lineage C). The Lineage C forms the sister group of Lineage A plus Lineage B (Fig. 1). The uncorrected p-distances among these lineages vary from 2.6% to 5.4% for the concatenated mtDNA and from 0.7% to 4.3% for the 16S rRNA fragment (Table 1). For COI, cytb, and H1, the distances vary from 5.0% to 9.3%, 4.6% to 9.0%, and 1.3% to 3.5%, respectively (Appendices VI, VII). None of the morphological and natural history characters of our matrix supported these lineages (Fig. 2; Appendices III, IV). Moreover, these lineages are not distinguishable on the basis of morphological characters analyzed for the taxonomic descriptions.

Within *Crossodactylodes izecksohni*, two well-supported and nonsympatric clades are recovered: a lineage from four different localities in the municipality of Santa Teresa, vicinities of the type locality (Lineage A), and a lineage from Estação Biológica de Santa Lúcia, also in the municipality of Santa Teresa (Lineage B). The range of uncorrected p-distances between the lineages is 5.3–5.4% for the concatenated mtDNA and 3.5–4.3% for the 16S rRNA fragment (Table 1). For COI, cytb, and H1, the ranges are 6.0–6.8%, 7.7–8.9%, and 3.8–3.9%, respectively (Appendices VI, VII). None of the morphological and natural history characters of our matrix supported these lineages (Fig. 2; Appendices III, IV). In addition, these lineages do not differ on the basis of morphological characters analyzed for the taxonomic descriptions.

Taxonomic Accounts

Crossodactylodes Cochran

Crossodactylodes Cochran 1938: Cochran 1938:41–42.

Type species.—*Crossodactylodes pintoi* Cochran 1938, by monotypy.

Diagnosis.—*Crossodactylodes* can be distinguished and diagnosed from the other genera of Paratelmatobiinae by the following combination of characters: (1) nuptial pads of males formed by few (less than 20) and well-developed keratinized spines; (2) discs of fingers II–IV expanded (i.e., more dilated than the base); (3) toes II–V lacking lateral ridges, fringes, or webs; (4) cloacal flap conspicuous (i.e., with long free distal portion); (5) reproductive mode 6 (i.e., eggs and exotrophic tadpoles in water in aerial plants; Haddad and Prado 2005); (6) deposition of single eggs, positioned isolated from other eggs; (7) tympanic middle ear (i.e., tympanic membrane, tympanic annulus, and columella; see Pereyra et al. 2016) completely lacking; (8) absence of

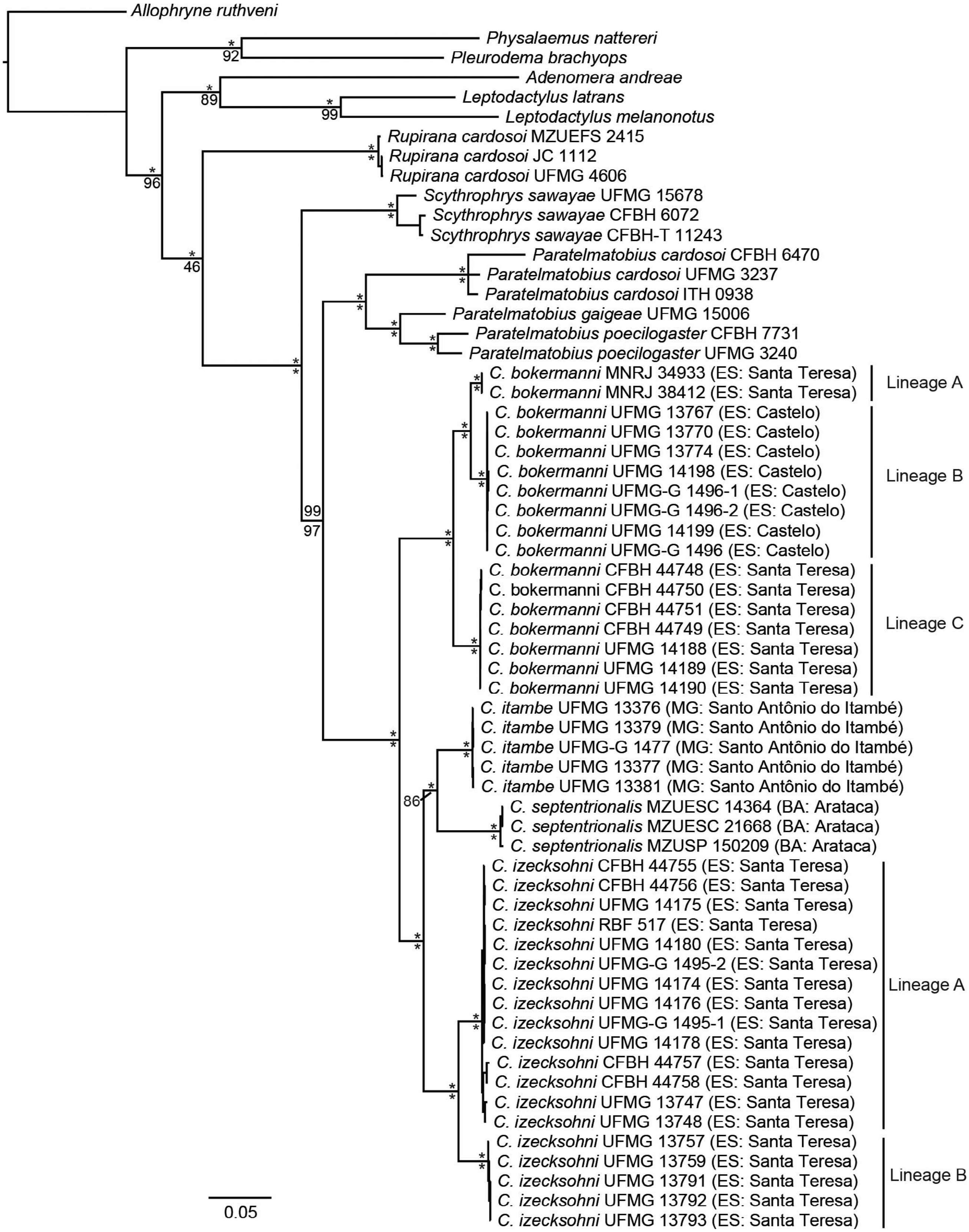

FIG. 1.—The 50% majority rule consensus tree from Bayesian phylogenetic inference of concatenated mtDNA (H1, COI, cytb) and nDNA (POMC, RAG-1, tyr) genes. Values above branches indicate posterior probabilities proportions and those under branches are jackknife proportions achieved in the parsimony analysis of the same matrix, which resulted in the same general topology (strict consensus available in Fig. S1). Asterisks indicate 100% values.

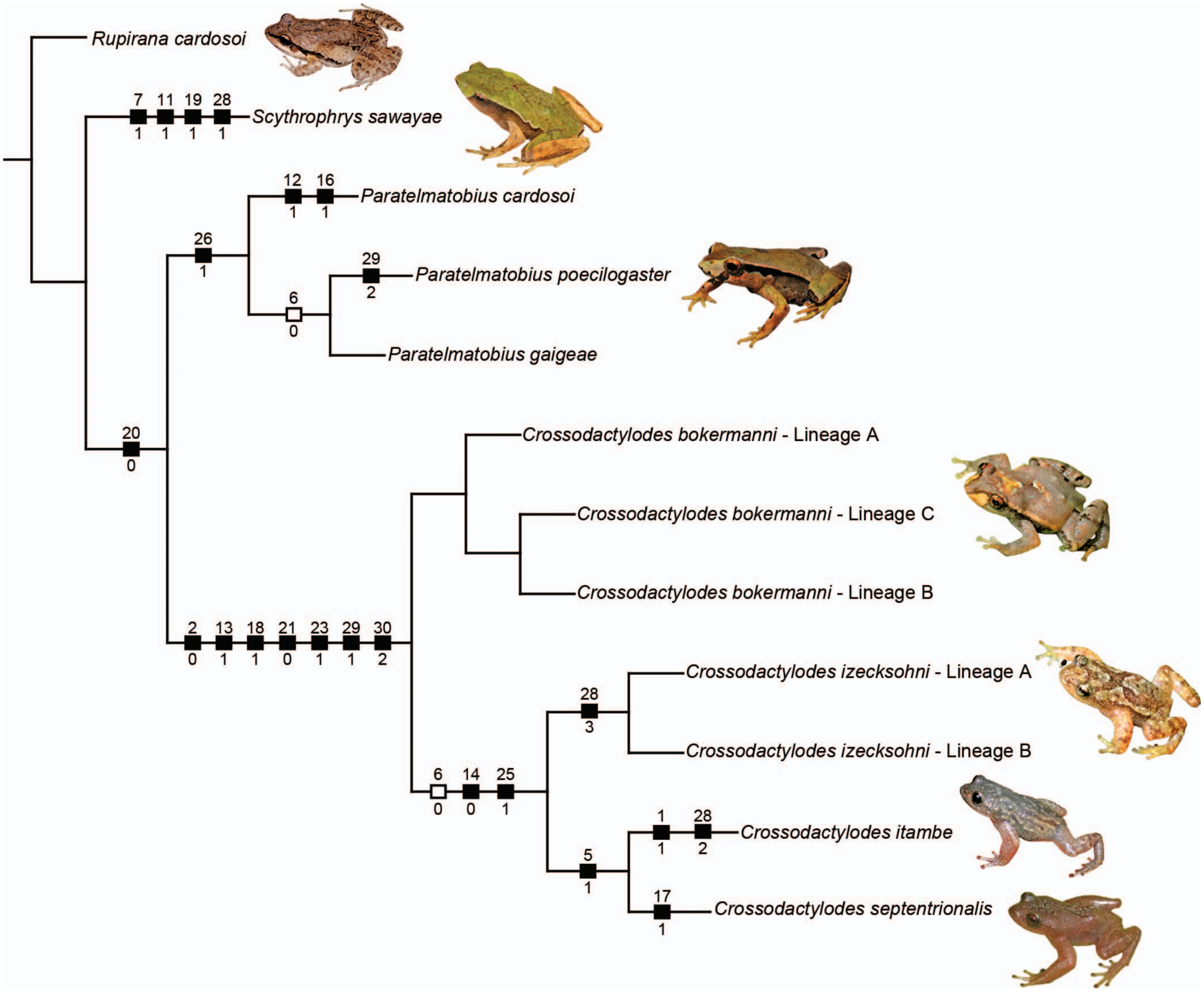

FIG. 2.—A simplified phylogenetic tree of Paratelmatobiinae showing optimization of unambiguous morphological and natural history characters (see Appendices III, IV). For each node the list of the unambiguous synapomorphies is given and each synapomorphy is represented by a black square (nonhomoplasic synapomorphy) or a white square (homoplasic synapomorphy). The upper numbers indicate the character number and the lower numbers their respective states. A color version of this figure is available online.

tarsal fold; (9) in life, ventral surfaces of arm lacking bright and contrasting coloration; (10) males lacking white tubercles on dorsum; (11) SVL 10.8–18.6 mm; (12) foot length/SVL 0.31–0.41; (13) snout rounded to truncate in dorsal view; (14) vocal sac absent, or externally indistinct; (15) tubercles on upper eyelid rounded or absent; (16) absence of a small meniscus on the upper iris; (17) absence of a tubercle on outer margin of heel; (18) in life, ventral surfaces of belly lacking bright and contrasting coloration. The characters 1–7 are putative synapomorphies of *Crossodactylodes* (Characters 2, 13, 18, 21, 23, 29, and 30 in Fig. 2 and Appendices III, IV).

Comparison with other genera of Paratelmatobiinae.—*Crossodactylodes* can be distinguished from all other genera of Paratelmatobiinae (characters in parentheses) by having nuptial pads of males formed by few (less than 20) and well-developed spines; Fig. 3A (nuptial pads lacking spines or spicules in *Paratelmatobius lutzii*, and formed by numerous (more than 20) small spicules in all remaining species of Paratelmatobiinae; Fig. 3B); discs of fingers II–IV expanded, i.e., more dilated than the base; Fig. 3C (narrow, i.e., same width or less dilated than the base in the other genera; Figs. 3D–F); toes II–V lacking lateral ridges, fringes, or webs; Fig. 3G (with lateral ridges in *Rupirana* and *Scythrophrys*, Figs. 3J, K; with well-developed webs in *P. lutzii*, Fig. 3I; and with well-developed flexible fringes in other species of *Paratelmatobius*, Fig. 3H); cloacal flap conspicuous, i.e., with long free distal portion; Fig. 4A (inconspicuous, i.e., with short free distal portion in the other genera; Figs. 4B, C); reproductive mode 6 sensu Haddad and Prado (2005), with eggs and exotrophic tadpoles associated to bromeliads (mode 18, eggs on rock above water, exotrophic tadpoles move to water) in *P. poecilogater* (mode 1, eggs and exotrophic tadpoles in lentic water) in other species of Paratelmatobiinae (Garcia 1996; Haddad and Prado 2005; Juncá and Lugli 2009); and deposition of

TABLE 1.—Uncorrected *p*-distances (percentage) among species and lineages of *Crossodactylodes*. Distances for all concatenated mtDNA fragments (ca. 3700 bp) are shown under the diagonal and distances for the 16S rRNA fragment (ca. 550 bp) are shown above the diagonal. Intraspecific or intralineage distances are shown as concatenated mitochondrial/16S rRNA (along diagonal). NC = not calculated because there was only one individual.

	C. bokermanni Lineage A	*C. bokermanni* Lineage B	*C. bokermanni* Lineage C	*C. itambe*	*C. izecksohni* Lineage A	*C. izecksohni* Lineage B	*C. septentrionalis*
C. bokermanni Lineage A	NC / 0 ($n = 2$)	0.7	3.3–3.6	5.1	4.9–5.5	6.6–6.8	6.1
C. bokermanni Lineage B	2.6–2.7	0.0–0.2 ($n = 7$) / 0 ($n = 8$)	4.0–4.3	5.1	4.9–5.5	6.6–6.8	6.1
C. bokermanni Lineage C	4.9–5.0	5.1–5.4	0.0–0.1 ($n = 3$) / 0 ($n = 7$)	4.9–5.3	5.7–6.3	7.1–7.9	6.1
C. itambe	10.2–10.4	10.0–10.2	9.9–10.1	0.1–0.2 ($n = 5$) / 0 ($n = 5$)	3.5–4.0	4.9–5.1	3.2
C. izecksohni Lineage A	10.8–10.9	10.5–10.9	11.0–11.2	8.0–8.4	0.0–0.7 ($n = 7$) / 0.0–0.4 ($n = 12$)	3.5–4.3	4.6–4.9
C. izecksohni Lineage B	11.0–11.2	10.8–11.2	11.1–11.4	8.5–8.8	5.3–5.4	0.1 ($n = 3$) / 0.0–0.2 ($n = 3$)	5.8–6.1
C. septentrionalis	11.4	11.1–11.4	11.2–11.3	7.8–7.9	9.4–9.7	9.9–10.2	NC / NC

single eggs, positioned isolated, i.e., not adjacent to any other egg (50–200 eggs in a single group in *Rupirana*; Juncá and Lugli 2009; 10–40 eggs positioned in haphazard groups, or in groups of 2–20 in other species of Paratelmatobiinae; Garcia 1996; Pombal and Haddad 1999). Moreover, *Crossodactylodes* differs from all other Paratelmatobiinae, except from *P. lutzii* (see Lynch 1971), by tympanic middle ear completely lacking (tympanic membrane, annulus, and columella present in *Rupirana*; tympanic membrane absent, tympanic annulus present and visible through the skin, columella present in *Scythrophrys*, *P. cardosoi*, *P. mantiqueira*, and *P. yepiranga*; and tympanic membrane absent, tympanic annulus present and concealed by skin, and columella present in *P. gaigeae* and *P. poecilogaster* (Figs. 5, 6).

Additionally, *Crossodactylodes* differs from *Rupirana* by the absence of a tarsal fold; Fig. 3G (presence; Fig. 3J), absence of white tubercles on males' dorsum; Fig. 5A (presence; Fig. 5D); by the smaller body size considering males and females, SVL = 10.8–18.6 mm (SVL = 27.8–34.4 mm; Heyer 1999), and smaller foot, foot length/SVL = 0.31–0.43 (foot length/SVL = 0.52–0.55). In addition, the optimization of the continuous character foot length showed a decrease of foot in *Crossodactylodes* compared with all other genera of Paratelmatobiinae (Fig. 7). From *Scythrophrys* it differs by having snout rounded to truncate in dorsal view (acuminate), vocal sac absent or externally indistinct (externally distinct), tubercle on upper eyelid rounded or absent (acuminate, which resembles a small dermal horn), absence of a small meniscus on the upper iris (presence), dorsolateral fold absent or weakly developed (well-developed), absence of a tubercle on outer margin of heel (presence), absence of a tarsal fold; Fig. 3G (presence; Fig. 3K), absence of bright and contrasting coloration on ventral surfaces of arm and forearm (presence). From *Paratelmatobius* it differs by the absence of bright and contrasting coloration on ventral surfaces of belly, arm, and forearm (presence).

Distribution.—Four of the five species of *Crossodactylodes* occur across the Atlantic Forest in the states of Bahia, Espírito Santo, and Rio de Janeiro, Brazil, at elevations between 770–1480 m (Cochran 1938; Peixoto 1983; Teixeira et al. 2013). A single species (*C. itambe*) occurs in the campo rupestre of the Espinhaço Range in the state of Minas Gerais, Brazil (Barata et al. 2013) at elevations between 1800–2000 m (Fig. 8).

Natural history.—In the Atlantic Forest domain, species of *Crossodactylodes* inhabit montane and submontane ombrophilous rain forests and are found in ground or epiphytic bromeliads. The only species that occupies the high-altitude campo rupestre of the Espinhaço Range is found exclusively in rupicolous bromeliads. The main locomotor mode of the species is a slow walking (Barata et al. 2018a; Ferreira et al. 2019a; this study). When disturbed, specimens dive quickly to the bottom of the water accumulated in bromeliad axils and rarely jump outside the bromeliads. When this occurs, some individuals display death-feigning on the ground. It is common to find adults together with different ontogenetic stages (e.g., eggs, tadpoles, and juveniles) in the same bromeliad or bromeliad cluster (Santos et al. 2017; Ferreira et al. 2019a; this study). Eggs are found as single large eggs

FIG. 3.—Some diagnostic characters for the genera of Paratelmatobiinae. Nuptial pads of males of (A) *C. itambe* UFMG 14032, showing few, and well-developed spines (this state is also observed in all other species of *Crossodactylodes*); and (B) *P. gaigeae* MZUSP 138661, showing numerous and small spicules (this state is also observed in *Scythrophrys*, *Rupirana*, and other species of *Paratelmatobius*, except in *P. lutzii*, for which nuptial pads lack spicules or spines). Scale bars = 0.2 mm. Left hand of (C) *C. itambe* UFMG 11239, showing expanded discs on fingers II–IV, i.e., more dilated than the base of finger (state also observed in other species of *Crossodactylodes*); and of (D) *P. cardosoi* CFBH 3269, (E) *R. cardosoi* UFMG 7924, and (F) *S. sawayae* UFMG 19546, showing narrow discs on fingers II–IV, i.e., same width or less dilated than the base of finger (state also observed in other species of *Paratelmatobius*). Scale bars = 0.5 mm. Right foot of (G) C. *bokermanni* UFMG 13767, showing absence of tarsal fold, and toes II–V lacking lateral ridges, fringes, or webs (states also observed in other species of *Crossodactylodes*); (H) *P. gaigeae* UFMG 15008, showing absence of tarsal fold, and toes II–V with well-developed flexible fringes (states also observed in other species of *Paratelmatobius*, except in *P. lutzii*); (I) *P. lutzii* MZUSP 94633, showing absence of tarsal fold, and toes II–V with well-developed webs; (J) *R. cardosoi* UFMG 4353, and (K) *S. sawayae* UFMG 19546, showing presence of tarsal fold, indicated by white arrowheads, and toes II–V with lateral ridges; some of them are indicated by black arrowheads. Scale bars = 1.0 mm. A color version of this figure is available online.

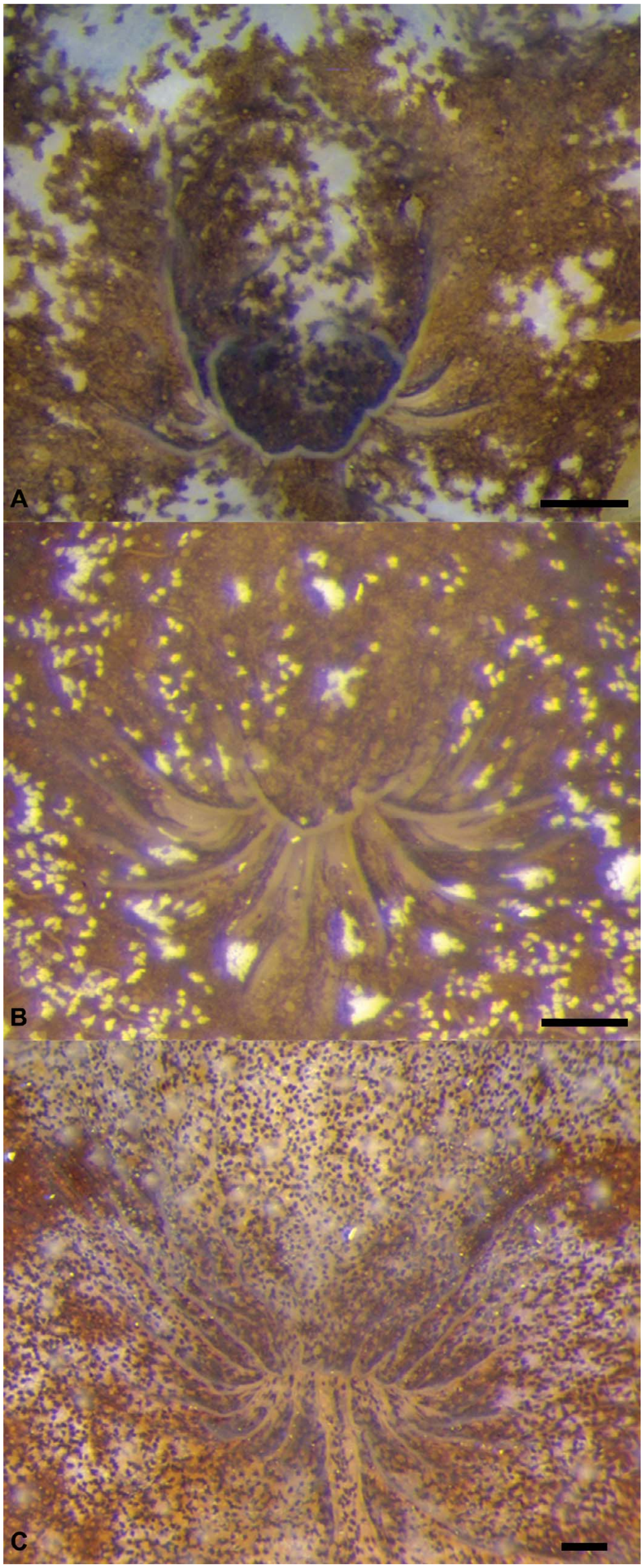

Fig. 4.—Some diagnostic characters for the genera of Paratelmatobiinae. Cloacal region of (A) *C. izecksohni* UFMG 14174, showing a conspicuous cloacal flap, i.e., with long free distal portion (state also observed in other species of *Crossodactylodes*), and of (B) *P. gaigeae* UFMG 15008, and (C) *R. cardosoi* UFMG 4353, showing an inconspicuous cloacal flap, i.e., with short free distal portion (state also observed in *Scythrophrys* and in other species of *Paratelmatobius*). Scale bars = 0.2 mm. A color version of this figure is available online.

submerged or slightly above the water surface, positioned isolated from other eggs (Santos et al. 2017; Ferreira et al. 2019a). We observed five well-formed eggs in the ovisac (i.e., posterior part of the oviduct) of one dissected female of *C. itambe* (UFMG 11237). As eggs were found singly in the field, at least females of *C. itambe* seem to partition their clutches into nearby axils or bromeliads. After hatching, tadpoles complete their development in the water accumulated in leaf axils (Peixoto 1983; Santos et al. 2017). Parental care (egg and tadpole guarding) was reported for *C. izecksohni* (Ferreira et al. 2019a) and hypothesized for *C. itambe* (Santos et al. 2017).

Content.—*Crossodactylodes pintoi* Cochran 1938, *C. bokermanni* Peixoto 1983 “1982”, *C. izecksohni* Peixoto 1983 “1982”, *C. septentrionalis* Teixeira, Recoder, Amaro, Damasceno, Cassimiro, and Rodrigues 2013, and *C. itambe* Barata, Santos, Leite, and Garcia 2013.

Species Accounts

Crossodactylodes pintoi Cochran

Figs. 9A, 10A–C

Crossodactylodes pintoi Cochran 1938: Cochran 1938:42. Holotype male (MZUSP 56467, formerly USNM 102606, examined in this study) from Serra de Macaé, municipality of Nova Friburgo, state of Rio de Janeiro, southeastern Brazil (Bokermann 1966), collected by E. Garbe between September and December 1909.

Referred specimens.—We examined four paratopotypes of *Crossodactylodes pintoi* including three males (MNRJ 4097 [formerly USNM 102610]; MZUSP 104; USNM 102608) and one female (MCZ 25707, formerly USNM 102609 [via photograph]). The specimen MNRJ 4097 was not considered in the Variation section due to its poor preservation condition.

Diagnosis.—*Crossodactylodes pintoi* is diagnosable from all congeners by the following combination of characters: (1) absence of vomerine odontophores; (2) snout not flattened in lateral view; (3) bilobed cloacal flap; (4) thumbs in adult males weakly widened; (5) zygomatic process of squamosal bone short, not passing the anterior margin of the optic foramen; (6) males lacking vocal slits; (7) absence of dorsolateral fold; (8) discs of fingers II–IV slightly expanded; (9) skin on males’ dorsum coarsely granular; (10) disc of Finger I rounded; (11) medial region of the upper lip not anteriorly projected; (12) SVL 15.9 mm (female) and 16.2–18.0 mm (males).

Comparisons.—*Crossodactylodes pintoi* is distinguished from its congeners (characters in parentheses) by the absence of vomerine odontophores; Fig. 11B (presence in *C. bokermanni* and *C. septentrionalis*; Fig. 11A); snout not flattened in lateral view; Fig. 10A (flattened in *C. bokermanni* [Fig. 10D] and *C. septentrionalis* [Fig. 11C]); thumbs in adult males weakly widened; Fig. 12D (broadly widened in *C. izecksohni* [Fig. 12C] and *C. septentrionalis* [Fig. 12E]); cloacal flap bilobed; Fig. 13B (undivided, or with a small indentation in *C. izecksohni* and *C. itambe*; Fig. 13A); zygomatic process of squamosal bone short, not passing the anterior margin of the optic foramen (long, passing the anterior margin of the optic foramen in *C. septentrionalis* and *C. itambe*; see Teixeira et al. 2013). Additionally, *C. pintoi* can be distinguished from *C. bokermanni* by the

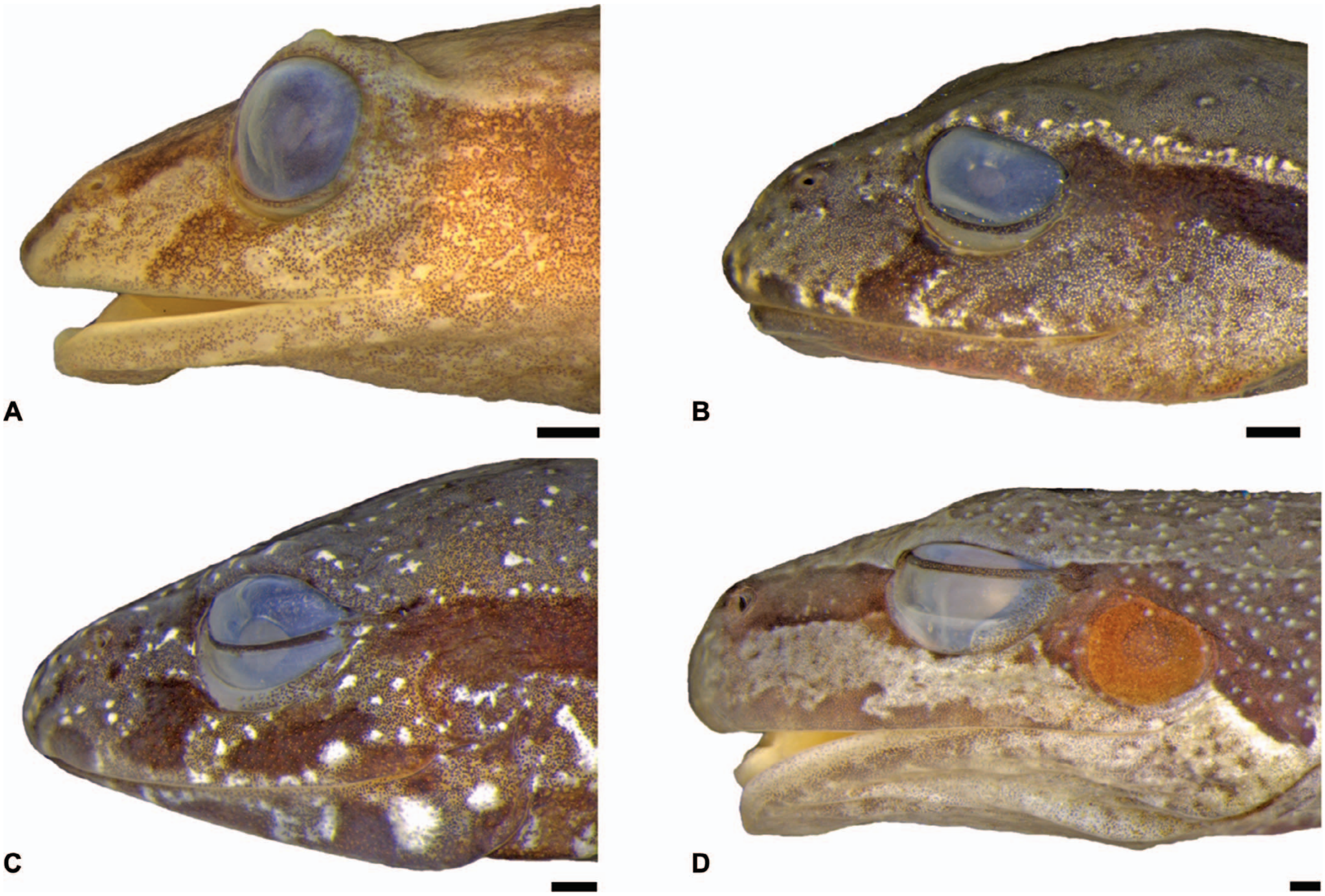

FIG. 5.—Some diagnostic characters related to tympanic middle ear elements for the genera of Paratelmatobiinae. Lateral side of the head in (A) *C. bokermanni* ZUFRJ 1933 and in (B) *P. gaigeae* UFMG 15005, showing absence of tympanic membrane and no apparent tympanic annulus externally (states also observed in other species of *Crossodactylodes*, and in *P. lutzii* and *P. poecilogaster*); in (C) *P. cardosoi* CFBH 28975, showing absence of tympanic membrane and tympanic annulus visible through the skin (states also observed in *P. mantiqueira*, *P. yepiranga*, and *S. sawayae*); in (D) *R. cardosoi* UFMG 4353, showing presence of tympanic membrane and tympanic annulus visible through the skin. Scale bars = 0.5 mm. A color version of this figure is available online.

absence of vocal slits in males (presence); absence of dorsolateral fold; Fig. 14B (presence; Fig. 14A); discs of fingers II–IV slightly expanded; Fig. 12D (broadly expanded; Fig. 12A); skin on males' dorsum coarsely granular (shagreen). Differs from *C. izecksohni* by its larger size, with SVL 15.9 mm in female and 16.2–18.0 mm in males (females SVL = 10.8–13.9 mm; males SVL = 10.8–15.0 mm; Table 2). It is distinguished from *C. septentrionalis* by having disc of Finger I rounded; Fig. 12D (acute; Fig. 12E). Differs from *C. itambe* by the absence of anterior projection in the medial region of the upper lip; Fig. 13C (presence; Figs. 11D, 13D).

Redescription of the holotype.—Adult male, SVL 16.2 mm; body slightly robust, dorsoventrally flattened; head slightly wider than long (head width/head length = 1.02); head width = 0.36 SVL; head length = 0.35 SVL; snout not flattened, truncated in dorsal view, rounded in lateral view; eye–nostril distance shorter than eye diameter (eye–nostril distance/eye diameter = 0.75); canthus rostralis slightly curved in dorsal view and rounded in cross-section; loreal region slightly concave; nostrils slightly protuberant, rounded, dorsolaterally directed, opening in the apices of small dermal elevations; interorbital area flat and approximately twice as long as eye diameter (interorbital distance/eye diameter = 2.00). Eyes medium-sized and protuberant (eye diameter/head length = 0.25; eye diameter/head width = 0.24), laterally oriented; upper eyelid margin smooth. Tympanic membrane and annulus absent. A poorly developed dermal fold from posterior edge of eye curving downward to arm insertion. Dorsolateral fold absent.

Choanae small, nearly rounded, spaced 1.6 mm from each other. Vomerine odontophores absent. Tongue ovoid, not notched, free behind for about one third of its length. Vocal slits absent; vocal sac externally indistinct. Single, small, toothlike process present on front of lower jaw with a socket between premaxillae.

Forelimb robust, hypertrophied, lacking fold or fringe; forearm nearly as robust as arm (forearm width/arm width = 1.02); fingers long; relative length of fingers I < II ≈ IV < III; discs of fingers II–IV slightly expanded, nearly rounded; disc of Finger I rounded, less expanded than the others; fingers II–IV slender; Finger I weakly widened, with nuptial pad formed by strongly aggregate keratinized spines covering most of its lateral margin and dorsal surface (12 spines on left and 13 on right thumbs); subarticular tubercles small, flat, oval in ventral view on Finger I and round in ventral view on fingers II–IV; supernumerary tubercles slightly distinct; inner metacarpal tubercle flat, elliptical; outer metacarpal

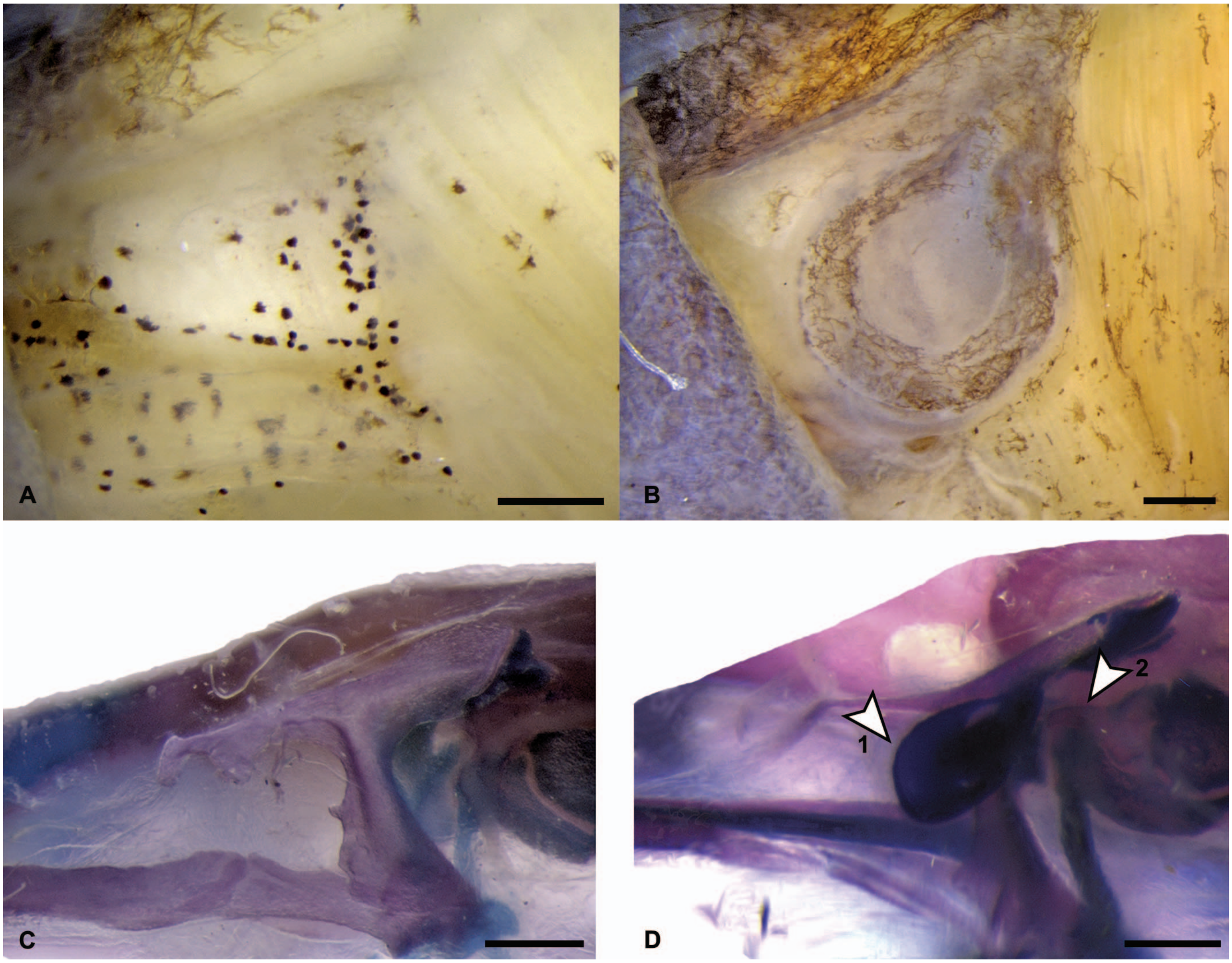

FIG. 6.—Some diagnostic characters related to tympanic middle ear elements for the genera of Paratelmatobiinae. Lateral side of the head shown after a dissection in the skin in (A) *C. bokermanni* UFMG 13769, showing absence of tympanic annulus (the same is observed in other species of *Crossodactylodes*), and in (B) *P. poecilogaster* UFMG 3240, showing presence of tympanic annulus concealed by the skin (the same state is observed in *P. gaigeae*). Scale bars = 0.25 mm. Cleared and double-stained specimens of (C) *C. itambe* UFMG 14033, showing absence of columella (state also reported for other species of *Crossodactylodes*), and of (D) *P. gaigeae* MZUSP 132608, showing presence of columella indicated by white arrowhead 2 (note also the presence of tympanic annulus, stained in blue and indicated by white arrowhead 1). Scale bars = 0.25 mm). A color version of this figure is available online.

tubercle large, flat, and nearly round in ventral view; vestigial digital webbing.

Hindlimb medium-sized and moderately robust (thigh length/SVL = 0.43; tibia length/SVL = 0.41); tarsal fold absent; toes long, slender, with expanded and nearly rounded discs, larger than finger discs (fourth toe disc diameter/third finger disc diameter = 1.29); relative length of toes I < II < III ≈ V < IV; subarticular tubercles small, flat, and rounded in ventral view; supernumerary tubercles indistinct; inner metatarsal tubercle large, flat, and elliptical in ventral view; outer metatarsal tubercle small, nearly rounded in ventral view, slightly conical in profile; digital webbing absent.

Skin on dorsal surface of body, dorsal and ventral surfaces of arm, flank, belly, and chest coarsely granular; skin on dorsal surface of head, dorsal and ventral surfaces of hindlimbs, and on throat shagreen. Cloacal opening directed posteriorly, at upper level of thighs, covered by a bilobed cloacal flap.

Measurements of the holotype (in mm).—SVL 16.2; head length 5.7; head width 5.8; eye diameter 1.4; eye–nostril distance 1.1; nostril–snout distance 0.8; internarial distance 1.2; interorbital distance 2.8; arm length 4.9; forearm length 2.8; hand length 4.1; third finger disk diameter 0.5; thigh length 6.8; tibia length 6.7; tarsal length 4.5; foot length 5.6; fourth toe disk diameter 0.6; arm width 1.8; forearm width 1.8.

Coloration of the holotype in preservative.—Translucent coloration on head and body, showing the superficial musculature. Dorsum and venter pale yellow; eyelids grayish; spines on nuptial pad black.

Variation.—Snout in dorsal view varies from truncate (MZUSP 56467) to rounded (MCZ 25707; MZUSP 104; USNM 102608) and in lateral view from rounded (MZUSP 56467; USNM 102608) to slightly sloping (MCZ 25707;

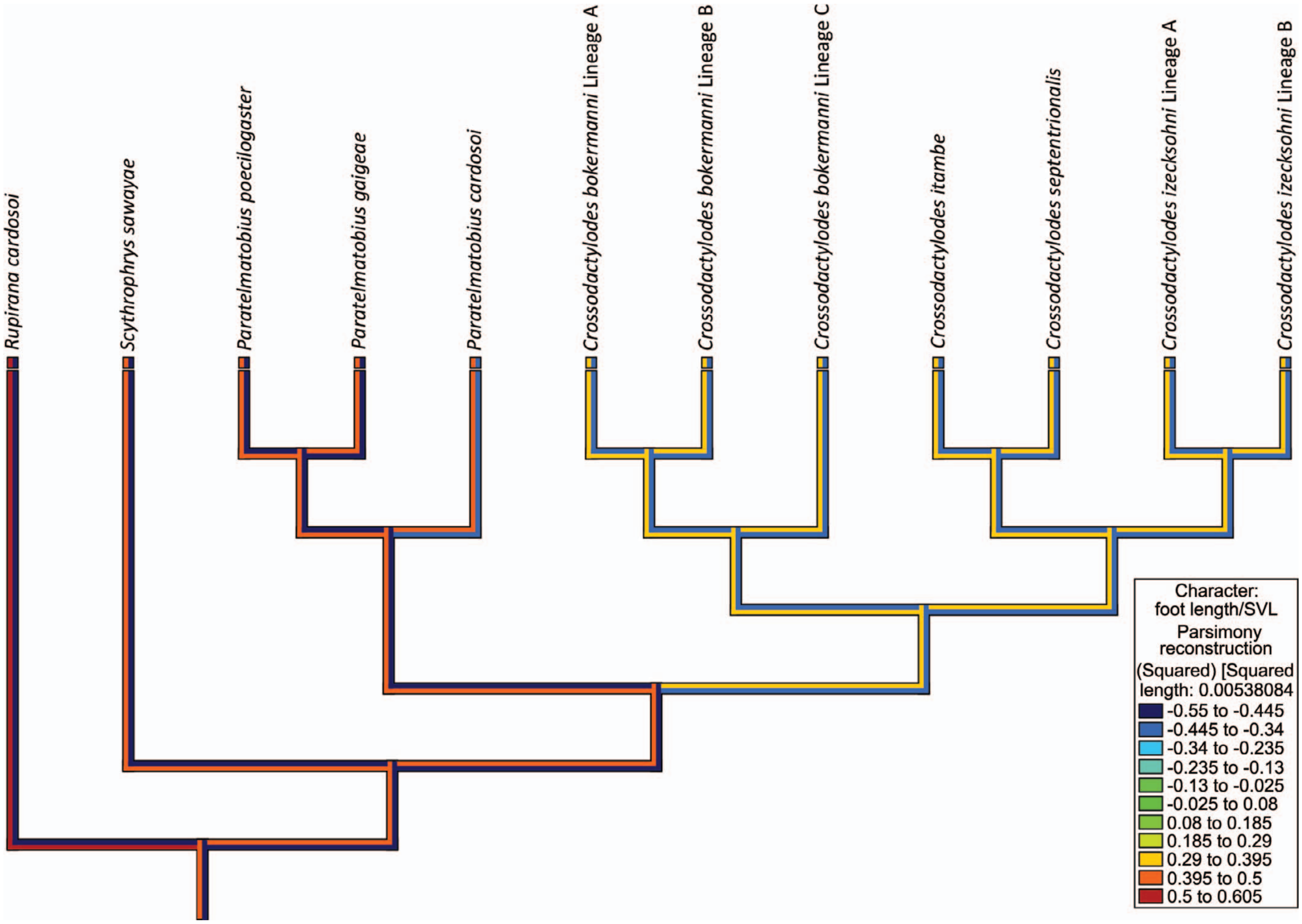

FIG. 7.—Optimization of the continuous character foot length, represented by minimum and maximum values of the ratio foot length/SVL, under Squared Change Parsimony model. Shades of the extremes blue and red represent, respectively, the highest values of minimum and maximum that indicate larger foots. Intermediate values represent smaller foots (i.e., lower values both in minimum and maximum). Note the decrease of foot length in *Crossodactylodes*. A color version of this figure is available online.

MZUSP 104). Males are distinguished from females by the presence of nuptial pads, hypertrophy of arms and forearms, and a rougher dorsal skin. The spines on nuptial pads vary in number (from one in a juvenile male to 13 in the holotype; the other males paratypes have 7–9 spines; Cochran 1955).

Distribution.—*Crossodactylodes pintoi* is known only from its type locality at Serra de Macaé, municipality of Nova Friburgo in the state of Rio de Janeiro, southeastern Brazil (Fig. 8).

Conservation.—*Crossodactylodes pintoi* is listed as Data Deficient by the IUCN Red List (Peixoto and Carvalho-e-Silva 2004) and the Brazilian Red List (Haddad et al. 2016a) due to the lack of information on its distribution and ecological requirements. On the other hand, Morais et al. (2013) suggested that the species status should be Critically Endangered based on the limited extent of occurrence and the long time no further individual is collected. It is noteworthy that Morais et al. (2013) used the publication year of *C. pintoi* description (1938) as evidence of the last collection, even though it is well documented that the species is known only from its type series collected in 1909.

The region of Serra de Macaé is also known as "Macaé de Cima" or headwaters of the Macaé River. It is located at the northern stretch of the escarpment of the Serra do Mar and covers the districts of Mury, Lumiar, and São Pedro da Serra in the municipality of Nova Friburgo. The region has extensive remnants of well-preserved ombrophilous dense forest (Instituto Estadual do Ambiente 2014). Two, short-term fieldworks were conducted in the region by MTTS (one between 18–24 January 2013 in the surroundings of the districts of Lumiar and São Pedro da Serra and one between 07–10 February 2017 in the surroundings of Macaé de Cima). Macaé de Cima was also visited by RBF between 11–15 December 2017, employing extensive bromeliad sampling at several sites with six collectors, totaling 46 sampling hours and 31.2 km tracked. We could not find new individuals of *Crossodactylodes pintoi*. The visited localities have high richness and abundance of bromeliads across different types of environments and strata. In this way, more sampling effort around the mountains of Nova Friburgo still needs to be done.

Although the type locality of *Crossodactylodes pintoi* has not been exactly recorded (see Remarks), all specimens of the type series were collected in the same locality (Cochran 1938). Thus, the estimated area of occupancy is $\sim$4 km^{2}. Following the precautionary approach (IUCN 2019) and based on the available evidence, *C. pintoi* can be listed as

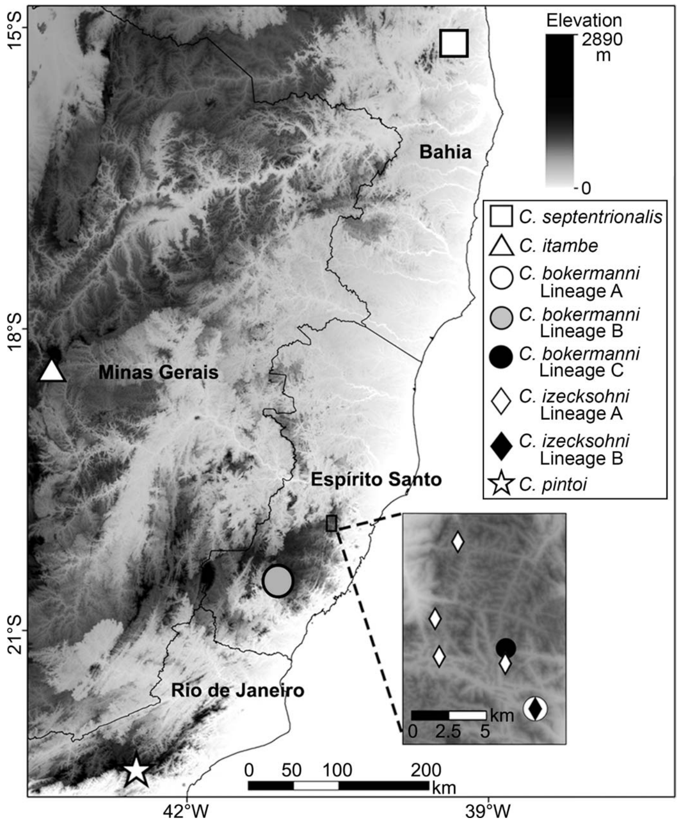

FIG. 8.—Geographic distribution of the species and lineages of *Crossodactylodes* on northeastern and southeastern Brazil. The black diamond overlapping the white circle indicates the sympatry of Lineage A of *C. bokermanni* and Lineage B of *C. izecksohni*.

Vulnerable under Criterion D2 because it is known from a single location and can become Critically Endangered or even Extinct within a short time period due to the effects of anthropic pressures or stochastic events.

Advertisement call.—Unknown.

Tadpole.—Unknown. A lot of tadpoles from municipality of Santa Teresa, described by Peixoto (1981), was wrongly assigned to *Crossodactylodes pintoi*. Later, Peixoto (1983) suggested that the same lot should belong to either one or both *C. bokermanni* or *C. izecksohni*.

Natural history.—Unknown.

Remarks.—Cochran (1938, 1955) reported that the tympanum of *Crossodactylodes pintoi* is hidden. However, Lynch (1971) and Teixeira et al. (2013) re-evaluated this character and considered the tympanum absent. We agree with Lynch (1971) and Teixeira et al. (2013) but considered all tympanic middle ear elements (i.e., tympanic membrane, tympanic annulus, and columella) absent. Cochran (1955) considered the snout of the holotype as rounded in dorsal view. However, our study and Teixeira et al. (2013) considered it truncated. This variation might be due to differences in interpretation or due to fixation artifact related to the long time the specimen was collected. Cochran (1955) and Barata et al. (2013) reported that *C. pintoi* has a median subgular vocal sac. However, after careful analysis, we conclude that the skinfold these authors interpreted as vocal sac is a fixation artifact and that a vocal sac is absent in *C. pintoi*. Peixoto (1983) erroneously reported MZUSP 56473 as the holotype of *C. pintoi*. Lynch (1971) reported natural history data for *C. pintoi*. However, the information refers to *C. bokermanni* or *C. izecksohni*, and the natural history of *C. pintoi* remains unknown.

It is well documented that Ernst Garbe (1853–1925), a traveling naturalist of the Museu de Zoologia of Universidade de São Paulo, was in the Serra de Macaé, municipality of Nova Friburgo, between September and December 1909, the year in which he collected the type series of *Crossodactylodes pintoi* (see Ihering and Ihering 1911; Pinto 1945; Paynter and Traylor 1991). According to Bokermann (1966), various species of birds collected by E. Garbe in the region are only found at elevations close to 1000 m. Because of this, Bokermann (1966) states that E. Garbe possibly collected the specimens along an old path that linked the municipality of Nova Friburgo to the headwaters of the Macaé River. However, it is not possible to precisely determine the type locality of *C. pintoi*.

Crossodactylodes bokermanni Peixoto
Figs. 9B, 10D–F

Crossodactylodes bokermanni Peixoto 1983 "1982": Peixoto 1983:619–621, 623, 626. Holotype male (EI 7173, examined in this study) from Alto Santo Antônio, municipality of Santa Teresa, state of Espírito Santo, southeastern Brazil, about 19°54′40.13″S, 40°35′29.37″W, 832 m, collected by O.L. Peixoto and colleagues on 22 December 1980 (O.L. Peixoto, personal communication).

Referred specimens.—We examined 33 paratopotypes of *Crossodactylodes bokermanni* including six males (EI 7174, 7180–7181; MZUSP 58077, 73759–73760 [formerly WCAB 48001–48002]), 15 females (EI 7175–7176, 7182–7183, 7189; MNRJ 4166, 14223–14226, 14237; MZUSP 58079; USNM 221885–87), and 12 juveniles (EI 7177–7179, EI 7184–7188; MNRJ 4165, 14222–14223; MZUSP 58078). To this species we refer four additional males (ZUFRJ 1377–1378, 1380, 1933) and two additional females (ZUFRJ 1382, 1934) from the type locality; one male (CFBH 44754) from Reserva Biológica Augusto Ruschi, municipality of Santa Teresa, state of Espírito Santo, southeastern Brazil, 19°53′50.31″S, 40°32′46.13″W, 811 m; one male (UFMG 14188), seven females (CFBH 44748–44753; UFMG 14189), and one juvenile (UFMG 14190) from Penha District, municipality of Santa Teresa, state of Espírito Santo, southeastern Brazil, 19°55′44.62″S, 40°32′55.33″W, 811 m; three males (MBML 3975, 3984–85), one female (MNRJ 38412), and one juvenile (MNRJ 34933) from Estação Biológica de Santa Lúcia, municipality of Santa Teresa, state of Espírito Santo, southeastern Brazil, 19°57′45.76″S, 40°31′55.66″W, 915 m; four males (UFMG 13767, 13769, 13774, 14197) and three females (UFMG 13770, 14198–14199) from Parque Estadual do Forno Grande, municipality of Castelo, state of Espírito Santo, southeastern Brazil, 20°30′40.07″S, 41°5′26.92″W, 1477 m; and one female (MBML 1774) and two juveniles (MBML 1779–80) from Sítio Fassarela, municipality of Domingos Martins, state of Espírito Santo, southeastern Brazil, 20°21′47.47″S, 41°4′47.16″W, 1018 m.

Diagnosis.—*Crossodactylodes bokermanni* is diagnosable from all congeners by the following combination of characters: (1) males with vocal slits; (2) presence of

Fig. 9.—Dorsal (left) and ventral (right) views of holotypes of (A) *C. pintoi* MZUSP 56467, male, SVL = 16.2 mm; (B) *C. bokermanni* EI 7173, male, SVL = 15.2 mm; and (C) *C. izecksohni* EI 7192, male, SVL = 13.4 mm. A color version of this figure is available online.

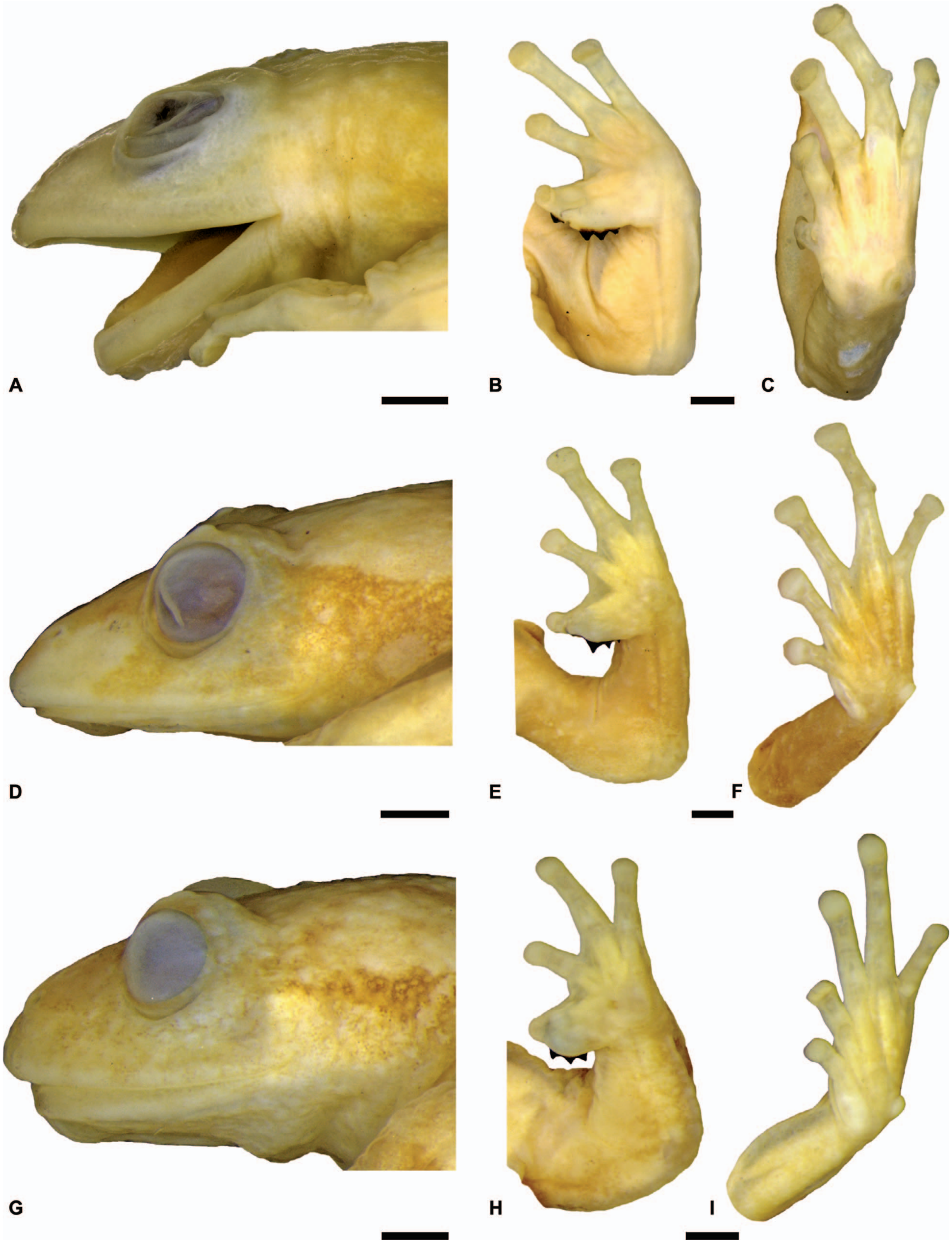

FIG. 10.—Head in lateral view, left hand, and left foot of holotypes of (A–C) *C. pintoi* MZUSP 56467, (D–F) *C. bokermanni* EI 7173, and (G–I) *C. izecksohni* EI 7192. Scale bars = 1 mm. A color version of this figure is available online.

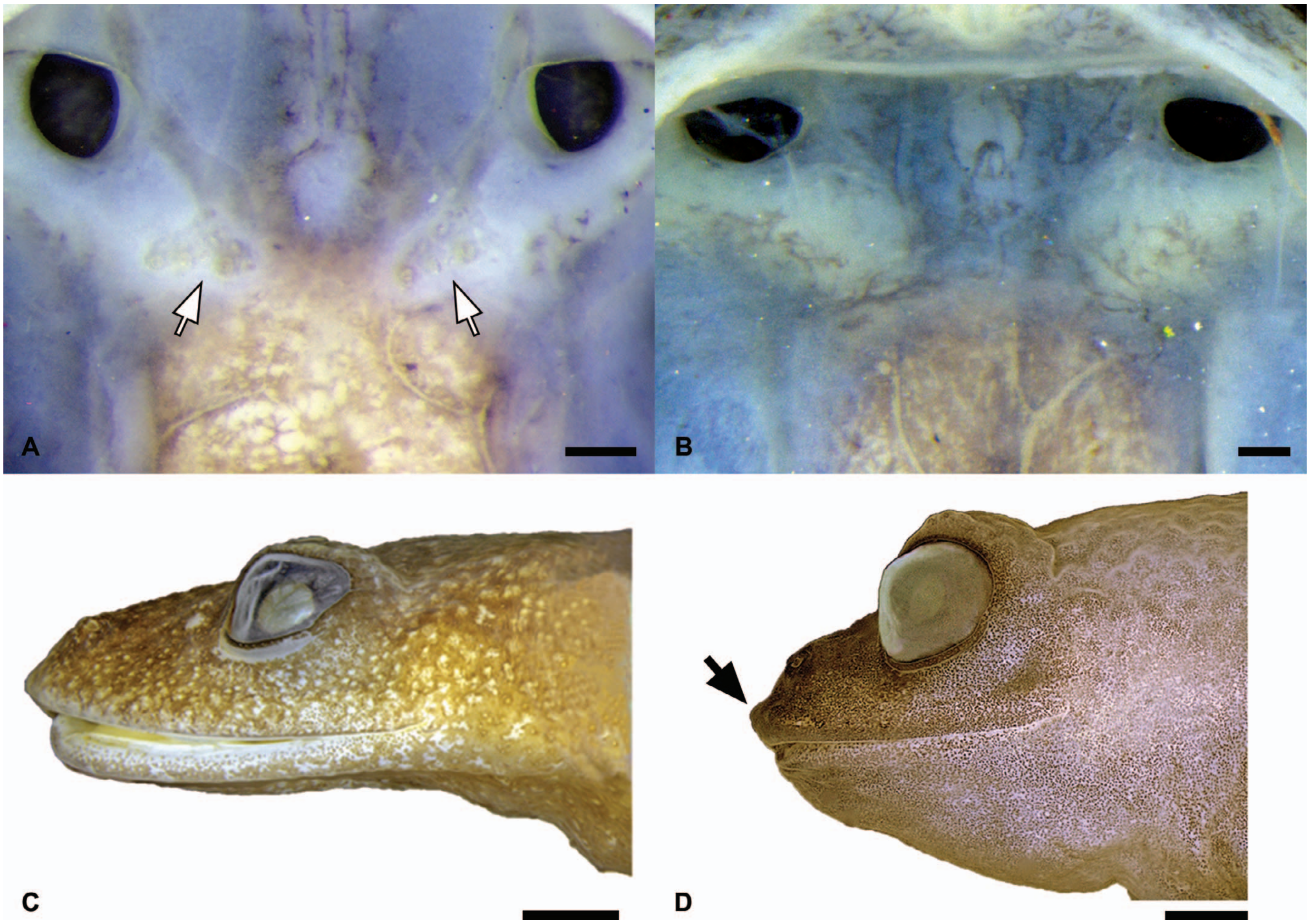

FIG. 11.—Some diagnostic characters for species of *Crossodactylodes*. Buccal roof in (A) *C. bokermanni* UFMG 14197, showing presence of vomerine odontophores indicated by white arrows (state also observed in *C. septentrionalis*), and in (B) *C. itambe* UFMG 14040, showing absence of vomerine odontophores (state also observed in *C. pintoi* and *C. izecksohni*). Scale bars = 0.2 mm. Head in lateral view in (C) *C. septentrionalis* MZUESC 14363, showing a flattened snout, and in (D) *C. itambe* UFMG 11239, showing a not-flattened snout and an anterior projection in the medial region of the upper lip indicated by a black arrow (for this character also refer to Fig. 13D). Scale bars = 1 mm. A color version of this figure is available online.

dorsolateral fold; (3) discs of fingers II–IV broadly expanded; (4) skin on males' dorsum shagreen; (5) presence of vomerine odontophores; (6) snout flattened in lateral view; (7) thumbs in adult males weakly widened; (8) in life, iris coppery or reddish with dark brown fine reticulations; (9) zygomatic process of squamosal bone short, not passing the anterior margin of the optic foramen; (10) presence of a black canthal stripe; (11) presence of a black lateral band from posterior corner of the eye to the posterior third of body; (12) hindlimbs with black transverse bars; (13) disc of Finger I rounded; (14) medial region of the upper lip not anteriorly projected; (15) in preservative, dorsal background coloration varying from pale cream to pale yellow, or brown.

Comparisons.—*Crossodactylodes bokermanni* is distinguished from its congeners (characters in parentheses) by the presence of vocal slits in males (absence in *C. pintoi*, *C. izecksohni*, *C. septentrionalis*, and *C. itambe*); presence of a dorsolateral fold from posterior corner of the eye to the posterior third of body; Fig. 14A (absence in *C. pintoi*, *C. izecksohni*, *C. septentrionalis*, and *C. itambe*; Fig. 14B); discs of fingers II–IV broadly expanded; Fig. 12A (slightly expanded in *C. pintoi*, *C. izecksohni*, *C. septentrionalis*, and *C. itambe*; Figs. 12B–E); skin on males' dorsum shagreen (coarsely granular in *C. pintoi*, *C. izecksohni*, *C. septentrionalis*, and *C. itambe*); presence of vomerine odontophores; Fig. 11A (absence in *C. pintoi*, *C. izecksohni*, and *C. itambe*; Fig. 11B); snout flattened in lateral view; Fig. 10D (not flattened in *C. pintoi* [Fig. 10A], *C. izecksohni* [Fig. 10G], and *C. itambe* [Fig. 11D]); thumbs in adult males weakly widened; Fig. 12A (broadly widened in *C. izecksohni* [Fig. 12C] and *C. septentrionalis* [Fig. 12E]); iris in life coppery to reddish, with dark brown fine reticulations; Fig. 15A (yellowish with dark brown fine reticulations, interrupted by a brown horizontal bar at the pupil level in *C. izecksohni* [Fig. 16A] and uniformly black or brownish black in *C. itambe* [Fig. 15B]); zygomatic process of squamosal bone short, not passing the anterior margin of the optic foramen (long, passing the anterior margin of the optic foramen in *C. septentrionalis* and *C. itambe*; see Teixeira et al. 2013); presence of a black canthal stripe; Fig. 14A (absence in *C. septentrionalis* and *C. itambe*; Fig. 14B); presence of a black lateral band from posterior corner of the eye to the posterior third of body; Fig. 14A (absence in *C. septentrionalis* and *C. itambe*; Fig. 14B); presence of black transverse bars on hindlimbs; Fig. 14A (absence in *C. septentrionalis* and *C. itambe*; Fig. 14B). Additionally, *C.*

Fig. 12.—Diagnostic characters for species of *Crossodactylodes*. Left hand of (A) a female (UFMG 13770) and a male (UFMG 13767) of *C. bokermanni*; (B) a female (UFMG 11246) and a male (UFMG 11239) of *C. itambe*; (C) a female (ZUFRJ 365) and a male (UFMG 14174) of *C. izecksohni*; (D) a male of *C. pintoi* (USNM 102608); and a female (MZUESC 14364) and a male (MZUESC 14363) of *C. septentrionalis*. Note the broadly expanded discs of fingers II–IV in *C. bokermanni* (A); the broadly widened thumbs in males of *C. izecksohni* (C), and *C. septentrionalis* (E); and the acute disc on Finger I in *C. septentrionalis* (E). Scale bars = 1 mm. A color version of this figure is available online.

bokermanni can be distinguished from *C. septentrionalis* by having disc of Finger I rounded; Fig. 12A (acute; Fig. 12E); from *C. itambe* by the absence of anterior projection in the medial region of the upper lip; Fig. 13C (presence; Figs. 11D, 13D); and dorsal background coloration in preservative pale cream, pale yellow, or brown; Fig. 17A (dark gray or brownish black; Fig. 17B).

Redescription of the holotype.—Adult male, SVL 15.2 mm; body slender, dorsoventrally flattened; head slightly longer than wide (head width/head length 0.97); head width 0.38 SVL; head length 0.40 SVL; snout flattened, rounded in dorsal view, slightly sloping in lateral view; eye–nostril distance slightly shorter than eye diameter (eye–nostril distance/eye diameter 0.97); canthus rostralis slightly curved in dorsal view and rounded in cross-section; loreal region slightly concave; nostrils protuberant, elliptical, dorsolaterally directed, opening in the apices of small dermal elevations; interorbital area flat and more than twice as long as eye diameter (interorbital distance/eye diameter = 2.24). Eyes medium-sized and protuberant (eye diameter/head length = 0.23; eye diameter/head width = 0.24), laterally oriented; upper eyelid margin with a prominent rounded tubercle in its medial region. Tympanic membrane and annulus absent. A poorly developed dermal fold from posterior edge of eye curving downward to arm insertion. A weakly developed dorsolateral fold extending from the posterior corner of the eye to the posterior third of body.

Choanae small, nearly rounded, spaced 1.5 mm from each other. Vomerine odontophores present, positioned posterior to the level of the choanae, broadly separated from each other. Tongue ovoid, not notched, free behind for about one third of its length. Vocal slits short, located at the level of the posterior third of tongue; vocal sac externally indistinct. Single, small tooth-like process present on front of lower jaw with a socket between premaxillae.

Forelimb slightly robust, moderately hypertrophied, lacking fold or fringe; forearm nearly as robust as arm (forearm width/arm width = 1.04); fingers long; relative length of fingers I ≈ II < IV < III; discs of fingers II–IV broadly expanded, elliptical; disc of Finger I rounded, less expanded than the others; fingers II–IV slender; Finger I weakly widened, with nuptial pad formed by regularly spaced keratinized spines covering most of its lateral margin and dorsal surface (eight spines on each thumb); subarticular tubercles small, flat, and rounded in ventral view; supernumerary tubercles slightly distinct; inner metacarpal tubercle flat, elliptical; outer metacarpal tubercle large, flat, and nearly round in ventral view; vestigial digital webbing.

Hindlimb medium-sized and slender (thigh length/SVL = 0.44; tibia length/SVL = 0.45); tarsal fold absent; toes long, slender; discs of toes II–V broadly expanded, elliptical; disc of Toe I rounded, less expanded than the others; discs with similar size to the finger discs (fourth toe disc diameter/third finger disc diameter = 1.02); relative length of toes I < II < V < III < IV; subarticular tubercles small, flat, and rounded

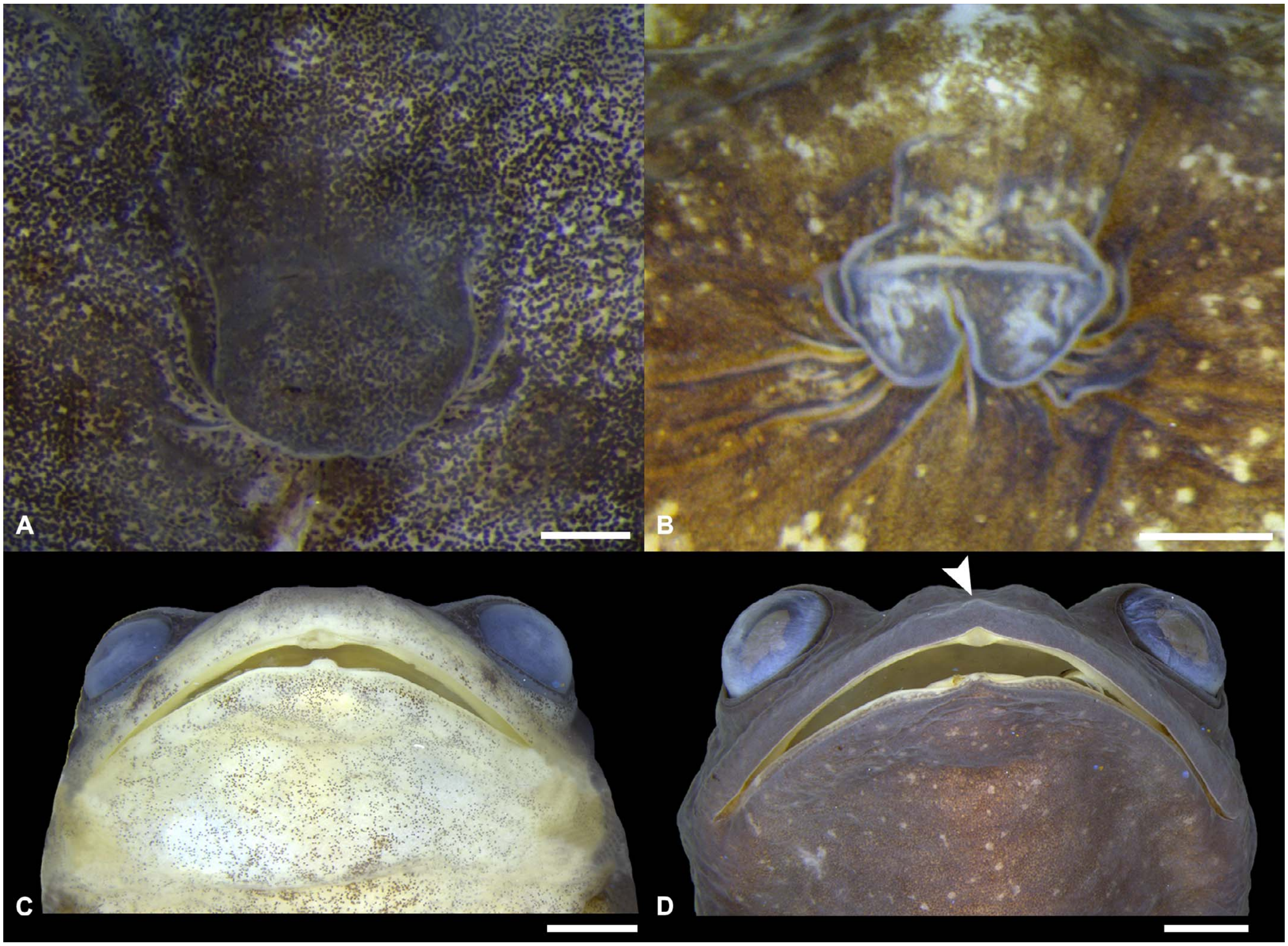

FIG. 13.—Diagnostic characters for species of *Crossodactylodes*. Cloacal region in (A) *C. itambe* UFMG 13382, showing an undivided cloacal flap (state also observed in *C. izecksohni*—in both species the flap can also show a small distal indentation); and in (B) *C. septentrionalis* MZUESC 14363, showing a bilobed cloacal flap (state also observed in *C. pintoi*). This character is polymorphic in *C. bokermanni*. Scale bars = 0.5 mm. Head in ventral view in (C) *C. bokermanni* UFMG 13767, showing medial region of the upper lip lacking an anterior projection (state also observed in *C. pintoi*, *C. izecksohni*, and *C. septentrionalis*); and in (D) *C. itambe* UFMG 13380, showing medial region of the upper lip with an anterior projection, indicated by a white arrow head. Scale bars = 1 mm. A color version of this figure is available online.

in ventral view; supernumerary tubercles indistinct; inner metatarsal tubercle large, flat, and elliptical in ventral view; outer metatarsal tubercle small, nearly rounded in ventral view, slightly conical in profile; digital webbing absent.

Skin on flank, dorsal, and ventral surfaces shagreen. Cloacal opening directed posteriorly, at upper level of thighs, covered by an undivided cloacal flap. Few small scattered tubercles near the cloacal opening.

Measurements of the holotype (in mm).—SVL 15.2; head length 6.0; head width 5.8; eye diameter 1.4; eye–nostril distance 1.3; nostril–snout distance 0.9; internarial distance 1.4; interorbital distance 3.1; arm length 4.2; forearm length 3.0; hand length 3.8; third finger disk diameter 0.6; thigh length 6.6; tibia length 6.9; tarsal length 3.8; foot length 5.7; fourth toe disk diameter 0.6; arm width 1.5; forearm width 1.5.

Coloration of the holotype in life.—Based on the description and photographs provided by Peixoto (1983), we could infer that the holotype had dorsal surfaces of head, body, and limbs reddish brown with scattered black flecks. Dorsum with two conspicuous reddish blotches lighter than the background, one with an inverted triangular shape on posterior third of head and the other somewhat rectangular extends from the scapular region to the posterior third of body. These blotches are delimited by whitish green flecks. Eyelid tubercle whitish. A black, rounded blotch in the lumbar region. Loreal region reddish, lighter than the background; a thick black canthal stripe and a black labial bar. A cream narrow dorsolateral fold extends from behind the eye to posterior third of body. Flank with a black band, dorsally delimited by the dorsolateral fold. This band is expanded after the arm insertion. A black transverse bar in the wrist; spines on nuptial pad black. Hindlimb with black transverse bars (three on thigh and tibia and one on tarsus). A thick black stripe on anterior surface of thigh. Venter dark brown with marbled blotches lighter than the background.

Coloration of the holotype in preservative.—The color is faded, turning into pale tones. The reddish-brown dorsal surfaces of head, body, and limbs become pale cream. The conspicuous reddish blotches on dorsum are translu-

FIG. 14.—Some diagnostic characters for species of *Crossodactylodes*. (A) *C. bokermanni* in life, showing the dorsolateral fold (white arrow), the black canthal stripe, the black lateral band from posterior corner of the eye to the posterior third of body, and the black transverse bars on hindlimbs (white arrowheads 1, 2, and 3, respectively). (B) *C. septentrionalis* in life, in which dorsolateral fold and the black stripe, band, and bars are absent. Dorsolateral fold is also absent in *C. pintoi*, *C. izecksohni*, and *C. itambe*. The black stripe, band, and bars are also absent in *C. itambe*, are polymorphic in *C. izecksohni* (Fig. S3), and states for these characters are unknown for *C. pintoi*. A color version of this figure is available online.

cent, as well as the dorsal and ventral surfaces of hand and foot. The black flecks, blotches, bands, and bars are pale brown and less evident. Venter continues darker than dorsum. Thoracic skin is translucent, showing pectoral musculature. Eyelid tubercle, dorsolateral fold, carpal, and tarsal tubercles are whitish.

Variation.—Snout in lateral view varies from slightly sloping (~71%) to acuminate (~29%). The cloacal flap is usually undivided (~61%), but may have a small distal indentation (~35%) and is rarely bilobed (~4%). Specimens from municipality of Castelo are slightly larger than specimens from municipality of Santa Teresa (Castelo, females SVL = 16.2–17.7 mm, mean = 17.2 mm, males SVL = 16.6–17.9 mm, mean = 17.1 mm; Santa Teresa, females SVL = 12.3–16.1 mm, mean = 14.1 mm, males SVL

TABLE 2.—Morphometric characters (mean ± SD, range in parentheses) in mm for males and females of species of *Crossodactylodes*.

	C. bokermanni		*C. izecksohni*		*C. itambe*		*C. septentrionalis*		*C. pintoi*
Character	Males (*n* = 20)	Females (*n* = 19)	Males (*n* = 39)	Females (*n* = 43)	Males (*n* = 17)	Females (*n* = 18)	Males (*n* = 1)	Females (*n* = 2)	Males (*n* = 3)
Snout–vent length	15.0 ± 1.5 (12.7–17.9)	14.5 ± 1.7 (12.2–17.7)	13.5 ± 1.0 (10.8–15.0)	12.4 ± 0.9 (10.8–13.9)	16.5 ± 1.3 (14.0–17.9)	16.4 ± 0.8 (15.2–18.0)	18.6	16.3 ± 0.3 (16.1–16.5)	17.0 ± 0.9 (16.2–18.0)
Head length	5.7 ± 0.4 (5.2–6.6)	5.6 ± 0.4 (4.9–6.5)	5.1 ± 0.3 (4.5–5.4)	4.8 ± 0.3 (4.3–5.2)	6.2 ± 0.3 (5.6–6.6)	6.1 ± 0.2 (5.7–6.5)	7.2	6.4 ±0.0 (6.4–6.4)	5.8 ± 0.1 (5.7–6.0)
Head width	5.6 ± 0.4 (5.0–6.4)	5.4 ± 0.5 (4.7–6.4)	5.4 ± 0.3 (4.6–5.8)	4.9 ± 0.3 (4.3–5.4)	6.6 ± 0.3 (6.2–7.2)	6.4 ± 0.2 (6.1–6.9)	7.3	6.3 ± 0.1 (6.2–6.3)	6.0 ± 0.2 (5.8–6.3)
Eye diameter	1.4 ± 0.1 (1.2–1.6)	1.4 ± 0.1 (1.1–1.6)	1.2 ± 0.1 (1.1–1.4)	1.2 ± 0.1 (1.1–1.3)	1.8 ± 0.1 (1.6–2.0)	1.8 ± 0.1 (1.4–2.0)	1.7	1.6 ± 0.1 (1.6–1.7)	1.4 ± 0.1 (1.4–1.5)
Interorbital distance	3.1 ± 0.3 (2.7–3.6)	3.0 ± 0.2 (2.6–3.5)	2.8 ± 0.2 (2.4–3.3)	2.7 ± 0.2 (2.3–3.0)	3.4 ± 0.2 (3.1–3.7)	3.3 ± 0.2 (2.9–3.6)	3.9	3.4 ± 0.1 (3.3–3.5)	3.1 ± 0.4 (2.8–3.5)
Eye–nostril distance	1.3 ± 0.2 (1.0–1.6)	1.2 ± 0.1 (1.0–1.5)	1.2 ± 0.1 (1.0–1.4)	1.1 ± 0.1 (0.9–1.3)	1.4 ± 0.1 (1.3–1.6)	1.4 ± 0.1 (1.3–1.5)	1.7	1.5 ± 0.0 (1.5–1.5)	1.2 ± 0.1 (1.1–1.3)
Nostril–snout distance	1.0 ± 0.1 (0.9–1.2)	1.0 ± 0.1 (0.9–1.2)	0.8 ± 0.1 (0.7–1.0)	0.8 ± 0.1 (0.7–0.9)	1.1 ± 0.1 (0.9–1.2)	1.0 ± 0.1 (0.9–1.1)	1.0	0.9 ± 0.0 (0.9–0.9)	0.9 ± 0.1 (0.8–0.9)
Internarial distance	1.3 ± 0.1 (1.1–1.5)	1.3 ± 0.1 (1.1–1.5)	1.1 ± 0.1 (1.0–1.3)	1.1 ± 0.1 (1.0–1.3)	1.3 ± 0.1 (1.2–1.4)	1.3 ± 0.1 (1.1–1.4)	1.4	1.2 ± 0.0 (1.2–1.2)	1.3 ± 0.2 (1.2–1.4)
Arm length	4.2 ± 0.5 (3.5–5.1)	4.0 ± 0.4 (3.3–4.8)	3.9 ± 0.4 (3.0–4.5)	3.4 ± 0.2 (3.0–3.8)	4.8 ± 0.3 (4.1–5.1)	4.6 ± 0.2 (4.2–4.9)	6.1	4.5 ± 0.1 (4.4–4.5)	4.7 ± 0.4 (4.2–5.0)
Arm width	1.3 ± 0.3 (0.9–1.9)	1.0 ± 0.1 (0.8–1.2)	1.6 ± 0.4 (0.8–2.1)	0.8 ± 0.1 (0.7–1.0)	1.8 ± 0.3 (1.3–2.3)	1.2 ± 0.1 (1.0–1.3)	2.4	1.1 ± 0.0 (1.1–1.1)	1.8 ± 0.0 (1.8–1.8)
Forearm length	2.9 ± 0.2 (2.6–3.4)	2.9 ± 0.3 (2.5–3.6)	2.5 ± 0.2 (2.0–3.0)	2.4 ± 0.2 (2.1–3.4)	3.6 ± 0.2 (3.1–3.9)	3.6 ± 0.2 (3.2–3.9)	3.4	3.3 ± 0.1 (3.2–3.3)	2.8 ± 0.2 (2.7–3.0)
Forearm width	1.4 ± 0.2 (1.1–1.9)	1.1 ± 0.1 (0.9–1.3)	1.5 ± 0.3 (1.0–1.9)	1.0 ± 0.1 (0.7–1.1)	1.9 ± 0.3 (1.5–2.4)	1.4 ± 0.1 (1.2–1.6)	2.3	1.1 ± 0.1 (1.1–1.2)	1.9 ± 0.1 (1.8–2.0)
Hand length	3.8 ± 0.4 (3.2–4.4)	3.5 ± 0.4 (2.9–4.5)	3.2 ± 0.3 (2.6–3.8)	2.8 ± 0.2 (2.5–3.4)	4.7 ± 0.3 (4.0–5.2)	4.4 ± 0.3 (3.8–4.9)	5.4	4.2 ± 0.1 (4.1–4.3)	4.2 ± 0.3 (4.0–4.5)
Third finger disc diameter	0.7 ± 0.1 (0.5–0.9)	0.6 ± 0.1 (0.5–0.9)	0.4 ± 0.1 (0.3–0.6)	0.4 ± 0.1 (0.3–0.5)	0.6 ± 0.1 (0.5–0.7)	0.6 ± 0.1 (0.5–0.7)	0.8	0.6 ± 0.1 (0.6–0.7)	0.6 ± 0.1 (0.5–0.6)
Thigh length	6.6 ± 0.6 (5.6–7.7)	6.4 ± 0.6 (5.4–7.6)	5.4 ± 0.4 (4.4–6.1)	4.9 ± 0.3 (4.3–5.8)	6.6 ± 0.3 (5.9–7.1)	6.6 ± 0.3 (6.0–7.3)	8.8	7.2 ± 0.3 (7.0–7.4)	7.1 ± 0.4 (6.8–7.6)
Tibia length	6. 7± 0.6 (5.7–7.6)	6.4 ± 0.6 (5.6–7.4)	5.4 ± 0.3 (4.5–6.0)	5.0 ± 0.3 (4.5–5.7)	6.3 ± 0.3 (5.5–6.7)	6.3 ± 0.3 (5.7–6.7)	8.6	6.8 ± 0.1 (6.7–6.9)	6.4 ± 0.3 (6.1–6.7)
Tarsal length	3.8 ± 0.3 (3.1–4.3)	3.5 ± 0.3 (3.0–4.1)	3.1 ± 0.2 (2.5–3.7)	2.9±0.2 (2.5–3.3)	3.7 ± 0.2 (3.4–4.1)	3.8 ± 0.2 (3.5–4.3)	5.2	4.1 ± 0.2 (4.0–4.2)	4.6 ± 0.2 (4.5–4.8)
Foot length	5.9 ± 0.6 (4.9–6.9)	5.4 ± 0.7 (4.5–7.0)	4.8 ± 0.4 (3.9–5.5)	4.4 ± 0.3 (3.8–5.1)	5.8 ± 0.4 (5.1–6.4)	5.8 ± 0.3 (5.3–6.3)	7.5	5.8 ± 0.3 (5.6–6.0)	5.7 ± 0.6 (5.1–6.3)
Fourth toe disk diameter	0.7 ± 0.1 (0.5–0.9)	0.6 ± 0.1 (0.5–0.9)	0.5 ± 0.1 (0.3–0.7)	0.4 ± 0.1 (0.4–0.6)	0.7 ± 0.1 (0.5–0.8)	0.7 ± 0.1 (0.5–0.8)	0.8	0.6 ± 0.0 (0.6–0.6)	0.7 ± 0.1 (0.6–0.8)

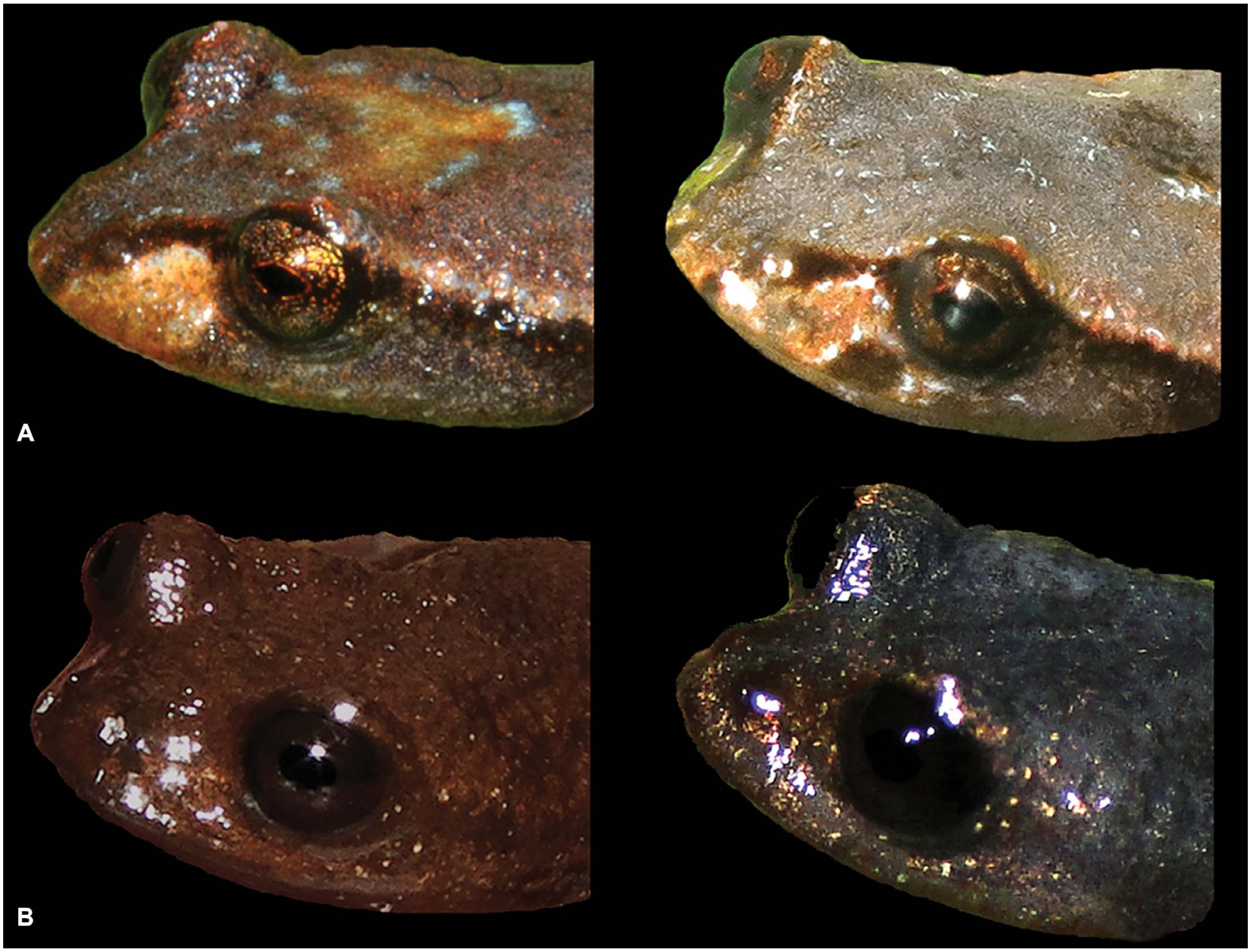

FIG. 15.—Diagnostic character states of iris coloration in life in *Crossodactylodes*. (A) Two specimens of *C. bokermanni*, showing a coppery or reddish iris with dark brown fine reticulations; (B) *C. itambe*, showing a uniformly black or brownish black iris. The state for this character is unknown for *C. pintoi*. For the states observed in *C. izecksohni* and *C. septentrionalis* refer to Fig. 16. A color version of this figure is available online.

= 12.7–16.3 mm, mean = 14.5 mm). Males are distinguished from females by the presence of nuptial pads, moderate hypertrophy of arms and forearms (females arm width/arm length = 0.20–0.27, mean = 0.24; forearm width/forearm length = 0.32–0.40, mean = 0.37; males arm width/arm length = 0.25–0.39, mean = 0.30; forearm width/forearm length = 0.40–0.61, mean = 0.46), and a slightly rougher dorsal skin. In addition, males have a single, median subgular vocal sac, visible only after dissection in the skin of gular region (e.g., UFMG 13769). The spines on nuptial pads vary in number (from one to eight), size, and degree of aggregation. The number of spines can vary between the right and left thumbs of a same specimen. Males with larger SVL and more-hypertrophied forelimbs have higher number and aggregation of spines. The dorsal background coloration in life varies from light gray, light lilac, and brown. The pattern of dorsal blotches is quite variable. The two conspicuous blotches described for the holotype vary in size and shape, can be black rather than reddish, and one or both may be absent. A black labial bar is usually present but can be absent. Some individuals have an orange coloration in different regions: loreal region; posterior surfaces of arm, thigh, tibia, and tarsus; and cloacal region (e.g., Fig. 14A). The black stripe, band, and bars vary in thickness and can be more or less marked. Venter might have orange scattered flecks on gular, abdominal, and cloacal regions.

Distribution.—*Crossodactylodes bokermanni* is only known from the state of Espírito Santo, southeastern Brazil. The species is known from four sites in the municipality of Santa Teresa: (1) Alto Santo Antônio (type locality), about 19°54′40.10″S, 40°35′29.37″W, 843 m (O.L. Peixoto, personal communication); (2) Reserva Biológica Augusto Ruschi, 19°53′50.31″S, 40°32′46.13″W, 811 m; (3) Penha district, 19°55′44.62″S, 40°32′55.33″W, 800 m; and (4) Estação Biológica de Santa Lúcia, about 19°57′47, 68″S, 40°31′55,85″W, 908 m. It is also recorded from another two localities: (1) Sítio Fassarela, municipality of Domingos Martins, 20°21′47.47″S, 41°4′47.16″W, 1018 m; and (2) Parque Estadual do Forno Grande, municipality of Castelo, 20°30′40.07″S, 41°5′26.92″W, 1477 m.

Peixoto (1983) used approximate geographic coordinates from the city of Santa Teresa. Other studies also used these coordinates, which misleads that *Crossodactylodes bokermanni* occurs between 650–675 m elevation (Silvano and

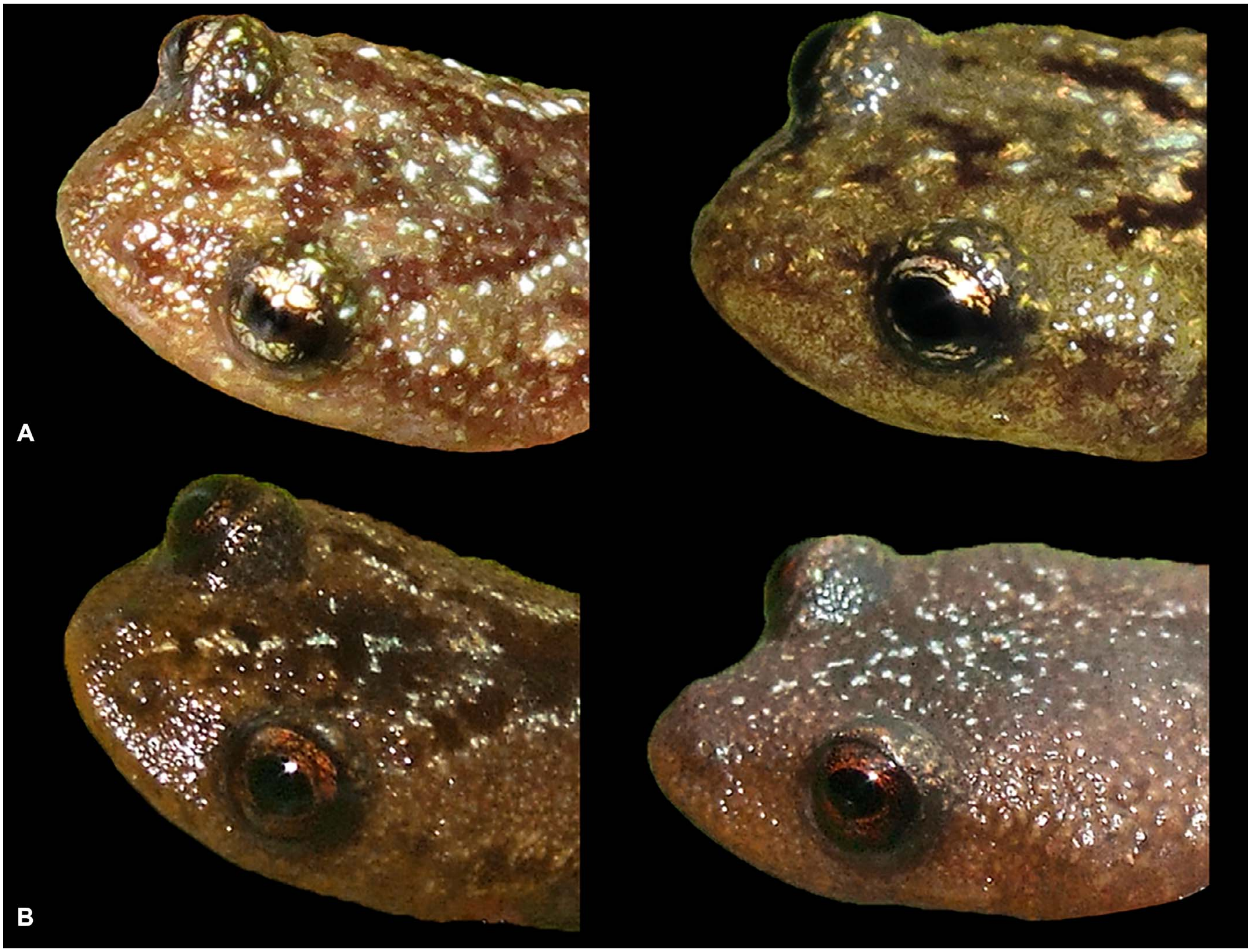

FIG. 16.—Diagnostic character states of iris coloration in life in *Crossodactylodes*. (A) Two specimens of *C. izecksohni*, showing a yellowish iris with dark brown fine reticulations, interrupted by a brown horizontal bar at the pupil level; (B) *C. septentrionalis*, showing a reddish iris with dark brown fine reticulations. The state for this character is unknown for *C. pintoi*. For the states observed in *C. bokermanni* and *C. itambe* refer to Fig. 15. A color version of this figure is available online.

Peixoto 2004a; Teixeira et al. 2013). In fact, *C. bokermanni* is known to occur between 800–1477 m elevations. Haddad et al. (2016b) stated that the species occurs in the Parque Estadual Mata das Flores, municipality of Castelo in the state of Espírito Santo, but we could not find voucher specimens from this locality in taxonomic collections.

Conservation.—According to the IUCN Red List, *Crossodactylodes bokermanni* has a decreasing population trend and is listed as Near Threatened (close to qualifying as Vulnerable) due to extent of occurrence <5000 km^2 and the probable declining on the extent and quality of habitat (Silvano and Peixoto 2004a). However, due to the extent of occurrence considered by the authors the species should almost qualify as Endangered, not Vulnerable (see IUCN 2019). In the Brazilian Red List, the species was also listed as Near Threatened, but close to qualifying as Endangered (Haddad et al. 2016b). According to these authors, there is no evidence that the species was more abundant in the past. Considering the six records currently known for *C. bokermanni*, our analysis shows an extent of occurrence of 765 km^2, with elevation ranging from 218–1718 m. Considering only areas above 700 m (see Materials and Methods), the extent of occurrence has 700 km^2, of which 174 km^2 are covered by Atlantic Forest remnants and 8 km^2 are inside protected areas.

Crossodactylodes bokermanni occurs at two strictly protected areas (IUCN category II; Dudley 2008): Reserva Biológica Augusto Ruschi (35.62 km^2) and Parque Estadual do Forno Grande (9.13 km^2). In addition, the species occurs at the Estação Biológica de Santa Lúcia (4.4 km^2). We point out that the main threat to the species is habitat loss in the private properties around the protected areas due to replacement of the forest by monocultures for wood production (*Pinus* and *Eucalyptus*), coffee plantations, and human settlements (Sabagh et al. 2017; Ferreira et al. 2019b). In addition, illegal collection of bromeliads, livestock grazing, logging, tourism (Silvano and Peixoto 2004a; Stuart et al. 2008; Haddad et al. 2016b), and burning (Scardua 2000) might be reducing the breeding habitat of *C. bokermanni*. Thus, following the IUCN (2019) guidelines, the species can be categorized as Near Threatened (close to qualifying as Endangered) due to its limited extent of occurrence (<5000 km^2; Criterion B1), fragmented popula-

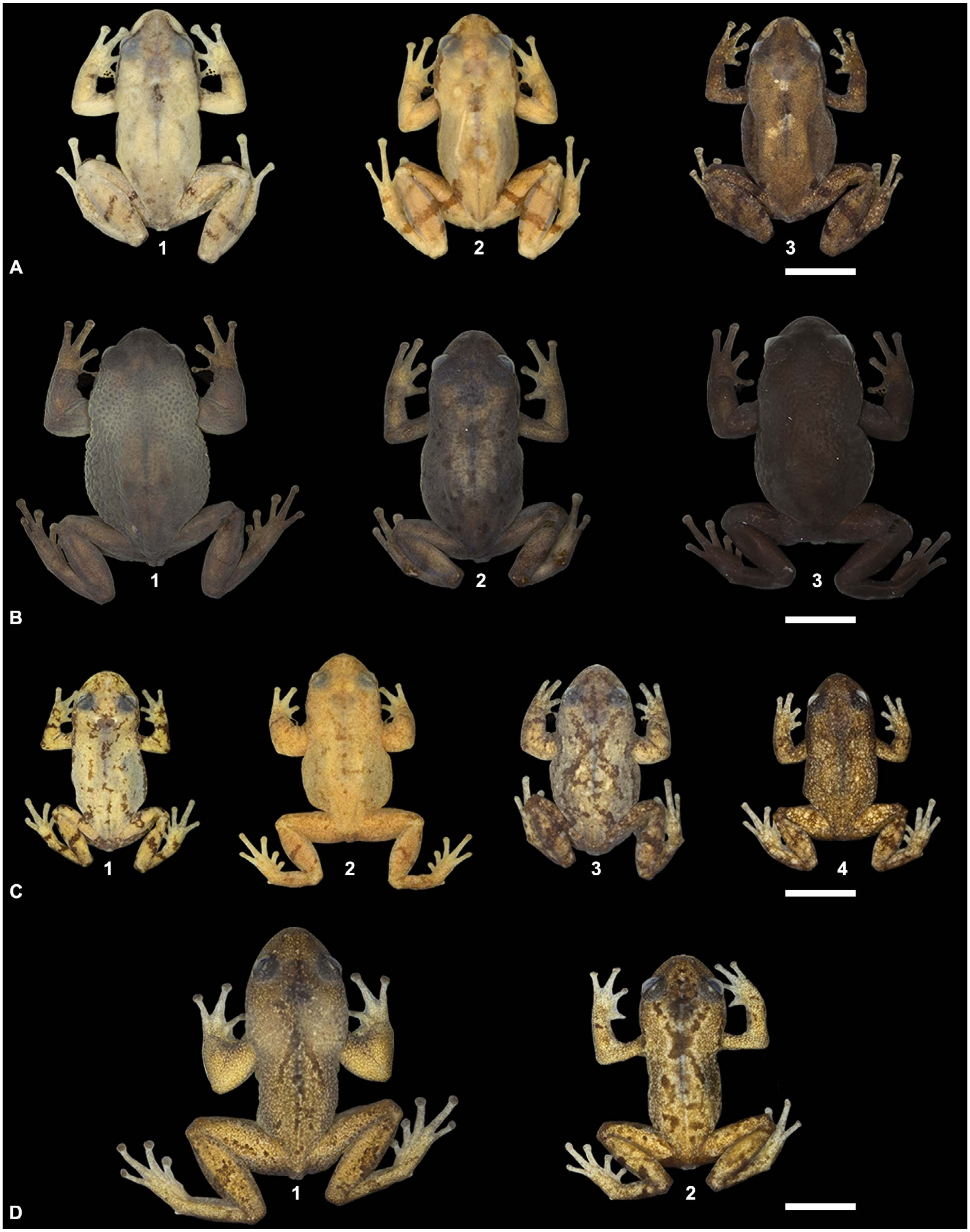

FIG. 17.—Dorsal background coloration in preservative in species of *Crossodactylodes*. (A) In *C. bokermanni*, the coloration varies from pale cream (1) UFMG 13767, pale yellow (2) ZUFRJ 1377, and brown (3) UFMG 14189. (B) In *C. itambe*, can be dark gray (1–2) UFMG 13377, and UFMG 13383, respectively, or brownish black (3) UFMG 11247. (C) In *C. izecksohni*, varies from pale cream (1) UFMG 13749, pale yellow (2) ZUFRJ 1935, and light brown (3–4) UFMG 14175, and UFMG 14216, respectively. (D) In *C. septentrionalis*, can be light brown (1) MZUESC 14363, and cream (2) MZUESC 14364. Note the difference comparing *C. itambe* with the other species. This character is not considered for *C. pintoi*, because all known specimens are faded. Scale bars = 5 mm. A color version of this figure is available online.

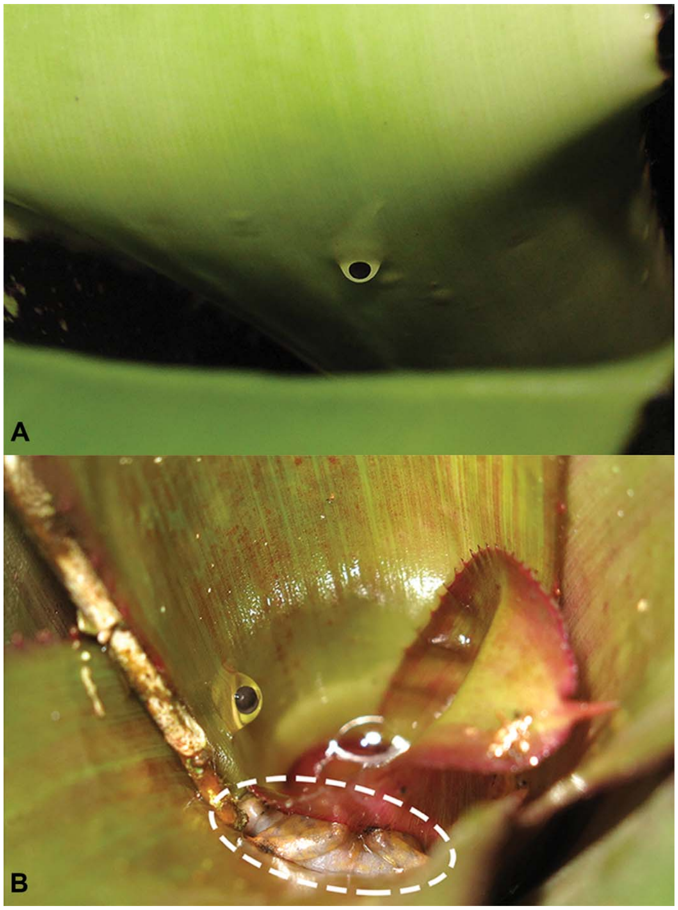

Fig. 18.—A single egg of (A) *C. bokermanni* attached to the abaxial surface of a *Billbergia* sp. from the Parque Estadual do Forno Grande, municipality of Castelo, Espírito Santo State, and of (B) *C. izecksohni* attached to the adaxial surface of a *Aechmea capixabae*, from Alto Santo Antônio, municipality of Santa Teresa, Espírito Santo State. Note the presence of a male (white ellipse), which was sitting alongside the egg, but dove quickly while being photographed. A color version of this figure is available online.

tions (Subcriterion a), and decline on the quality of habitat outside and around protected areas (approaching Subcriterion b[iii]).

Advertisement call.—Unknown.

Tadpole.—Unknown. The tadpole described by Peixoto (1981) was wrongly attributed to *Crossodactylodes pintoi* (Peixoto 1983) and might belong to either or both *C. bokermanni* or *C. izecksohni*.

Natural history.—*Crossodactylodes bokermanni* was found throughout the year inside bromeliads in the montane and submontane ombrophilous rain forest at the northern portion of the Mantiqueira Mountain Range (sensu Gontijo-Pascutti et al. 2012), in the Atlantic Forest domain. In the municipality of Santa Teresa, *C. bokermanni* was recorded in epiphytic (i.e., from 33 cm to 12 m from the ground) and terrestrial bromeliads of the following species: *Billbergia* sp., *Edmundoa lindenii*, *Neoregelia guttata*, *N. macrosepala*, *N. pauciflora*, and *Vriesea bituminosa*. The species was mostly found using large epiphytic bromeliads with many axils (e.g., *V. bituminosa*). In the municipality of Castelo, *C. bokermanni* was recorded in terrestrial and epiphytic bromeliads (i.e., up to 4 m from the ground) exclusively of the genus *Billbergia* (a small-sized bromeliad with few axils), despite the occurrence of several other species of bromeliads in the visited areas.

Individuals of *Crossodactylodes bokermanni* were mostly found partially submerged inside the water accumulated in bromeliads but were also found fully submerged or on the leaf out of the water. Most individuals were found alone or in pairs in the bromeliads. In one occasion, a male was found with two females in a *Billbergia* spp. cluster. The field observations indicate that individuals of *C. bokermanni* are found much more rarely and sparsely than are individuals of *C. izecksohni* and *C. itambe*. In the municipality of Santa Teresa, *C. bokermanni* occurs in sympatry with *C. izecksohni*, but they were not found in syntopy. Females lay single large eggs, positioned isolated from other eggs. Eggs are uniformly dark pigmented, submerged or above the water surface, attached to bromeliad leaves (Fig. 18A).

Remarks.—Peixoto (1983) stated that males of *Crossodactylodes bokermanni* have a less modified thumb, compared to males of *C. pintoi*, without specifying in which aspect. Possibly, Peixoto (1983) referred to a higher enlargement of the thumb and a higher number and degree of aggregation of spines on nuptial pads of *C. pintoi*. Our examination indicates that this is valid considering most of the individuals of both species. However, a few males of *C. bokermanni* show a similar thumb to that observed in males of *C. pintoi* and thus this character is not diagnostic between these species. Peixoto (1983) considered the iris in life of *C. bokermanni* black with intense, copper-colored dots while Teixeira et al. (2013) considered that the iris is brown. Our examination of specimens in life indicates that the iris coloration varies from coppery to reddish, with dark brown fine reticulations (Fig. 15A).

Crossodactylodes izecksohni Peixoto
Figs. 9C, 10G–I

Crossodactylodes izecksohni Peixoto 1983 “1982”: Peixoto: 1983:621–622, 625–626. Holotype male (EI 7192, examined in this study) from Alto Santo Antônio, municipality of Santa Teresa, state of Espírito Santo, southeastern Brazil, about 19°54′40.13″S, 40°35′29.37″W, 832 m, collected by O.L. Peixoto and colleagues on 22 December 1980 (O.L. Peixoto, personal communication).

Referred specimens.—We examined 45 paratopotypes of *Crossodactylodes izecksohni* including 18 males (EI 7193, 7196, 7198, 7200, 7206–7207, 7209, 7213, 7217, 7220; MZUSP 58080, 58082, 58084, 58086; USNM 221878–221880, 221884) and 27 females (EI 7194–7195, 7197, 7199, 7201–7205, 7208, 7210–7212, 7214–7216, 7218–7219, 7221–7222; MNRJ 4167; MZUSP 58081, 58083, 58085; USNM 221881–221883). To this species we refer 10 additional topotypes including six males (UFMG 397, 13747; ZUFRJ 361, 1400, 1932, 1935) and four females (UFMG 399; ZUFRJ 365, 1392, 1401); 12 males (UFMG 14174–14175, 14177–14181, 14215, 14219–14220, 14222–14223) and 11 females (UFMG 14176, 14182–14186, 14214, 14216–14217, 14221, 14224) from another locality in Alto Santo Antônio, municipality of Santa Teresa, state of Espírito Santo, southeastern Brazil, 19°51′53.28″S, 40°34′39.68″W, 933 m; seven males (MBML 3835–3836, 3977–3979; UFMG 13753, 14030) and four females (MBML 3834; UFMG

13748–13749, 14029) from hill in front of Escola Superior São Francisco de Assis, municipality of Santa Teresa, state of Espírito Santo, southeastern Brazil, 19°56′01.02″S, 40°35′21.68″W, 770 m; two males (UFMG 14222–14223) and one female (UFMG 14224) from the vicinity of Reserva Biológica Augusto Ruschi, municipality of Santa Teresa, state of Espírito Santo, southeastern Brazil, 19°54′35,97″S, 40°32′9,89″W, 888 m; six males (MBML 3958–3959, 4605, 6784; UFMG 13760, 13791) and five females (MBML 3956–3957; UFMG 13757, 13759, 13793) from Estação Biológica de Santa Lúcia, municipality of Santa Teresa, state of Espírito Santo, southeastern Brazil, 19°57′45.76″S, 40°31′55.66″W, 915 m; and one female (MBML 768) from Nova Lombardia, municipality of Santa Teresa, state of Espírito Santo, southeastern Brazil (not georeferenced).

Diagnosis.—*Crossodactylodes izecksohni* is diagnosable from all known congeners by the following combination of characters: (1) thumbs in adult males broadly widened; (2) SVL 10.8–13.9 mm (females) and 10.8–15.0 mm (males); (3) in life, iris yellowish with dark brown fine reticulations, interrupted by a brown horizontal bar at the pupil level; (4) cloacal flap undivided or with a small distal indentation; (5) absence of vomerine odontophores; (6) snout not flattened in lateral view; (7) zygomatic process of squamosal bone short, not passing the anterior margin of the optic foramen; (8) males lacking vocal slits; (9) absence of dorsolateral fold; (10) discs of fingers II–IV slightly expanded; (11) skin on male dorsum coarsely granular; (12) disc of Finger I rounded; (13) medial region of the upper lip not anteriorly projected; (14) in preservative, dorsal background coloration varying from pale cream to pale yellow, or light brown.

Comparisons.—*Crossodactylodes izecksohni* is distinguished from its congeners (characters in parentheses) by having thumbs in adult males broadly widened; Fig. 12C (weakly widened in *C. pintoi* [Fig. 12D], *C. bokermanni* [Fig. 12A], and *C. itambe* [Fig. 12B]); iris in life yellowish with dark brown fine reticulations, interrupted by a brown horizontal bar at the pupil level; Fig. 16A (coppery to reddish with dark brown fine reticulations in *C. bokermanni* [Fig. 15A], reddish with dark brown fine reticulations in *C. septentrionalis* [Fig. 16B], uniformly black or brownish black in *C. itambe* [Fig. 15B]); males and females with smaller size, SVL 10.8–13.9 mm in females and 10.8–15.0 mm in males (female SVL = 15.9 mm, males SVL = 16.2–18.0 mm in *C. pintoi*; females SVL = 16.1–16.5 mm, male SVL = 18.6 mm in *C. septentrionalis*; Table 2); females with a smaller size, SVL 10.8–13.9 mm (females SVL = 15.2–18.0 mm in *C. itambe*; Table 2); cloacal flap undivided or with a small indentation; Fig. 13A (bilobed in *C. pintoi* and *C. septentrionalis*; Fig. 13B); absence of vomerine odontophores; Fig. 11B (presence in *C. bokermanni* and *C. septentrionalis*; Fig. 11A); snout not flattened in lateral view; Fig. 10G (flattened in *C. bokermanni* [Fig. 10D] and *C. septentrionalis* [Fig. 11C]); zygomatic process of squamosal bone short, not passing the anterior margin of the optic foramen (long, passing the anterior margin of the optic foramen in *C. septentrionalis* and *C. itambe*; see Teixeira et al. 2013). Additionally, *C. izecksohni* can be distinguished from *C. bokermanni* by the absence of vocal slits in males (presence); absence of dorsolateral fold; Fig. 14B (presence; Fig. 14A); discs of fingers II–IV slightly expanded; Fig. 12C (broadly expanded; Fig. 12A); skin on male dorsum coarsely granular (shagreen). From *C. septentrionalis* by having disc of Finger I rounded; Fig. 12C (acute; Fig. 12E). It differs from *C. itambe* by the absence of anterior projection in the medial region of the upper lip; Fig. 13C (presence; Figs. 11D, 13D); and dorsal background coloration in preservative pale cream, pale yellow, or light brown; Fig. 17C (dark gray or brownish black; Fig. 17B).

Redescription of the holotype.—Adult male, SVL 13.4 mm; body slightly robust, dorsoventrally flattened; head wider than long (head width/head length = 1.09); head width 0.43 SVL; head length = 0.40 SVL; snout not flattened, rounded in dorsal and lateral views; eye–nostril distance slightly longer than eye diameter (eye–nostril distance/eye diameter = 1.05); canthus rostralis slightly curved in dorsal view and rounded in cross-section; loreal region slightly concave; nostrils protuberant, elliptical, dorsolaterally directed, opening in the apices of small dermal elevations; interorbital area flat, more than twice as long as eye diameter (interorbital distance/eye diameter = 2.48). Eyes medium-sized and protuberant (eye diameter/head length = 0.23; eye diameter/head width = 0.21), laterally oriented; upper eyelid margin granular, with a nearly elliptic tubercle in its medial region. Tympanic membrane and annulus absent. A poorly developed dermal fold from posterior edge of eye curving downward to arm insertion. Dorsolateral fold absent.

Choanae small, nearly rounded, spaced 1.4 mm from each other. Vomerine odontophores absent. Tongue ovoid, not notched, free behind for about one third of its length. Vocal slits absent; vocal sac externally indistinct. Single, small, tooth-like process present on front of lower jaw with a socket between premaxillae.

Forelimb robust, hypertrophied, lacking fold or fringe; forearm less robust than arm (forearm width/arm width = 0.82); fingers medium-sized; relative length of fingers I < II ≈ IV < III; discs of fingers II–IV slightly expanded, rounded; disc of Finger I rounded, less expanded than the others; fingers II–IV slender; Finger I broadly widened, with nuptial pad formed by strongly aggregate keratinized spines covering most of its lateral margin and dorsal surface (nine spines on left and 10 on right thumbs); subarticular tubercles small, flat, and rounded in ventral view; supernumerary tubercles slightly distinct; inner metacarpal tubercle flat, elliptical; outer metacarpal tubercle large, flat, and nearly round in ventral view; vestigial digital webbing.

Hindlimb medium-sized and moderately robust (thigh length/SVL = 0.39; tibia length/SVL = 0.43); tarsal fold absent; toes long, slender, with slightly expanded and nearly rounded discs, slightly larger than finger discs (fourth toe disc diameter/third finger disc diameter = 1.07); relative length of toes I < II < V < III < IV; subarticular tubercles small, flat, and rounded in ventral view; supernumerary tubercles indistinct; inner metatarsal tubercle large, flat, and elliptical in ventral view; outer metatarsal tubercle small, nearly rounded in ventral view, slightly conical in profile; digital webbing absent.

Skin on dorsal surfaces of head, body and arm, flanks, belly, chest, and ventral surface of arm coarsely granular; skin on dorsal and ventral surfaces of hindlimbs and on throat shagreen. Cloacal opening directed posteriorly, at upper level of thighs, covered by a cloacal flap with a small distal indentation.

Measurements of the holotype (in mm).—SVL 13.4; head length 5.3; head width 5.8; eye diameter 1.2; eye–nostril distance 1.3; nostril–snout distance 0.8; internarial distance 1.2; interorbital distance 3.1; arm length 4.3; forearm length 2.7; hand length 3.4; third finger disk diameter 0.4; thigh length 5.3; tibia length 5.7; tarsal length 3.4; foot length 5.2; fourth toe disk diameter 0.5; arm width 2.0; forearm width 1.6.

Coloration of the holotype in life.—Based on description and photographs provided by Peixoto (1983), we could infer that the holotype had cream dorsal surfaces of head, body, and limbs, with scattered brown flecks and blotches. An X-shaped brown blotch extends from the scapular region to the middle third of body; an oblique band of the same color, connected to this blotch, extends into the lumbar region. Flank with a brown band extending from behind the eye to the arm insertion. A brown transverse bar in the wrist; nuptial pads black colored. Hindlimbs with brown marbled blotches and interrupted bands. Venter lighter than the dorsum and with few brown flecks and blotches.

Coloration of the holotype in preservative.—The color is faded, turning into pale tones. The cream dorsal surfaces of head, body, and limbs become pale yellow. The brown blotches, flecks, and bands become pale brown and less evident. Venter continues lighter than dorsum. The ventral surfaces of hand and foot are translucent, showing superficial musculature. Eyelid tubercles, carpal, and tarsal tubercles are whitish.

Variation.—Snout in lateral view varies from rounded (~67%) to slightly sloping (~33%). The cloacal flap has a small distal indentation (~69%) or is undivided (~31%). The tubercle on medial region of upper eyelid margin is usually present (~70%) but can be absent (~30%). The shape of this tubercle is usually elliptical (~73%) but can be elongated (~27%). Few specimens have 2–4 elliptical tubercles arranged in a line (~11%) or scattered (~4%). Males are distinguished from females by the presence of nuptial pads, hypertrophy of arms and forearms (males arm width/arm length = 0.28–0.54, mean = 0.41; females arm width/arm length = 0.21–0.28, mean = 0.25; and males forearm width/forearm length = 0.46–0.80, mean = 0.61; females forearm width/forearm length = 0.29–0.45, mean = 0.40), and a rougher dorsal skin. In addition, males have wider thumbs than do females. This is possibly related to the presence of a well-developed prepolex in males (see Gomes 1988). The spines on nuptial pads vary in number (from two to 14), size, and degree of aggregation. The number of spines can vary between the right and left thumbs of a same specimen. Males with larger SVL and pronounced hypertrophy of forelimbs have a higher number and aggregation of spines, wider thumbs, and rougher skin.

The coloration pattern in life shows high variation. The dorsal background coloration can be pale pink, pale cream, beige, pale lilac, light brown, brownish gray, pale yellow, and brownish yellow (Fig. S3). Froglets are usually dark brown with numerous small white, bluish, and/or yellowish spots. The pattern of blotches, flecks, bands, and bars is also highly variable. Most specimens have a dorsal X-shaped blotch that can be strongly or weakly marked, continuous, or interrupted, but this blotch can be absent. A few specimens have a black lateral band from posterior corner of the eye to the posterior third of body, but this band is usually incomplete or fragmented. A few specimens have transverse bars on hindlimbs that can be strongly or weakly marked (Fig. S3). In preservative, the dorsal background coloration varies from pale cream, pale yellow, until light brown, and the pattern of blotches, flecks, bands, and bars is also highly variable (Fig. 17C).

Distribution.—*Crossodactylodes izecksohni* is known only from the municipality of Santa Teresa in the state of Espírito Santo, from seven sites: (1) Alto Santo Antônio (type locality), about 19°54′40.10″S, 40°35′29.37″W, 843 m (O.L. Peixoto, personal communication); (2) another locality in Alto Santo Antônio 19°51′53.28″S, 40°34′39.68″W, 933 m; (3) hill in front of the Escola Superior São Francisco de Assis (ESFA), 19°56′1.02″S, 40°35′21.68″W, 770 m; (4) Penha district, 19°56′17.45″S, 40°32′56.96″W, 867 m; (5) vicinity of Reserva Biológica Augusto Ruschi, 19°54′35, 97″S, 40°32′9, 89″W, 888 m; (6) Estação Biológica de Santa Lúcia, 19°57′45.76″S, 40°31′55.66″W, 915 m; and (7) Lombardia (not georeferenced data).

Peixoto (1983) used geographic coordinates from the city of Santa Teresa. Other studies used these approximate coordinates, which misleads that *Crossodactylodes izecksohni* occurs between 650–675 m elevation. (Silvano and Peixoto 2004b; Teixeira et al. 2013). In fact, *C. izecksohni* is only known from elevations between 770–933 m.

Conservation.—*Crossodactylodes izecksohni* is listed as Near Threatened (close to qualifying as Vulnerable) by the IUCN Red List due to extent of occurrence <5000 km^2 and the probable declining on the extent and quality of habitat (Silvano and Peixoto 2004b). However, due to the extent of occurrence considered by the authors, the species should almost qualify as Endangered, not Vulnerable (see IUCN 2019). It is listed as Data Deficient by the Brazilian Red List (Haddad et al. 2016c). These authors erroneously stated that the species has not been found in the last 30 yr, sampling effort has not been enough, and that the extent of occurrence is 435.73 km^2. Actually, the species was recorded in 1997, 2005, 2006, 2012, and 2013 (vouchered in MBML), and the sampling effort has been extensively conducted since 2012. Our analysis indicates an extent of occurrence of 39 km^2, of which 23 km^2 are covered by Atlantic Forest remnants and 12 km^2 are inside protected areas with elevations ranging from 689–933 m.

Crossodactylodes izecksohni occurs inside and in vicinities of Reserva Biológica Augusto Ruschi (35.62 km^2), a strictly protected area (IUCN Category II; Dudley 2008), and in the Estação Biológica de Santa Lúcia (4.4 km^2). These areas possibly mitigate negative impacts on lineages A and B, respectively. We point out that the main threat to *C. izecksohni* is habitat loss in the private properties around the protected areas due to wood plantations (*Pinus* and *Eucalyptus*), coffee plantations, and human settlements. In addition, illegal collection of bromeliads for gardening might be reducing the breeding habitat of *C. izecksohni* (Silvano and Peixoto 2004b; Stuart et al. 2008; Haddad et al. 2016c; Sabagh et al. 2017; Ferreira et al. 2019b). Despite these threats, almost 31% of the extent of occurrence of *C. izecksohni* is under protected areas. Therefore, following the IUCN (2019) guidelines, the species can be categorized as Near Threatened (close to qualifying as Critically Endangered) due to its limited extent of occurrence (<100 km^2; Criterion B1), fragmented populations (Subcriterion a), and decline on the quality of habitat outside and around protected areas (approaching Subcriterion b[iii]).

Advertisement call.—*Crossodactylodes izecksohni* call has not been described. Ferreira et al. (2019a) video recorded males calling but the infrared video camera did not record high standard calls.

Tadpole.—Unknown. The tadpole described by Peixoto (1981) was wrongly attributed to *Crossodactylodes pintoi* (Peixoto 1983) and might belong to either or both *C. izecksohni* or *C. bokermanni*.

Natural history.—The natural history of *Crossodactylodes izecksohni* was described in detail by Ferreira et al. (2019a). A photograph of a single egg of *C. izecksohni* is provided (Fig. 18B) for comparison with the egg of *C. bokermanni*.

Remarks.—Teixeira et al. (2013) stated that the iris of *Crossodactylodes izecksohni* is brown. However, our examination indicates that the iris coloration is yellowish with dark brown fine reticulations, interrupted by a brown horizontal bar at the pupil level (Fig. 16A).

Crossodactylodes septentrionalis Teixeira, Recoder, Amaro, Damasceno, Cassimiro, and Rodrigues

Crossodactylodes septentrionalis Teixeira, Recoder, Amaro, Damasceno, Cassimiro, and Rodrigues 2013: Teixeira et al. 2013:461–469. Holotype female (MZUSP 150209, examined in this study) from Peito de Moça, Parque Nacional da Serra das Lontras, municipality of Arataca, state of Bahia, northeastern Brazil, 15°9′47.68″S, 39°20′34.03″W, 931 m, collected by M. Teixeira, Jr., R.S, Recoder, R.C Amaro, R.P. Damasceno, J. Cassimiro, and M.T. Rodrigues on 6 March 2009.

Referred specimens.—We examined two topotypes of *Crossodactylodes septentrionalis*, one male (MZUESC 14363) and one female (MZUESC 14364).

Diagnosis.—*Crossodactylodes septentrionalis* is diagnosable from all congeners by the following combination of characters: (1) disc of Finger I acute (no apparent disc); (2) zygomatic process of squamosal bone long, passing the anterior margin of the optic foramen; (3) thumbs in adult males broadly widened; (4) presence of vomerine odontophores; (5) snout flattened in lateral view; (6) cloacal flap bilobed; (7) in life, iris reddish with dark brown fine reticulations; (8) males lacking vocal slits; (9) absence of dorsolateral fold; (10) discs of fingers II–IV slightly expanded; (11) absence of a black canthal stripe; (12) absence of a black lateral band from posterior corner of the eye to the posterior third of body; (13) hindlimbs lacking transverse bars; (14) skin on male dorsum coarsely granular; (15) SVL 16.1–16.5 mm (females) and 18.6 mm (male); (16) medial region of the upper lip not anteriorly projected; (17) in preservative, dorsal background coloration varying from light brown to cream.

Comparisons.—*Crossodactylodes septentrionalis* is distinguished from its congeners (characters in parentheses) by having disc of Finger I acute; Fig. 12E (rounded in *C. pintoi*, *C. bokermanni*, *C. izecksohni*, and *C. itambe*; Figs. 12A–D); zygomatic process of squamosal bone long, passing the anterior margin of the optic foramen (short, not passing the anterior margin of the optic foramen in *C. pintoi*, *C. bokermanni*, and *C. izecksohni*; see Teixeira et al. 2013); thumbs in adult males broadly widened; Fig. 12E (weakly widened in *C. pintoi*, Fig. 12D; *C. bokermanni*, Fig. 12A; and *C. itambe*, Fig. 12B); presence of vomerine odontophores; Fig. 11A (absence in *C. pintoi*, *C. izecksohni*, and *C. itambe*; Fig. 11B); snout flattened in lateral view; Fig. 11C (not flattened in *C. pintoi*, Fig. 10A; *C. izecksohni*, Fig. 10G; and *C. itambe*, Fig. 11D); cloacal flap bilobed; Fig. 13B (undivided or with a small indentation in *C. izecksohni* and *C. itambe*; Fig. 13A); iris in life reddish with dark brown fine reticulations; Fig. 16B (yellowish with dark brown fine reticulations, interrupted by a brown horizontal bar at the pupil level in *C. izecksohni*, Fig. 16A; uniformly black or brownish black in *C. itambe*, Fig. 15B). Additionally, *C. septentrionalis* can be distinguished from *C. bokermanni* by the absence of vocal slits in males (presence); discs of fingers II–IV slightly expanded; Fig. 12E (broadly expanded; Fig. 12A); absence of dorsolateral fold; Fig. 14B (presence; Fig. 14A); absence of a black canthal stripe; Fig. 14B (presence; Fig. 14A); absence of a black lateral band from posterior corner of the eye to the posterior third of body; Fig. 14B (presence; Fig. 14A); absence of black transverse bars on hindlimbs; Fig. 14B (presence; Fig. 14A); and skin on male dorsum coarsely granular (shagreen). From *C. izecksohni* by its larger size, with SVL 16.1–16.5 mm in females and 18.6 mm in male (females SVL = 10.8–13.9 mm; males SVL = 10.8–15.0 mm; Table 2). It differs from *C. itambe* by the absence of anterior projection in the medial region of the upper lip; Fig. 13C (presence; Figs. 11D, 13D); and dorsal background coloration in preservative light brown or cream; Fig. 17D (dark gray or brownish black; Fig. 17B).

Description of the holotype.—See Teixeira et al. (2013).

Variation.—The separation between the two lobes of cloacal flap can be strongly (MZUESC 14363; MZUSP 150209) or moderately developed (MZUESC 14364). A tubercle on medial region of upper eyelid margin can be present (MZUESC 14363–14364) or absent (MZUSP 150209). The shape of this tubercle can be elliptical (MZUESC 14364) or elongated (MZUESC 14363). The only known male (MZUESC 14363) is distinguished from females by the presence of nuptial pads formed by regularly spaced keratinized spines covering most of the lateral margin and dorsal surface of thumbs (nine spines on each thumb) and by hypertrophy of arms and forearms (male arm width/arm length = 0.39; females arm width/arm length = 0.23–0.24; and male forearm width/forearm length = 0.66; females forearm width/forearm length = 0.34–0.35). In addition, the male has rougher dorsal skin and wider thumbs than a female.

Distribution.—*Crossodactylodes septentrionalis* is known only from the type locality at Peito de Moça in the Parque Nacional da Serra das Lontras, 15°09′47.68″S, 39°20′34.03″W, 931 m, municipality of Arataca, in the state of Bahia, northeastern Brazil (Fig. 8).

Conservation.—*Crossodactylodes septentrionalis* has not been assessed by the IUCN and Brazilian red lists. So far, only three adult specimens have been recorded from Peito de Moça summit in the Parque Nacional da Serra das Lontras, a strictly protected area of 113.36 km^2 (IUCN category II; Dudley 2008). Another eight mountainous sites (above 700 m) in the Atlantic Forest of the state of Bahia were surveyed by IRD, sampling at least 50 h/person in each area (Fig. S4). In one of these sites (Reserva Particular do Patrimônio Natural Serra Bonita), a sampling effort of ∼16 mo was performed (see Dias et al. 2014). Bromeliads were inspected in all sites, but no other specimen of *C. septentrionalis* was found. Thus, the known area of occupancy of the species is ∼4 km^2.

The type locality of *Crossodactylodes septentrionalis* is quite distinct from the other visited sites and also from the surrounding forest areas in the Parque Nacional da Serra das Lontras. At the type locality, the vegetation develops over a rocky formation composed predominantly of low-height trees with a high abundance of epiphytes (lichens, mosses, and bromeliads). Although the species occurs in a strictly protected area, the available data on geographic distribution, ecological requirements, and possible threats are insufficient to classify the taxon into a category. Thus, *C. septentrionalis* can be categorized as Data Deficient.

Advertisement call.—Unknown.

Tadpole.—Unknown.

Natural history.—All known specimens of *Crossodactylodes septentrionalis* were found in the bromeliad *Vriesea dictyographa*, a species recorded from few highland areas, being endemic to the Atlantic Forest of Bahia State (Martinelli et al. 2008). A female (MZUESC 14364), a male (MZUESC 14363), and a tadpole of *C. septentrionalis* were found together in an ∼1-m diameter bromeliad partially exposed to the sun at ∼1 m above the ground. Four froglets were found together in a bromeliad at 1.5 m above the ground and 15–20 m apart from the bromeliad where the adults were found. In a neighboring bromeliad, two tadpoles were found at ∼2.5 m above the ground. All the tadpoles were lost in the field. Apparently, *C. septentrionalis* has low abundance or prefers high canopy bromeliads.

Remarks.—*Crossodactylodes septentrionalis* has an iris in vivid red with dark brown fine reticulations (instead of only vivid red as in Teixeira et al. 2013). Some characters used by Teixeira et al. (2013) to distinguish *C. septentrionalis* from other species show polymorphisms. The SVL of *C. septentrionalis* is only larger than *C. izecksohni* (instead of *C. bokermanni* and *C. izecksohni*). The absence of well-defined bars pattern on hindlimb distinguish *C. septentrionalis* only from *C. bokermanni* (instead of *C. bokermanni* and *C. izecksohni*) because this character is polymorphic in *C. izecksohni*.

Crossodactylodes itambe Barata, Santos, Leite, and Garcia

Crossodactylodes itambe Barata, Santos, Leite, and Garcia 2013: Barata et al. 2013:553–559. Holotype male (UFMG 11239, examined in this study) from Parque Estadual do Pico do Itambé, municipality of Santo Antônio do Itambé, state of Minas Gerais, southeastern Brazil, 18°23′53.1″S, 43°20′39.6″W, 1921 m, collected by I.M. Barata, C.M. Correia, and R. Ancântara on 13 January 2010.

Referred specimens.—We examined 24 paratopotypes of *Crossodactylodes itambe* including 10 males (UFMG 11241–11242, 11244, 11247, 11249, 13375, 13377, 13379, 13382, 13384) and 14 females (UFMG 11236–11238, 11240, 11243, 11245–11246, 13376, 13378, 13380–13381, 13383, 13385, 13387). To this species we refer 10 additional topotypes including six males (UFMG 14031–14036) and four females (UFMG 14037–14040).

Diagnosis.—*Crossodactylodes itambe* is diagnosable from all known congeners by the following combination of characters: (1) medial region of the upper lip anteriorly projected; (2) in preservative, dorsal background coloration varying from dark gray to brownish black; (3) zygomatic process of squamosal bone long, passing the anterior margin of the optic foramen; (4) in life, iris uniformly black or brownish black; (5) cloacal flap undivided or with a small distal indentation; (6) absence of vomerine odontophores; (7) snout not flattened in lateral view; (8) thumbs in adult males weakly widened; (9) males lacking vocal slits; (10) absence of dorsolateral fold; (11) discs of fingers II–IV slightly expanded; (12) absence of a black canthal stripe; (13) absence of a black lateral band from posterior corner of the eye to the posterior third of body; (14) hindlimbs lacking transverse bars; (15) skin on male dorsum coarsely granular; (16) SVL 15.2–18.0 mm (females) and 14.0–17.9 mm (males); (17) disc of Finger I rounded.

Comparisons.—*Crossodactylodes itambe* is distinguished from its congeners (characters in parentheses) by having medial region of the upper lip anteriorly projected; Figs. 11D, 13D (not anteriorly projected in *C. pintoi*, *C. bokermanni*, *C. izecksohni*, and *C. septentrionalis*; Fig. 13C); dorsal background coloration in preservative dark gray or brownish black; Fig. 17B (pale cream, pale yellow, or brown in *C. bokermanni*, Fig. 17A; pale cream, pale yellow, or light brown in *C. izecksohni*, Fig. 17C; light brown or cream in *C. septentrionalis*, Fig. 17D); iris in life uniformly black or brownish black; Fig. 15B (coppery to reddish with dark brown fine reticulations in *C. bokermanni*, Fig. 15A; yellowish with dark brown fine reticulations, interrupted by a brown horizontal bar at the pupil level in *C. izecksohni*, Fig. 16A; reddish with dark brown fine reticulations in *C. septentrionalis*, Fig. 16B); zygomatic process of squamosal bone long, passing the anterior margin of the optic foramen (short, not passing the anterior margin of the optic foramen in *C. pintoi*, *C. bokermanni*, and *C. izecksohni*; see Teixeira et al. 2013); cloacal flap undivided or with a small distal indentation, Fig. 13A (bilobed in *C. pintoi* and *C. septentrionalis*; Fig. 13B); thumbs in adult males weakly widened, Fig. 12B (broadly widened in *C. izecksohni*, Fig. 12C; and *C. septentrionalis*, Fig. 12E); absence of vomerine odontophores, Fig. 11B (presence in *C. bokermanni* and *C. septentrionalis*, Fig. 11A); snout not flattened in lateral view; Fig. 11D (flattened in *C. bokermanni*, Fig. 10D; and *C. septentrionalis*, Fig. 11C). Additionally, *C. itambe* can be distinguished from *C. bokermanni* by the absence of vocal slits in males (presence); discs of fingers II–IV slightly expanded; Fig. 12B (broadly expanded; Fig. 12A); absence of a dorsolateral fold; Fig. 14B (presence; Fig. 14A); absence of a black canthal stripe; Fig. 14B (presence; Fig. 14A); absence of a black lateral band from posterior corner of the eye to the posterior third of body; Fig. 14B (presence; Fig. 14A); absence of black transverse bars on hindlimbs; Fig. 14B (presence; Fig. 14A); skin on male dorsum coarsely granular (shagreen). From *C. izecksohni* by females with larger size, SVL 15.2–18.0 mm (females SVL = 10.8–13.9 mm; Table 2). It differs from *C. septentrionalis* by having disc of Finger I rounded; Fig. 12B (acute; Fig. 12E).

Description of the holotype.—See Barata et al. (2013).

Variation.—The cloacal flap is usually undivided (~71%) but can have a small distal indentation (~29%). A tubercle on medial region of upper eyelid margin can be absent (~60%) or present (~40%). When present, this tubercle can be elongated (~57%) or elliptical (~43%). Few specimens have 2–3 elliptical tubercles arranged in a line (~6%). For differences between males and females, and other variations, see Barata et al. (2013).

Distribution.—*Crossodactylodes itambe* is known only from its type locality at Itambé summit in the Parque Estadual do Pico do Itambé, 18°23′53.1″S, 43°20′39.6″W, 1921 m, municipality of Santo Antônio do Itambé, in the state of Minas Gerais, southeastern Brazil (Fig. 8).

Conservation.—*Crossodactylodes itambe* has not been assessed by the IUCN and is listed as Data Deficient in the Brazilian Red List (Haddad et al. 2016d). The Itambé summit (type locality) is a singular environment within the Espinhaço Range due to its high elevation, humid microclimate, and high abundance of bromeliads (Barata et al. 2013). The most similar nearby area is the Pico Dois Irmãos (18°12′27.84″S; 43°18′36.60″W, ~1800 m) in the Parque Estadual do Rio Preto, at the boundaries of the municipalities of São Gonçalo do Rio Preto and Felício dos Santos in the state of Minas Gerais. This site is ~20 km distant from the type locality and harbors the same species of bromeliad (*Vriesea medusa*) which *C. itambe* inhabits. This bromeliad is only known from these two localities (Versieux et al. 2010). Fieldwork was conducted by MTTS on March 2015 at the Pico Dois Irmãos, surveying bromeliads, and he did not find any individual of *C. itambe*. The same locality was visited by another researcher in 2015 and 2017, who also did not find any individual (I. Barata, personal communication).

Occasional fires could lead to continuous decline in the area, extent and/or quality of habitat of *Crossodactylodes itambe*, even the species occurring in a strictly protected area (Barata et al. 2013, 2018b). Indeed, in November 2015, a fire destroyed natural vegetation at the Itambé summit (S.J. Duarte, personal communication) and burned part of the reproductive habitat of *C. itambe* (i.e., clumps of bromeliads). The species is known only from a single location, thus having a very small extent of occurrence and area of occupancy (i.e., 4 km^2) in an environment which was and still could be threatened by fires. Therefore, following the IUCN (2019) guidelines, *C. itambe* can be listed as Critically Endangered under criteria B1ab(iii) and B2ab(iii), as previously suggested by Barata et al. (2018b).

Advertisement call.—Barata et al. (2018a) have reported that *Crossodactylodes itambe* exhibits calling activity but have not recorded the call.

Tadpole.—Tadpole was described by Santos et al. (2017).

Natural history.—See Barata et al. (2013), Santos et al. (2017), Barata et al. (2018a,b).

Remarks.—Some morphological characters used by Barata et al. (2013) to distinguish *Crossodactylodes itambe* from other species are misinterpreted or polymorphic. The absence of marks on the dorsum and limbs cannot be used to distinguish *C. itambe* from *C. izecksohni* because a few specimens of *C. izecksohni* have no marks. The absence of vocal sac cannot distinguish *C. itambe* from *C. pintoi* (see Remarks of *C. pintoi*).

KEY TO SPECIES OF *CROSSODACTYLODES*

1a. Males with vocal slits; fingers II–IV broadly expanded (Fig. 12A); presence of dorsolateral fold (Fig. 14A)....... .... *C. bokermanni*
1b. Males lacking vocal slits; fingers II–IV slightly expanded (Figs. 12B–E); absence of dorsolateral fold (Fig. 14B) 2
2a. Presence of vomerine odontophores (Fig. 11A); disc of Finger I acute (no apparent disc; Fig. 12E)...................... .... *C. septentrionalis*
2b. Absence of vomerine odontophores (Fig. 11B); disc of Finger I rounded (Figs. 12A–D).................................... 3
3a. Medial region of the upper lip anteriorly projected (Figs. 11D, 13D).. *C. itambe*
3b. Medial region of the upper lip not anteriorly projected (Fig. 13C) 4
4a. Thumbs in adult males broadly widened (Fig. 12C); cloacal flap undivided or with a small distal indentation (Fig. 13A).. *C. izecksohni*
4b. Thumbs in adult males weakly widened (Fig. 12D); cloacal flap bilobed (Fig. 13B) .... *C. pintoi*

DISCUSSION

We recovered *Crossodactylodes* as a monophyletic and unambiguously supported clade, in accordance with the two previous phylogenetic hypotheses (Fouquet et al. 2013; Teixeira et al. 2013). We also recovered a monophyletic Paratelmatobiinae, and the relationships among the four genera were consistent with the two analyses that included all of them (Fouquet et al. 2013; Faivovich et al. 2014). We found a well-supported position of *Rupirana* as the sister taxon of the remaining Paratelmatobiinae in the Bayesian analysis, with 100% posterior probability. Nevertheless, this relationship was poorly supported in the parsimony analysis, with a jackknife frequency <50% (Fig. 1; Fig. S1). These methods tend to differ considerably, with an underestimation of support values by jackknife and an overestimation by the Bayesian method (Simmons et al. 2004). Moreover, these support indices are not directly comparable (Simmons et al. 2004), especially in our analyses in which each index was based on a distinct method of phylogenetic reconstruction. The same phylogenetic placement for *Rupirana* was recovered with high support under other parsimony and Bayesian analyses (Fouquet et al. 2013; Faivovich et al. 2014). This may be a result of differences in taxon and character sampling, as these authors used few terminals of Paratelmatobiinae but a considerably larger outgroup sampling and a larger number of nDNA fragments.

Similar to other phylogenetic hypotheses, we recovered the subfamily Leptodactylinae as the sister taxon of Paratelmatobiinae (Fouquet et al. 2013, complete matrix approach; Faivovich et al. 2014). However, other analyses recovered Paratelmatobiinae as the sister taxon of Leiuperinae (Pyron and Wiens 2011) or as the sister taxon of Leiuperinae plus Leptodactylinae (Fouquet et al. 2013, super matrix approach; Pyron 2014), but with low support values. These studies employed a more comprehensive coverage of outgroups and a larger number of DNA fragments but used fewer sequences of Paratelmatobiinae and have more missing data per species on average. Moreover, Pyron and Wiens (2011) and Pyron (2014) employed the maximum likelihood method of phylogenetic reconstruction. All these methodological differences might explain the contrasting results.

Within *Crossodactylodes*, we recovered *C. bokermanni* as the sister taxon of the remaining species (Fig. 1), in accordance with Teixeira et al. (2013). This phylogenetic placement is consistent with the distinct morphology of *C. bokermanni* in comparison with congeners. Some of the morphological diagnostic characters of *C. bokermanni* seem to be plesiomorphic among Paratelmatobiinae (e.g., presence of dorsolateral fold, skin on male dorsum shagreen, and presence of vocal slits). Also, *C. bokermanni* seems to be ecologically distinct by having sparse distribution and low population abundance and by selecting epiphyte bromeliads in higher vertical strata. The higher expansion on finger II–IV discs found in the species (Fig. 12A) is likely an adaptation to arboreality.

Crossodactylodes pintoi was strongly supported as part of a clade which also includes *C. itambe*, *C. septentrionalis*, and *C. izecksohni* (Fig. S2) and shares three putative morphological synapomorphies with these species: absence of vocal slit, absence of dorsolateral fold, and coarsely granular skin texture of males (Appendices III, IV). However, the phylogenetic relationships within this clade were not fully resolved and should be further investigated, either by means of DNA sequences of *C. pintoi* from historical museum specimens (see Rowe et al. 2011) or by incorporating a more robust phenotypic dataset in phylogenetic reconstruction.

The subfamily Paratelmatobiinae is a morphologically diverse group of frogs, with remarkable characters distinguishing the genera (e.g., presence of numerous white tubercles on males' dorsum in *Rupirana*; presence of a meniscus on the upper iris in *Scythrophrys*; presence of well-developed and flexible fringes or webs on foot in *Paratelmatobius*; and nuptial pads of males formed by few and well-developed keratinized spines in *Crossodactylodes*; Figs. 2–6; Appendices III, IV). Stochastic events associated with the long divergence times between the genera (Fouquet et al. 2013), and the divergent selection associated with different habitats or environments in which the genera occur (i.e., shallow temporary ponds and backwaters in campo rupestre in *Rupirana*; temporary ponds and backwaters in forest areas in *Scythrophrys* and *Paratelmatobius*; and bromeliads in forest areas or campo rupestre in *Crossodactylodes*), might explain these differences. *Crossodactylodes* exhibits a life cycle strictly associated with bromeliads, which is a synapomorphic character within Leptodactylidae (Fouquet et al. 2013; this study). Some of the putative morphological synapomorphies that we found for the genus (Figs. 2–6; Appendices III, IV) seem to be related to this bromeligenous habit. The expanded discs on fingers and the lack of lateral ridges, fringes, or webs on toes seem to be adaptations to a distinct locomotor mode (i.e., slow walking on bromeliad leaves). On the other hand, other Paratelmatobiinae have narrow discs on fingers and the presence of lateral ridges, fringes, or webs on toes, which seem to be adaptions to semiaquatic habits (to varying degrees). The decrease in foot length in *Crossodactylodes*, compared with other Paratelmatobiinae (Fig. 7), might also be related to the distinct locomotor mode. A smaller foot might perform better while walking whereas a larger foot might favor higher propulsive forces during swimming and jumping (Emerson 1978; Pough 2007).

The absence of columella was already reported for *Crossodactylodes pintoi*, *C. bokermanni*, *C. izecksohni*, and *C. septentrionalis* (Lynch 1971; Gomes 1988; Teixeira et al. 2013) and we report it for *C. itambe* (Fig. 6C). Based on examination of external morphology, dissection of the skin on the lateral head of some specimens, and following the assumption of Pereyra et al. (2016), i.e., absence of columella implies absence of tympanic annulus and tympanic membrane, we consider the tympanic middle ear as completely lacking in all species of *Crossodactylodes*. This is another putative synapomorphy for the genus (Figs. 2, 5, 6; Appendices III, IV). However, among other Paratelmatobiinae, the absence of columella was reported for *Paratelmatobius lutzii* (Lynch 1971), and the knowledge of the phylogenetic placement of this species is important for a more accurate optimization of this character (Pereyra et al. 2016). Extratympanic hearing pathways were already reported for many species of different anuran families (Pereyra et al. 2016). In *Crossodactylodes* it might be related to the evolution of a different type of communication associated with breeding in bromeliads, as at least *C. izecksohni* and *C. itambe* are known to exhibit calling activity (Barata et al. 2018a; Ferreira et al. 2019a).

The nuptial pad formed by a few, well-developed spines (Figs. 2, 3A; Appendices III, IV) is another putative synapomorphy of *Crossodactylodes* (Fouquet et al. 2013; this study). Agonistic encounters between males were reported for *C. izecksohni* (Ferreira et al. 2019a). Therefore, this character seems to be associated with territoriality. Bromeliads, tree holes, and pools in torrential streams are limited resources which select males with the ability to defend them (e.g., Mendelson et al. 2008; Magalhães et al. 2018; Ferreira et al. 2019a). Territorial males usually have secondary sexual characters such as tusks, spines, odontids, keratinized nuptial pads, and hypertrophied forearms (Kupfer 2007); these last two are present in *Crossodactylodes*. However, the spines can also be used to attack potential predators of eggs and tadpoles, as *C. izecksohni* and *C. itambe* are known to exhibit egg and/or tadpole guarding behavior (Santos et al. 2017; Ferreira et al. 2019a). Therefore, both territoriality and parental care might be related to the evolution of the different type of nuptial pad in *Crossodactylodes* males. In addition, *C. izecksohni* females have also been observed displaying egg and tadpole guarding as well as in female–female combat (Ferreira et al. 2019a). The deposition of single eggs positioned isolated from other eggs, another putative synapomorphy of *Crossodactylodes* (Figs. 2, 18; Appendices III, IV), is another indication of high maternal investment and parental care (Santos et al. 2017; Ferreira et al. 2019a).

The sexual dimorphism related to hypertrophy of arms and forearms is more accentuated in *Crossodactylodes izecksohni* and *C. itambe* than it is in *C. bokermanni* (Table 2). This dimorphism seems also to be accentuated in *C. pintoi* and *C. septentrionalis*, but a higher number of specimens need to be analyzed for confirmation. In addition, *C. izecksohni* and *C. itambe* were found in higher abundance, with aggregations of individuals occupying the same bromeliad or bromeliad patch (Santos et al. 2017; Ferreira et al. 2019a). This favors agonistic encounters which probably increase the selective pressure on characters related to territoriality. Therefore, we hypothesize that territoriality might be an important issue in the evolution and diversification of the clade comprising *C. izecksohni*, *C. itambe*, *C. septentrionalis*, and *C. pintoi*.

We found high genetic distances and striking relationships among lineages within both *Crossodactylodes bokermanni* and *C. izecksohni* (Fig. 1; Table 1; Appendices VI, VII). In *C. bokermanni*, Lineage A is more closely related to Lineage B (which occurs ~85 km apart) than to Lineage C (which occurs ~5 km apart; Figs. 1, 8). In *C. izecksohni*, we found two distinct lineages which occur ~5 km apart (Figs. 1, 8). Fouquet et al. (2007) suggested a mean genetic distance of 3% for 16S rDNA to identify lineages that could correspond to candidate species in Neotropical frogs. The distances between Lineages A and C and Lineages B and C of *C. bokermanni*, and between Lineages A and B of *C. izecksohni*, are above this threshold (Table 1). In addition, these same distances are similar to some interspecific distances (e.g., between *C. itambe* and Lineage A of *C. izecksohni* and between *C. itambe* and *C. septentrio*nalis) and much higher than all other intraspecific or intralineage distances (Table 1). The same pattern occurs in the other mtDNA fragments (Appendices VI, VII). Although thresholds for species recognition based in genetic distances are arbitrary because different phenomena drive the evolutionary processes in different species (Padial et al. 2009), the mtDNA distances among these lineages are unexpectedly high considering the small geographic distances separating them. The small body size and the occurrence in topographically complex forests have been associated with high genetic divergences in other taxa of tropical anurans (Pabijan et al. 2012; Rodríguez et al. 2015). In *Crossodactylodes*, the high genetic distances might be related to ecological barriers to gene flow associated with a high concentration of bromeliads in mountaintops and unfavorable conditions in depressions, forming islands with low connectivity. This type of isolation in highland environments was already reported for other Atlantic Forest anurans (Pie et al. 2018; Ramos et al. 2019). Alternatively, this might be related to multiple bottlenecks or founder events, isolating lineages which previously had a continuous distribution, as observed for some African montane frogs (Lawson et al. 2015). These scenarios (i.e., gradual isolation or bottlenecks/founder events) could be tested with a more extensive sampling using demographic simulations (Knowles 2009).

Despite the high genetic divergences among the lineages within *Crossodactylodes bokermanni* and *C. izecksohni*, we did not detect morphological characters distinguishing them. For this reason, we considered that these lineages are deep conspecific lineages (sensu Padial et al. 2010). However, we suggest further investigation using alternative character systems and methods such as a multispecies coalescent in an integrative taxonomic approach (Fujita et al. 2012). Acoustic and larval characters, which are poorly known for *Crossodactylodes*, may provide the alternative source of characters for a more accurate identification of these lineages. These characters constitute important sources of evidence to delimit cryptic species in anurans (Randrianiaina et al. 2009; Grosjean et al. 2015; Köhler et al. 2017). Furthermore, samples from more localities will be required to discern between true allopatry or extremes of clinal variation.

Moreover, and in addition to the possible morphologically cryptic species, the high discontinuity among the geographic range of the different species of *Crossodactylodes*, associated with the recent findings of new species and populations (Teixeira et al. 2013; Barata et al. 2013; this study), indicate that the real diversity within the genus might be underestimated. The geographic distribution of the genus resembles that of other taxa of small-sized anurans with a high proportion of narrow endemic species associated with highland forest islands (e.g., *Brachycephalus* Fitzinger 1826; *Ischnocnema venancioi* species series; and *Paratelmatobius* [Pie et al. 2013; Taucce et al. 2018; Santos et al. 2019, respectively]). In *Brachycephalus*, 22 of its 36 constituent species were described in the last 10 yr (Frost 2019).

The phylogenetic placement of *Crossodactylodes itambe* (Figs. 1, 2), the only nonforest species of the genus, suggests that the common ancestor of *Crossodactylodes* inhabited forests and the colonization of campo rupestre was secondary. *Crossodactylodes itambe* was recovered as the sister taxon of *C. septentrionalis* (Fig. 1), indicating a close relationship between campo rupestre and southern Bahia Atlantic Forest. This relation was also reported by Ramos et al. (2019) based on the close relationships between the treefrog *Pithecopus megacephalus* (Miranda-Ribeiro 1926), endemic from campo rupestre, and one lineage of *P. rohdei* (Mertens 1926) that occurs on southern Bahia. On the other hand, Sabbag et al. (2018) found that the rock frog *Thoropa megatympanum* Caramaschi and Sazima 1984, another endemic species from campo rupestre, diverged after *T. saxatilis* Cocroft and Heyer 1988 from southern Atlantic Forest and before a clade comprising lineages from southeastern and northeastern Atlantic Forest, including one inhabiting southern Bahia. Our results support the idea that at least part of the endemic anuran fauna from campo rupestre originates from Atlantic Forest ancestors, even though the relationships between these two regions are complex.

The genus *Crossodactylodes* is distributed in highland forest islands in the Atlantic Forest domain and in one location in the campo rupestre of the Espinhaço Range (Fig. 8). According to current knowledge, all species are restricted to very small geographic ranges (i.e., *C. pintoi*, *C. itambe*, and C. *septentrionalis* are known only from their type locality; and the predicted extent of occurrence is 174 km^2 for *C. bokermanni*, and 23 km^2 for *C. izecksohni*). Both the Atlantic Forest domain and the campo rupestre of the Espinhaço Range are considered very endangered environments (Myers et al. 2000; Silveira et al. 2016). Among the threats to global amphibian conservation, habitat loss and fragmentation are considered the most prominent (Cushman 2006; Stuart et al. 2008), as they lead to isolation of populations and loss of genetic diversity (Weeks et al. 2016). Furthermore, the extinction associated with fragmentation is inversely proportional to species dispersal capacity (Cushman 2006), an important factor for species of *Crossodactylodes* due to their small body size and dependency on bromeliads, which probably limits their dispersal. In addition, species with restricted ranges are more vulnerable to natural stochastic events and the negative anthropogenic activities, and hence are more prone to extinction (Sodhi et al. 2008; Pimm et al. 2014; Toledo et al. 2014; Weeks et al. 2016). All these factors emphasize the need for effective conservation measures to safeguard *Crossodactylodes* species.

Acknowledgments.—We thank H.Q. Boudet (MBML), J.P. Pombal, Jr. (MNRJ), H. Zaher, T. Grant (MZUSP), O.L. Peixoto (EI), S.P. Carvalho-e-Silva (ZUFRJ), W.R. Heyer and K. de Queiroz (USNM), and V.G.D. Orrico (MZUESC) for loan of specimens or providing access to the collections. J. Rosado and J. Woodward (MCZ) provided photographs of a specimen under their care. P.P.G. Taucce took pictures of some specimens at USNM. We are grateful to the Centro de Estudos de Insetos Sociais (CEIS), UNESP, Rio Claro, Brazil, for allowing the utilization of the facilities for some molecular analyses. P. Shea and C. French helped with English. P.D.P. Pinheiro helped with dissections and phylogenetic analyses. D. Baêta and B.F. Zaidan helped with cleared and double-stained specimens. We are grateful to G.H.F. Azevedo, I.L.F. Magalhães, B. Faleiro, J.V.A. Lacerda, F. Leal, I.R. Fernandes, A.P. Motta, M.B. Harvey, and two anonymous reviewers for comments and suggestions that improved the manuscript. M. Vancine helped with the map. We thank L. Kollman, A. Amorin, M. Sena, and T. Mota for identification of bromeliads. J.E. Santos, Jr. and M.L. Lyra provide laboratory assistance. We thank P.H. Martins, P. Rocha, B.H. Fehlberg, C.Z. Zocca, A.T. Monico, F.C. Lirio, and R.S. Cipriano for fieldwork assistance, and the Bromeligenous project for logistical support. This work was financed by Fundação de Amparo à Pesquisa do Estado de São Paulo (FAPESP), Grant 2013/50741-7; Fundação de Amparo à Pesquisa do Estado de Minas Gerais (FAPEMIG), Grant APQ-01120-16; Mohamed bin Zayed; Utah State University; and Rufford Foundation. This study was financed in part by the Coordenação de Aperfeiçoamento de Pessoal de Nível Superior – Brasil (CAPES) – Finance Code 001. Support was provided to MTTS by FAPEMIG and CAPES (Grants 88881.189822/2018-01 and 88882.434124/2019-01); to RFM by CAPES (Programa Nacional de Pós-Doutorado); and IRD thanks Conselho Nacional de Desenvolvimento Científico e Tecnológico (CNPq), Grant 155198/2018-1 and FSFL thanks FAPEMIG and Vale, Grants APQ-01796-15 and RDP-00004-17. In addition, CFBH, FRS, and PCAG were supported by research fellowships from CNPq. Sampling permits were issued by ICMBio (28607, 35198-2, and 50402); Instituto Estadual de Florestas, Minas Gerais 108/12; Instituto Estadual de Meio Ambiente e Recursos Hídricos, Espírito Santo 021-2012 and 005-2016; Institutional Animal Care and Use Committee, Utah State University 2002; and Comissão de Ética no Uso de Animais, Universidade Vila Velha 355-2015.

SUPPLEMENTAL MATERIAL

Supplemental material associated with this article can be found online at https://doi.org/10.1655/HERPMONOGRAPHS-D-19-00008.S1; https://doi.org/10.1655/HERPMONOGRAPHS-D-19-00008.S2; https://doi.org/10.1655/HERPMONOGRAPHS-D-19-00008.S3; https://doi.org/10.1655/HERPMONOGRAPHS-D-19-00008.S4.

LITERATURE CITED

Altig, R., and R.W. McDiarmid. 2007. Morphological diversity and evolution of egg and clutch structure in amphibians. Herpetological Monographs 21:1–32.

Barata, I.M., M.T.T. Santos, F.S.F. Leite, and P.C.A. Garcia. 2013. A new species of *Crossodactylodes* (Anura: Leptodactylidae) from Minas Gerais, Brazil: First record of genus within the Espinhaço Mountain Range. Zootaxa 3731:552–560.

Barata, I.M., R.A. Griffiths, and G.B. Ferreira. 2018a. Activity pattern and behavior of an endemic bromeliad frog observed through camera trapping. Herpetological Review 49:432–438.

Barata, I.M., E.P. Silva, and R.A. Griffiths. 2018b. Predictors of abundance of a rare bromeliad-dwelling frog (*Crossodactylodes itambe*) in the Espinhaço Mountain Range of Brazil. Journal of Herpetology 52:321–326.

Bornschein, M.R., C.R. Firkowski, D. Baldo, L.F. Ribeiro, R. Belmonte-Lopes, L. Corrêa, S.A.A. Morato, and M.R. Pie. 2015. Three new species of phytotelm-breeding *Melanophryniscus* from the Atlantic Rainforest of southern Brazil (Anura: Bufonidae). PLoS ONE 10:e0142791. DOI: https://dx.doi.org/10.1371/journal.pone.0142791

Bossuyt, F., and M.C. Milinkovitch. 2000. Convergent adaptive radiations in Madagascan and Asian ranid frogs reveal covariation between larval and adult traits. Proceedings of the National Academy of Science of the United States of America 97:6585–6590.

Bokermann, W.C.A. 1966. Lista Anotada das Localidades Tipo de Anfíbios Brasileiros. Serviço de Documentação da Reitoria da Universidade de São Paulo, Brasil.

Caramaschi, U., and I. Sazima. 1984. Uma nova espécie de *Thoropa* da Serra do Cipó, Minas Gerais, Brasil (Amphibia, Leptodactylidae). Revista Brasileira de Zoologia 2:139–146.

Carvalho, T.R., C.S. Cassini, P.P.G. Taucce, and C.F.B. Haddad. 2019. A new, morphologically cryptic species of *Adenomera* closely related to *Adenomera araucaria* from the Atlantic Forest of southern Brazil (Anura, Leptodactylidae). Journal of Herpetology 53:131–143.

Cochran, D.M. 1938. Diagnoses of new frogs from Brazil. Proceedings of the Biological Society of Washington 51:41–42.

Cochran, D.M. 1955. Frogs of southeastern Brazil. United States National Museum Bulletin 206:1–423.

Cocroft, R.B., and W.R. Heyer. 1988. Notes on the frog genus *Thoropa* (Amphibia: Leptodactylidae) with a description of a new species (*Thoropa saxatilis*). Proceedings of the Biological Society of Washington 101:209–220.

Cope, E.D. 1865. Sketch of the primary groups of Batrachia s. Salientia. Natural History Review, New Series 5:97–120.

Cope, E.D. 1866. On the structures and distribution of the genera of the arciferous Anura. Journal of the Academy of Natural Sciences of Philadelphia, Series 2 6:67–112.

Costello, M.J., B. Vanhoorne, and W. Appeltans. 2015. Conservation of biodiversity through taxonomy, data publication, and collaborative infrastructures. Conservation Biology 29:1094–1099.

Cushman, S.A. 2006. Effects of habitat loss and fragmentation on amphibians: A review and prospectus. Biological Conservation 128:231–240.

Dias, I.R., T.T. Medeiros, M.V. Nova, and M. Solé. 2014. Amphibians of Serra Bonita, southern Bahia: A new hotpoint within Brazil's Atlantic Forest hotspot. Zookeys 449:105–130.

Dubois, A. 2005. Amphibia Mundi 1.1. An ergotaxonomy of recent amphibians. Alytes 23:1–24.

Dubois, A. 2013. Crossodactylodinae Fouquet, Blotto, Maronna, Verdade, Juncá, de Sá and Trefaut Rodrigues, 2013 is an invalid junior synonym of Paratelmatobiinae Ohler and Dubois, 2012 (Amphibia, Anura). Zootaxa 3700:499–500.

Dudley, N. 2008. Guidelines for Applying Protected Areas Management Categories. International Union for Conservation of Nature, Switzerland.

Duellman, W.E. 1970. The hylid frogs of Middle America. Monograph of the Museum of Natural History, The University of Kansas 1:1–754.

Duellman, W.E., and E. Lehr. 2009. Terrestrial Breeding Frogs (Strabomantidae) in Peru. Natur und Tier-Verlag, Germany.

Duméril, A.M.C., and G. Bibron. 1841. Erpétologie Générale ou Histoire Naturelle Complète des Reptiles, Volume 8. Librairie Encyclopédique de Roret, France.

Emerson, S.B. 1978. Allometry and jumping in frogs: Helping the twain to meet. Evolution 32:551–564.

Faivovich, J., C.F.B. Haddad, P.C.A. Garcia, D.R. Frost, J.A. Campbell, and W.C. Wheeler. 2005. Systematic review of the frog family Hylidae, with special reference to Hylinae: Phylogenetic analysis and taxonomic revision. Bulletin of the American Museum of Natural History 294:1–240.

Faivovich, J., L. Nicoli, B.L. Blotto, M.O. Pereyra, D. Baldo, J.S. Barrionuevo, M. Fabrezi, E.R. Wild, and C.F.B. Haddad. 2014. Big, bad, and beautiful: Phylogenetic relationships of the horned frogs (Anura: Ceratophryidae). South American Journal of Herpetology 9:207–227.

Farris, J.S., V.A. Albert, M. Kallersjo, D. Lipscomb, and A.G. Kluge. 1996. Parsimony jackknifing outperforms neighbor-joining. Cladistics 12:99–124.

Feller, A.E., and S.B. Hedges. 1998. Molecular evidence for the early history of living amphibians. Molecular Phylogenetics and Evolution 9:509–516.

Ferreira, R.B., A.T. Mônico, C.Z. Zocca,… C. Duca. 2019a. Uncovering the natural history of the bromeligenous frog *Crossodactylodes izecksohni* (Leptodactylidae, Paratelmatobiinae). South American Journal of Herpetology 14:136–145.

Ferreira, R.B., A.T. Mônico, E.T. Silva, F.C.F. Lírio, C.Z. Zocca, M.M. Mageski, J.F.R. Tonini, K.H. Beard, C. Duca, and T. Silva-Soares. 2019b. Amphibians of Santa Teresa, Brazil: The hotspot further evaluated. ZooKeys 857:139–162.

Fitzinger, L.J.F.J. 1826. Neue Classification der Reptilien nach ihren

Natürlichen Verwandtschaften nebst einer Verwandtschafts-Tafel und einem Verzeichnisse der Reptilien-Sammlung des K.K. Zoologisch Museum's zu Wien. J.G. Heubner, Austria.

Forlani, M.C., J.F.R. Tonini, C.A.G. Cruz, H. Zaher, and R.O. de Sá. 2017. Molecular and morphological data reveal three new cryptic species of *Chiasmocleis* (Mehely 1904) (Anura, Microhylidae) endemic to the Atlantic Forest, Brazil. PeerJ 5:e3005. DOI: http://dx.doi.org/10.7717/peerj.3005

Fouquet, A., A. Gilles, M. Vences, C. Marty, M. Blanc, and N.J. Gemmell. 2007. Underestimation of species richness in Neotropical frogs revealed by mtDNA analyses. PLoS ONE 2:e1109. DOI: http://dx.doi.org/10.1371/journal.pone.0001109

Fouquet, A., B.L. Blotto, M.M. Maronna, V.K. Verdade, F.A. Juncá, R. de Sá, and M.T. Rodrigues. 2013. Unexpected phylogenetic positions of the genera *Rupirana* and *Crossodactylodes* reveal insights into the biogeography and reproductive evolution of leptodactylid frogs. Molecular Phylogenetics and Evolution 67:445–457.

Frost, D.R. 2019. Amphibian Species of the World: An Online Reference, Version 6.0. Available at http://research.amnh.org/herpetology/amphibia/index.html. American Museum of Natural History, USA. Archived by WebCite at http://www.webcitation.org/6qp8hUYGQ on 29 May 2017.

Frost, D.R., T. Grant, J. Faivovich,… W.C. Wheeler. 2006. The amphibian tree of life. Bulletin of the American Museum of Natural History 297:1–370.

Fujita, M.K., A.D. Leaché, F.T. Burbrink, J.A. McGuire, and C. Moritz. 2012. Coalescent-based species delimitation in an integrative taxonomy. Trends in Ecology and Evolution 27:480–488.

Gaige, H.T. 1926. A new frog from British Guiana. Occasional Papers of the Museum of Zoology, University of Michigan 176:1–3.

Garcia, P.C.A. 1996. Recaracterização de *Scythrophrys sawayae* (Cochran, 1953) Baseada em Morfologia, Osteologia e Aspectos da Miologia e História Natural (Amphibia, Anura, Leptodactylidae). M.S. thesis, Universidade Católica do Rio Grande do Sul, Brasil.

Giaretta, A.A., and L.M. Castanho. 1990. Nova espécie de *Paratelmatobius* (Amphibia, Anura, Leptodactylidae) da Serra do Mar, Brasil. Papéis Avulsos de Zoologia, São Paulo 37:133–139.

Goebel, A.M., J.M. Donnely, and M.E. Atz. 1999. PCR primers and amplification methods for 12S ribosomal DNA, the control region, cytochrome oxidase I, and cytochrome b in bufonids and other frogs, and an overview of PCR primers which have amplified DNA in amphibians successfully. Molecular Phylogenetics and Evolution 11:163–199.

Goloboff, P., and S. Catalano. 2016. TNT version 1.5, including a full implementation of phylogenetic morphometrics. Cladistics 32:221–238.

Gomes, N. 1988. Osteologia comparada de duas espécies do gênero *Crossodactylodes* Cochran, 1938 (Amphibia, Anura, Leptodactylidae). Memórias do Instituto Butantan 50:51–61.

Gontijo-Pascutti, A.H.F., Y. Hasui, M. Santos, A.V. Soares, Jr., and I.A. Souza. 2012. As serras do Mar e da Mantiqueira. Pp. 549–571 in Geologia do Brasil (Y. Hasui, C.D.R. Carneiro, F.F.M. Almeida, and A. Bartorelli, eds.). Beca, Brazil.

Graybeal, A. 1997. Phylogenetic relationships of bufonid frogs and tests of alternate macroevolutionary hypotheses characterizing their radiation. Zoological Journal of the Linnean Society 119:297–338.

Grosjean, S., S. Bordoloi, Y. Chuaynkern, P. Chakravarty, and A. Ohler. 2015. When young are more conspicuous than adults: A new ranid species (Anura: Ranidae) revealed by its tadpole. Zootaxa 4058:471–498.

Haddad, C.F.B., and C.P.A. Prado. 2005. Reproductive modes in frogs and their unexpected diversity in the Atlantic Forest of Brazil. BioScience 55:207–217.

Haddad, C.F.B., L.F. Toledo, C.P.A. Prado, D. Loebmann, J.L. Gasparini, and I. Sazima. 2013. Guide to the Amphibians of the Atlantic Forest: Diversity and Biology. Anolis Books, Brazil.

Haddad, C.F.B., I.F. Machado, J.G.R. Giovanelli,… R.P. Bastos. 2016a. Avaliação do Risco de Extinção de *Crossodactylodes pintoi* Cochran, 1938. Available at http://www.icmbio.gov.br/portal/biodiversidade/fauna-brasileira/estado-de-conservacao/7647-anfibios-crossodactylodes-pintoi.html. Processo de Avaliação do Risco de Extinção da Fauna Brasileira, ICMBio, Brazil. Archived by WebCite at http://www.webcitation.org/6uaCmZKjy on 29 October 2017.

Haddad, C.F.B., M.V. Segalla, Y.S.L. Bataus,… U. Caramaschi. 2016b Avaliação do Risco de Extinção de *Crossodactylodes bokermanni* Peixoto 1983 ''1982''. Available at http://www.icmbio.gov.br/portal/faunabrasileira/carga-estado-de-conservacao/8116-anfibios-crossodactylodes-bokermanni. Processo de Avaliação do Risco de Extinção da Fauna Brasileira, ICMBio, Brazil. Archived by WebCite at http://www.webcitation.org/6uaDE2Sbl on 29 October 2017.

Haddad, C.F.B., M.V. Segalla, Y.S.L. Bataus,… U. Caramaschi. 2016c. Avaliação do Risco de Extinção de *Crossodactylodes izecksohni* Peixoto 1983 ''1982''. Available at http://www.icmbio.gov.br/portal/biodiversidade/fauna-brasileira/estado-de-conservacao/7701-anfibios-crossodactylodes-izecksohni.html. Processo de Avaliação do Risco de Extinção da Fauna Brasileira, ICMBio, Brazil. Archived by WebCite at http://www.webcitation.org/6uaDUh4w4 on 29 October 2017.

Haddad, C.F.B., Y.S.L. Bataus, V.M. Uhlig,… R. Lingnau. 2016d. Avaliação do Risco de Extinção de *Crossodactylodes itambe* Barata, Santos, Leite, and Garcia 2013. Available at http://www.icmbio.gov.br/portal/biodiversidade/fauna-brasileira/estado-de-conservacao/7700-anfibios-crossodactylodes-itambe.html. Processo de Avaliação do Risco de Extinção da Fauna Brasileira, ICMBio, Brazil. Archived by WebCite at http://www.webcitation.org/6ua8FrJ61on 29 October 2017.

Hedges, S.B. 1994. Molecular evidence for the origin of birds. Proceedings of the National Academy of Sciences of the United States of America 91:2621–2624.

Heyer, W.R. 1975. A preliminary analysis of the intergeneric relationships of the frog family Leptodactylidae. Smithsonian Contributions to Zoology 199:1–55.

Heyer, W.R. 1999. A new genus and species of frog from Bahia, Brazil (Amphibia: Anura: Leptodactylidae) with comments on the zoogeography of the Brazilian campos rupestres. Proceedings of The Biological Society of Washington 112:19–30.

Heyer, W.R., A.S. Rand, C.A.G. Cruz, O.L. Peixoto, and C. Nelson. 1990. Frogs of Boracéia. Arquivos de Zoologia do Estado de São Paulo 31:231–410.

Hortal, J., F. de Bello, J.A.F. Diniz-Filho, T.M. Lewinsohn, J.M. Lobo, and R.J. Ladle. 2015. Seven shortfalls that beset large-scale knowledge of biodiversity. Annual Review of Ecology, Evolution, and Systematics 46:523–549.

Ihering, H., and R. Ihering. 1911. O Museu Paulista nos annos de 1906 a 1909. Revista do Museu Paulista 8:1–22.

Instituto Chico Mendes de Conservação da Biodiversidade (ICMBio). 2017. Unidades de Conservação. Available at http://icmbio.gov.br/portal/unidadesdeconservacao/biomas-brasileiros. Accessed on 13 November 2019. Ministério do Meio Ambiente, Brasil.

Instituto Estadual do Ambiente. 2014. APA Estadual de Macaé de Cima: Plano de Manejo: Informações Sintetizadas da UC. Executive Report. Instituto Estadual do Ambiente, Brazil.

International Union for Conservation of Nature (IUCN) Standards and Petitions Committee. 2019. Guidelines for Using the IUCN Red List Categories and Criteria, Version 14. International Union for Conservation of Nature, Switzerland.

Juncá, F.A., and L. Lugli. 2009. Reproductive biology, vocalizations, and tadpole morphology of *Rupirana cardosoi*, an anuran with uncertain affinities. South American Journal of Herpetology 4:173–178.

Katoh, K., and D.M. Standley. 2013. MAFFT multiple sequence alignment software Version 7: Improvements in performance and usability. Molecular Biology and Evolution 30:772–780.

Katoh, K., J. Rozewicki, and K.D. Yamada. 2019. MAFFT online service: Multiple sequence alignment, interactive sequence choice and visualization. Briefings in Bioinformatics 20:1160–1166.

Köhler, J., M. Jansen, A. Rodríguez, P.J.R. Kok, L.F. Toledo, M. Emmrich, F. Glaw, C.F.B. Haddad, M. Rödel, and M. Vences. 2017. The use of bioacoustics in anuran taxonomy: Theory, terminology, methods and recommendations for best practice. Zootaxa 4251:1–124.

Knowles, L.L. 2009. Statistical phylogeography. Annual Review of Ecology, Evolution, and Systematics 40:593–612.

Kumar, S., G. Stecher, and K. Tamura. 2016. MEGA7: Molecular evolutionary genetics analysis version 7.0 for bigger datasets. Molecular Biology and Evolution 33:1870–1874.

Kupfer, A. 2007. Sexual size dimorphism in amphibians: An overview. Pp. 50–59 in Sex, Size and Gender Roles: Evolutionary Studies of Sexual Size Dimorphism (D.J. Fairbairn, W.U. Blanckenhorn and T. Szekely, eds.). Oxford University Press, UK.

Lanfear, R., P.B. Frandsen, A.M. Wright, T. Senfeld, and B. Calcott. 2017. PartitionFinder 2: New methods for selecting partitioned models of evolution for molecular and morphological phylogenetic analyses. Molecular Biology and Evolution 34:772–773.

Lawson, L.P., J.M. Bates, M. Menegon, and S.P. Loader. 2015. Divergence at the edges: Peripatric isolation in the montane spiny throated reed frog complex. BMC Evolutionary Biology 15:1–15. DOI: http://dx.doi.org/10.1186/s12862-015-0384-3

Lutz, B., and A.L. de Carvalho. 1958. Novos anfíbios anuros das serras costeiras do Brasil. Memórias do Instituto Oswaldo Cruz 56:239–249.

Lynch, J.D. 1971. Evolutionary relationships, osteology, and zoogeography of leptodactyloid frogs. Miscellaneous Publications of the Museum of Natural History, University of Kansas 53:1–238.

Lyra, M.L., C.F.B. Haddad, and A.M.L. de Azeredo-Espin. 2017. Meeting the challenge of DNA barcoding Neotropical amphibians: Polymerase chain reaction optimization and new COI primers. Molecular Ecology Resources 17:966–980.

Maddison, W.P., and D.R. Maddison. 2017. Mesquite: A modular system for evolutionary analysis, Version 3.2. Available at http://mesquiteproject.org. Mesquite Project, USA. Archived by WebCite at http://www.webcitation.org/6r3FdSuUV on 07 June 2017.

Magalhães, R.F., J.V.A. Lacerda, L.P. Reis, P.C.A. Garcia, and P.D.P. Pinheiro. 2018. Sexual dimorphism in *Bokermannohyla martinsi* (Bokermann, 1964) (Anura, Hylidae) with a report of male–male combat. South American Journal of Herpetology 13:202–209.

Martinelli, G., C.M. Vieira, M. González, P. Leitman, A. Piratininga, A.F. da Costa, and R.C. Forzza. 2008. Bromeliaceae da Mata Atlântica brasileira: Lista de espécies, distribuição e conservação. Rodriguésia 59:209–258.

Mendelson, J.R., J.M. Savage, E. Griffith, H. Ross, B. Kubicki, and R. Gagliardo. 2008. Spectacular new gliding species of *Ecnomiohyla* (Anura: Hylidae) from central Panama. Journal of Herpetology 42:750–759.

Mertens, R. 1926. Herpetologischen Mitteilungen VIII–XV. Senckenbergiana Biologica 8:137–155.

Miller, M.A., W. Pfeiffer, and T. Schwartz. 2010. Creating the CIPRES Science Gateway for inference of large phylogenetic trees. Proceedings of the Gateway Computing Environments Workshop 2010:1–8. DOI: https://dx.doi.org/10.1109/GCE.2010.5676129

Miranda-Ribeiro, A. 1923. *Elosia* Tsch. e os generos correlatos. Revista do Museu Paulista 13:813–821.

Miranda-Ribeiro, A. 1926. Notas para servirem ao estudo dos gymnobatrachios (Anura) brasileiros. Arquivos do Museu Nacional, Rio de Janeiro 27:1–227.

Morais, A.R., M.N. Siqueira, P. Lemes, N.M. Maciel, P. De Marco, Jr., and D. Brito. 2013. Unraveling the conservation status of Data Deficient species. Biological Conservation 166:98–102.

Moritz, C., C.J. Schneider, and D.B. Wake. 1992. Evolutionary relationships within the *Ensatina eschscholtzii* complex confirm the ring species interpretation. Systematic Biology 41:273–291.

Müller, L. 1922. Über eine Sammlung Froschlurche von Sta. Catharina nebst Beschriebung zweier neuer Arten. Blätter für Aquarien- und Terrarienkunde 33:167–171.

Myers, N., R.A. Mittermeier, C.G. Mittermeier, G.A.B. da Fonseca, and J. Kent. 2000. Biodiversity hotspots for conservation priorities. Nature 403:853–858.

Nixon, K. 2002. WinClada, Version 1.00.08. Published by the author, USA.

Ohler, A., and A. Dubois. 2012. Validation of two familial nomina nuda of Amphibia Anura. Alytes 28:162–167.

Oliveira, U., A.P. Paglia, A.D. Brescovit,… A.J. Santos. 2016. The strong influence of collection bias on biodiversity knowledge shortfalls of Brazilian terrestrial biodiversity. Diversity and Distributions 22:1232–1244.

Pabijan, M., K.C. Wollenberg, and M. Vences. 2012. Small body size increases the regional differentiation of populations of tropical mantellid frogs (Anura: Mantellidae). Journal of Evolutionary Biology 25:2310–2324.

Padial, J.M., S. Castroviejo-Fisher, J. Köhler, C. Vilà, J.C. Chaparro, and I. De la Riva. 2009. Deciphering the products of evolution at the species level: The need for an integrative taxonomy. Zoologica Scripta 38:431–447.

Padial, J.M., A. Miralles, I. De la Riva, and M. Vences. 2010. The integrative future of taxonomy. Frontiers in Zoology 7:16. DOI: http://dx.doi.org/10.1186/1742-9994-7-16

Palumbi, S.R., A.P. Martin, B.D. Kessing, and W.O. McMillan. 1991. Detecting population structure using mitochondrial DNA. Pp. 271–278 in Genetic Ecology of Whales and Dolphins (A.R. Hoelzel, ed.). International Whaling Commission, UK.

Paynter, R.A.J., and M.A. Traylor. 1991. Ornithological Gazetteer of Brazil, vol. 2. Cambridge Harvard College Press, USA.

Peixoto, O.L. 1981. Notas sobre o girino de *Crossodactylodes pintoi* Cochran (Amphibia, Anura, Leptodactylidae). Revista Brasileira de Biologia 41:339–341.

Peixoto, O.L. 1983 “1982”. Duas novas espécies de *Crossodactylodes* de Santa Tereza, estado do Espírito Santo, Brasil. (Amphibia, Anura, Leptodactylidae). Revista Brasileira de Biologia 42:619–626.

Peixoto, O.L. 1995. Associação de anuros a bromeliáceas na Mata Atlântica. Revista da Universidade Federal Rural do Rio de Janeiro, Série Ciências da Vida 17:75–83.

Peixoto, O.L., and S.P. Carvalho-e-Silva. 2004. *Crossodactylodes pintoi*. The IUCN Red List of Threatened Species 2004:e.T56346A11465671. DOI: http://dx.doi.org/10.2305/IUCN.UK.2004.RLTS.T56346A11465671.en

Pereyra, M.O., M.C. Womack, Barrionuevo,J.S. … J. Faivovich. 2016. The complex evolutionary history of the tympanic middle ear in frogs and toads (Anura). Scientific Reports 6:34130. DOI: http://dx.doi.org/10.1038/srep34130

Pie, M.R., A.L.S. Meyer, C.R. Firkowski, L.F. Ribeiro, and M.R. Bornschein. 2013. Understanding the mechanisms underlying the distribution of microendemic montane frogs (*Brachycephalus* spp., Terrarana: Brachycephalidae) in the Brazilian Atlantic Rainforest. Ecological Modelling 250:165–176.

Pie, M.R., B.C. Faircloth, L.F. Ribeiro, M.R. Bornschein, and J.E. McComarck. 2018. Phylogenomics of montane frogs of the Brazilian Atlantic Forest is consistent with isolation in sky islands followed by climatic stability. Biological Journal of the Linnean Society 125:72–82.

Pimm, S.L., C.N. Jenkins, R. Abell, T.M. Brooks, J.L. Gittleman, L.N. Joppa, P.H. Raven, C.M. Roberts, and J.O. Sexton. 2014. The biodiversity of species and their rates of extinction, distribution, and protection. Science 344:1246752. DOI: http://dx.doi.org/10.1126/science.1246752

Pinto, O.M.O. 1945. Cinqüenta anos de investigação ornitológica. Arquivos de Zoologia do Estado de São Paulo 4:261–340.

Pombal, J.P., Jr., and C.F.B. Haddad. 1999. Frogs of the genus *Paratelmatobius* (Anura: Leptodactylidae) with descriptions of two new species. Copeia 1999:1014–1026.

Pough, F.H. 2007. Amphibian biology and husbandry. ILAR Journal 48:203–213.

Pyron, R.A. 2014. Biogeographic analysis reveals ancient continental vicariance and recent oceanic dispersal in amphibians. Systematic Biology 63:779–797.

Pyron, R.A., and J.J. Wiens. 2011. A large-scale phylogeny of Amphibia with over 2800 species, and a revised classification of extant frogs, salamanders, and caecilians. Molecular Phylogenetics and Evolution 61:543–583.

Rambaut, A., M.A. Suchard, D. Xie, and A.J. Drummond. 2014. Tracer, version 1.6. Available at http://tree.bio.ed.ac.uk/software/tracer. Archived by WebCite at http://www.webcitation.org/6qpoA3u3h on 29 May 2017.

Ramos, E.K.S., R.F. Magalhães, N.C.S. Marques, D. Baêta, P.C.A. Garcia, and F.R. Santos. 2019. Cryptic diversity in Brazilian endemic monkey frogs (Hylidae, Phyllomedusinae, *Pithecopus*) revealed by multispecies coalescent and integrative approaches. Molecular Phylogenetics and Evolution 132:105–116.

Randrianiaina, R.D., R.N. Antúnez, J. Canitz,… M. Vences. 2009. Vogue or adaptive character? A tadpole’s goatee helps to distinguish two cryptic treefrog species of the genus *Boophis*. Herpetology Notes 2:165–173.

Rodríguez, A., M. Börner, M. Pabijan, M. Gehara, C.F.B. Haddad, and M. Vences. 2015. Genetic divergence in tropical anurans: Deeper phylogeographic structure in forest specialists and in topographically complex regions. Evolutionary Ecology 29:765–785.

Ronquist, F., M. Teslenko, P. van der Mark, D.L. Ayres, A. Darling, S. Höhna, B. Larget, L. Liu, M.A. Suchard, and J.P. Huelsenbeck. 2012. MrBayes 3.2: Efficient Bayesian phylogenetic inference and model choice across a large model space. Systematic Biology 61:539–542.

Rossa-Feres, D.C., M.V. Garey, U. Caramaschi,… C.F.B. Haddad. 2017. Anfíbios da Mata Atlântica: Lista de espécies, histórico dos estudos, biologia e conservação. Pp. 237–314 in Revisões em Zoologia: Mata Atlântica (E.L.A Monteiro-Filho and C.E. Conte, eds.). Editora UFPR, Brazil.

Rowe, K.C., S. Singhal, M.D. Macmanes, J.F. Ayroles, T.L. Morelli, E.M. Rubidge, K. Bi, and C.C. Moritz. 2011. Museum genomics: Low-cost and high-accuracy genetic data from historical specimens. Molecular Ecology Resources 11:1082–1092.

Sabagh, L.T., R.B. Ferreira, and C.F.D. Rocha. 2017. Host bromeliads and their associated frog species: Further considerations on the importance of species interactions for conservation. Symbiosis 73:201–211.

Sabbag, A.F., M.L. Lyra, K.R. Zamudio, C.F.B. Haddad, R.N. Feio, F.S.F. Leite, J.L. Gasparini, and C.A. Brasileiro. 2018. Molecular phylogeny of Neotropical rock frogs reveals a long history of vicariant diversification in the Atlantic Forest. Molecular Phylogenetics and Evolution 122:142–156.

Sabaj, M.H. 2016. Standard Symbolic Codes for Institutional Resource Collections in Herpetology and Ichthyology: An Online Reference, Version 6.5. Available at http://www.asih.org/. American Society of Ichthyologists and Herpetologists, USA. Archived by WebCite at http://www.webcitation.org/6qpZPWPt3 on 29 May 2017.

Sambrook, J., and D.W. Russel. 2001. Molecular Cloning: A Laboratory Manual. Cold Spring Harbor Laboratory Press, USA.

Santos, J.E., Jr., F.R. Santos, and F.A. Silveira. 2015. Hitting an unintended target: Phylogeography of *Bombus brasiliensis* Lepeletier, 1836 and the first new Brazilian bumblebee species in a century (Hymenoptera: Apidae). PLoS ONE 10:e0125847. DOI: https://dx.doi.org/10.1371/journal.pone.0125847

Santos, M.T.T., T.L. Pezzuti, I.M. Barata, F.S.F. Leite, and P.C.A. Garcia. 2017. The tadpole of the microendemic, bromeligenous *Crossodactylodes itambe* (Anura, Leptodactylidae) from the endangered 'campo rupestre' of southeastern Brazil, with additional comments on natural history. South American Journal of Herpetology 12:14–23.

Santos, M.T.T., S.H. Oliveira, T.R. Carvalho, B.F. Zaidan, N.R. Silva, B.V. Berneck, and P.C.A. Garcia. 2019. A new species of *Paratelmatobius* (Anura: Leptodactylidae: Paratelmatobiinae) from the Atlantic Forest of southern Brazil. Zootaxa 4648:473–493.

Scardua, F.P. 2000. Plano de Manejo do Parque Estadual do Forno Grande. Technical Report. Instituto Estadual de Meio Ambiente e Recursos Hídricos, Brasil.

Segalla, M.V., U. Caramaschi, C.A.G. Cruz, P.C.A. Garcia, T. Grant, C.F.B. Haddad, D.J. Santana, L.F. Toledo, and J.A. Langone. 2019. Brazilian amphibians: List of species. Herpetologia Brasileira 8:65–96.

Silvano, D., and O.L. Peixoto. 2004a. *Crossodactylodes bokermanni*. The IUCN Red List of Threatened Species 2004:e.T56344A11465382. DOI: http://dx.doi.org/10.2305/IUCN.UK.2004.RLTS.T56344A11465382.en

Silvano, D., and O.L. Peixoto. 2004b. *Crossodactylodes izecksohni*. The IUCN Red List of Threatened Species 2004:e.T56345A11465530. DOI: http://dx.doi.org/10.2305/IUCN.UK.2004.RLTS.T56345A11465530.en

Silveira, F.A.O., D. Negreiros, N.P.U. Barbosa,… H. Lambers. 2016. Ecology and evolution of plant diversity in the endangered campo rupestre: A neglected conservation priority. Plant and Soil 403:129–152.

Simmons, M.P., K.M. Pickett, and M. Miya. 2004. How meaningful are Bayesian support values? Molecular Biology and Evolution 21:188–199.

Sodhi, N.S., D. Bickford, A.C. Diesmos, T.M. Lee, L.P. Koh, B.W. Brook, C.H. Sekercioglu, and C.J.A. Bradshaw. 2008. Measuring the meltdown: Drivers of global amphibian extinction and decline. PLoS ONE 3:e1636. DOI: https://dx.doi.org/10.1371/journal.pone.0001636

SOS Mata Atlântica and Instituto Nacional de Pesquisas Espaciais. 2018. Atlas dos Remanescentes Florestais da Mata Atlântica, Período 2016–2017. Available at http://mapas.sosma.org.br. Accessed on 13 November 2019.

Steindachner, F. 1867. Reise der österreichischen Fregatte Novara um die Erde in den Jahren 1857, 1858, 1859 unter den Bafehlen des Commodore B. von Wüllerstorf-Urbair. Zologischer Theil. 1. Amphibien. K.K. Hof- und Staatsdruckerei, Austria.

Stuart, S., M. Hoffmann, J. Chanson, N. Cox, R. Berridge, P. Ramani, and B. Young. 2008. Threatened Amphibians of the World. Lynx Edicions, IUCN, and Conservation International, Spain, Switzerland, and USA.

Tapley, B., C.J. Michaels, R. Gumbs, M. Böhm, J. Luedtke, P. Pearce-Kelly, and J.J.L. Rowley. 2018. The disparity between species description and conservation assessment: A case study in taxa with high rates of species discovery. Biological Conservation 220:209–214.

Taylor, W.R., and G.C. Van Dyke. 1985. Revised procedures for staining and clearing small fishes and other vertebrates for bone and cartilage study. Cybium 9:107–119.

Taucce, P.P.G., C. Canedo, J.S. Parreiras, L.O. Drummond, P. Nogueira-Costa, and C.F.B. Haddad. 2018. Molecular phylogeny of *Ischnocnema* (Anura: Brachycephalidae) with the redefinition of its series and the description of two new species. Molecular Phylogenetics and Evolution 128:123–146.

Teixeira, M., Jr., R.S. Recoder, R.C. Amaro, R.P. Damasceno, J. Cassimiro, and M.T. Rodrigues. 2013. A new *Crossodactylodes* Cochran, 1938 (Anura: Leptodactylidae: Paratelmatobiinae) from the highlands of the Atlantic Forests of southern Bahia, Brazil. Zootaxa 3702:459–472.

Titus, T.A., and A. Larson. 1996. Molecular phylogenetics of desmognathine salamanders (Caudata: Plethodontidae): A reevaluation of evolution in ecology, life history, and morphology. Systematic Biology 45:451–472.

Toledo, L.F., C.G. Becker, C.F.B. Haddad, and K.R. Zamudio. 2014. Rarity as an indicator of endangerment in Neotropical frogs. Biological Conservation 179:54–62.

Tschudi, J.J. 1838. Classification der Batrachier, Mit Berücksichtigung der Fossilen Thiere Dieser Abtheilung der Reptilien. In der Buchdruckerei von Petitpierre, Switzerland.

Valeriano, M.M., and D.F. Rossetti. 2012. Topodata: Brazilian full coverage refinement of SRTM data. Applied Geography 32:300–309.

Vasconcelos, T.S., V.H.M. Prado, F.R. da Silva, and C.F.B. Haddad. 2014. Biogeographic distribution patterns and their correlates in the diverse frog fauna of the Atlantic Forest hotspot. PLoS ONE 9:e104130. DOI: https://dx.doi.org/10.1371/journal.pone.0104130

Versieux, L.M., R.B. Louzada, P.L. Viana, N. Mota, and M.G.L. Wanderley. 2010. An illustrated checklist of Bromeliaceae from Parque Estadual do Rio Preto, Minas Gerais, Brazil, with notes on phytogeography and one new species of *Cryptanthus*. Phytotaxa 10:1–16.

Villalobos, F., R. Dobrovolski, D.B. Provete, and S.F. Gouveia. 2013. Is rich and rare the common share? Describing biodiversity patterns to inform conservation practices for South American anurans. PLoS ONE 8:e56073. DOI: https://dx.doi.org/10.1371/journal.pone.0056073

Weeks, A.R., J. Stoklosa, and A.A. Hoffmann. 2016. Conservation of genetic uniqueness of populations may increase extinction likelihood of endangered species: The case of Australian mammals. Frontiers in Zoology 13:31. DOI: https://dx.doi.org/10.1186/s12983-016-0163-z

Werner, F. 1896. Beiträge zur Kenntniss der Reptilien und Batrachier von Centralamerika und Chile, sowie einiger seltenerer Schlangenarten. Verhandlungen des Zoologisch-Botanischen Vereins in Wien 46:344–365.

Wilcox, D.C., B.S Dove, D.W. McDaid, and D.B. Greer. 1996. Imagetool. Available at http://compdent.uthscsa.edu/imagetool.asp. The University of Texas Health Science Center at San Antonio, USA. Archived by WebCite at http://www.webcitation.org/6qpeHshHN on 29 May 2017.

Wiens, J.J., J.W. Fetzner, C.L. Parkinson, and T.W. Reeder. 2005. Hylid frog phylogeny and sampling strategies for speciose clades. Systematic Biology 54:778–807.

Accepted on 22 November 2019
Published on 20 May 2020

Appendix I.—GenBank accession numbers for sequences employed in this study. Museum voucher numbers are reported only for sequences generated for this article. For other voucher information, refer to the GenBank accession numbers. A dash (—) indicates missing data.

		GenBank accession numbers					
Species	Museum number	H1	COI	cytb	POMC	RAG-1	Tyr
Adenomera andreae		KC520683	KC520689	JQ321766	KC604061	KC604037/ KF674220	KC520698
Allophryne ruthveni		AY843564	KU494331	AY843786	AY819077	AY844361	KC604076
Crossodactylodes bokermanni		KC593358	—	—	—	—	—
C. bokermanni	MNRJ 38412	KC593359	MN610690	MN610722	MN610759	MN609871	MN610796
C. bokermanni	UFMG 14188	MN610833	MN610691	MN610723	MN610760	MN609872	MN610797
C. bokermanni	UFMG 14189	MN610834	MN610692	MN610724	MN610761	MN609873	MN610798
C. bokermanni	UFMG 14190	MN610835	MN610693	MN610725	MN610762	MN609874	MN610799
C. bokermanni	UFMG 13767	MN610836	MN610694	MN610726	MN610763	MN609875	MN610800
C. bokermanni	UFMG 13770	MN610837	MN610695	MN610727	MN610764	MN609876	MN610801
C. bokermanni	UFMG 13774	MN610838	MN610696	MN610728	MN610765	MN609877	MN610802
C. bokermanni	UFMG 14198	MN610839	MN610697	MN610729	MN610766	—	MN610803
C. bokermanni	UFMG 14199	MN610840	MN610698	MN610730	MN610767	MN609878	MN610804
C. bokermanni	UFMG-G 1496-1	MN610841	MN610699	MN610731	MN610768	MN609879	MN610805
C. bokermanni	UFMG-G 1496-2	MN610842	MN610700	MN610732	MN610769	MN609880	MN610806
C. bokermanni	UFMG-G 1496-3	MN610843	—	—	—	—	—
C. bokermanni		KF534637/ KF534647	KF534656	KF534665	—	—	—
C. bokermanni		KF534638/ KF534648	KF534657	KF534666	—	—	KF534683
C. bokermanni		KF534639/ KF534649	KF534658	KF534667	—	—	KF534684
C. bokermanni		KF534640/ KF534650	KF534659	KF534668	—	—	KF534685
Crossodactylodes itambe	UFMG-G 1477	MN610844	KY362547	MN610733	MN610770	MN609881	MN610807
C. itambe	UFMG 13376	MN610845	KY362548	MN610734	MN610771	MN609882	MN610808
C. itambe	UFMG 13377	MN610846	KY362549	MN610735	MN610772	MN609883	MN610809
C. itambe	UFMG 13379	MN610847	KY362550	MN610736	MN610773	MN609884	MN610810
C. itambe	UFMG 13381	MN610848	KY362551	MN610737	MN610774	MN609885	MN610811
Crossodactylodes izecksohni	UFMG 13757	MN610849	MN610701	MN610738	MN610775	MN609886	MN610812
C. izecksohni	UFMG 13759	MN610850	MN610702	MN610739	MN610776	MN609887	MN610813
C. izecksohni	UFMG 13791	MN610851	MN610703	MN610740	MN610777	MN609888	MN610814
C. izecksohni	UFMG 13792	—	MN610704	MN610741	MN610778	MN609889	MN610815
C. izecksohni	UFMG 13793	—	MN610705	MN610742	MN610779	MN609890	MN610816
C. izecksohni	UFMG 13747	MN610852	MN610706	MN610743	MN610780	MN609891	MN610817
C. izecksohni	UFMG 13748	MN610853	MN610707	MN610744	MN610781	MN609892	MN610818
C. izecksohni	UFMG 14174	MN610854	MN610708	MN610745	MN610782	MN609893	MN610819
C. izecksohni	UFMG 14175	MN610855	MN610709	MN610746	MN610783	MN609894	MN610820
C. izecksohni	UFMG 14176	MN610856	MN610710	MN610747	MN610784	MN609895	MN610821
C. izecksohni	UFMG 14178	MN610857	MN610711	MN610748	MN610785	MN609896	MN610822
C. izecksohni	UFMG 14180	MN610858	MN610712	MN610749	MN610786	MN609897	MN610823
C. izecksohni	UFMG-G 1495-1	MN610859	MN610713	MN610750	MN610787	MN609898	MN610824
C. izecksohni	UFMG-G 1495-2	MN610860	MN610714	MN610751	MN610788	MN609899	MN610825
C. izecksohni		KF534632/ KF534641	KF534651	KF534660	—	—	KF534678
C. izecksohni		KF534633/ KF534642	KF534652	KF534661	—	—	KF534679
C. izecksohni		KF534634/ KF534644	KF534653	KF534662	—	—	KF534680
C. izecksohni		KF534635/ KF534645	KF534654	KF534663	—	—	KF534681
C. izecksohni		KF534636/ KF534646	KF534655	KF534664	—	—	KF534682
Crossodactylodes septentrionalis		KC603957/ KC603958	KC603985	KC603963	KC604048	KC604033	KC604077
C. septentrionalis	MZUESC 14363	—	MN610715	MN610752	MN610789	MN609900	MN610826
C. septentrionalis	MZUESC 21668	—	MN610716	MN610753	MN610790	MN609901	MN610827
Leptodactylus latrans		AY843688	KC603989	AY843934	KP295578	AY844470	KC604082
Leptodactylus melanonotus		JX564873	JX564873	JX564873	—	—	—
Paratelmatobius cardosoi		EU224413	KU494618	—	—	—	—
P. cardosoi		—	JX298372	JX298413	JX298143	JX298195	JX298242
P. cardosoi	UFMG 3237	—	MN610717	MN610754	MN610791	MN609902	MN610828
Paratelmatobius gaigeae	UFMG 15006	—	MN610718	MN610755	MN610792	MN609903	MN610829
Paratelmatobius poecilogaster		EU224398	KU494620	—	—	—	—
P. poecilogaster	UFMG 3240	—	MN610719	MN610756	MN610793	MN609904	MN610830
Physalaemus nattereri		—	KC603984	KC603965	KC604053	—	KC604079
Pleurodema brachyops		AY843733	KP295702	AY843979	KP295582	AY844503	—
Rupirana cardosoi		KC593361	—	KC593351	—	—	KC593368
R. cardosoi		KC603955/ KC603956	KC603987	KC603964	KC604049	KC604034	KC604078
R. cardosoi	UFMG 4606	—	MN610720	MN610757	MN610794	MN609905	MN610831
Scythrophrys sawayae		DQ283099	—	—	—	—	DQ282926
S. sawayae		KU495580	KU494787	—	—	—	—
S. sawayae	UFMG 15678	—	MN610721	MN610758	MN610795	MN609906	MN610832

APPENDIX II.—Sequence of primers, temperature, and time melting used for each fragment and the correlated sources.

Locus	Primer name and sequence (5′→3′)	Temperature (°C)	Time (s)	Source
12S	MVZ59: ATAGCACTGAAAAYGCTDAGATG MVZ50: TYTCGGTGTAAGYGARAKGCTT	54	60	Graybeal (1997)
16S	12SL13: TTAGAAGAGGCAAGTCGTAACATGGTA 16STitus1: GGTGGCTGCTTTTAGGCC	51	60	Feller and Hedges (1998) Titus and Larson (1996)
16S	16SL2A: CCAAACGAGCCTAGTGATAGCTGGTT 16SH10: TGATTACGCTACCTTTGCACGGT	51	60	Hedges (1994)
16S	16Sar: CGCCTGTTTATCAAAAACAT 16Sbr: CCGGTCTGAACTCAGATCACGT	51	60	Palumbi et al. (1991)
COI	ANF1: ACHAAYCAYAAAGAYATYGG ANR1: CCRAARAATCARAADARRTGTTG	51	40	Lyra et al. (2017)
cytb	CytbAR-H: TAWAAGGGTCTTCTACTGGTTG MVZ15: GAACTAATGGCCCACACWWTACGNAA	53	30	Goebel et al. (1999) Moritz et al. (1992)
cytb	CytbF: TTTCTAGCAATACAYTACACAGCYGAT CytbC-R: CTACTGGTTGTCCTCCGATTCATGT	50	50	M.L. Lyra (personal communication)
POMC	POMC-1: AATGTATYAAAGMMTGCAAGATGGWCCT POMC-2: TAYTGRCCCTTYTTGTGGGCRTT	60	40	Wiens et al. (2005)
RAG-1	R1-GFF: GAGAAGTCTACAAAAAVGGCAAAG R1-GFR: GAAGCGCCTGAACAGTTTATTAC	61	40	Faivovich et al. (2005)
Tyr	Tyr1C: GGCAGAGGAWCRTGCCAAGATGT Tyr1G: TGCTGGGCRTCTCTCCARTCCCA	61	40	Bossuyt and Milinkovitch (2000)

APPENDIX III

List of morphological/natural history and morphometric characters and characters states coded for terminals of Paratelmatobiinae. To see the character states coded for each terminal, refer to Appendix IV.

Morphological and Natural History Characters

(1) Anterior projection in medial region of the upper lip: (0) absent (Fig. 13C); (1) present (Figs. 11D, 13D).

(2) Tympanic middle ear (Figs. 5, 6): (0) absent; (1) present. The tympanic middle ear, when complete, is composed by tympanic membrane, tympanic annulus, and columella. However, one or more elements can be absent (see Pereyra et al. 2016). We coded this character as absent only when all the three elements are lacking. The absence of columella in species of *Crossodactylodes* was coded following literature data for *C. pintoi*, *C. bokermanni*, *C. izecksohni*, and *C. septentrionalis* (Lynch 1971; Gomes 1988; Teixeira et al. 2013) or by direct examination (for *C. itambe*).

(3) Tympanic membrane: (0) absent (Figs. 5A–C); (1) present (Fig. 5D).

(4) Tympanic annulus visibility (Figs. 5, 6A, B): (0) not visible through the skin; (1) visible through the skin. We made dissections to determine the presence of tympanic annulus concealed by the skin.

(5) Size of zygomatic process of squamosal bone: (0) short, not passing the anterior margin of the optic foramen; (1) long, passing the anterior margin of the optic foramen. This character was previously proposed by Teixeira et al. (2013).

(6) Vocal slit: (0) absent; (1) present.

(7) Vocal sac condition: (0) externally indistinct; (1) externally distinct. Although Heyer (1999) considered the vocal sac of *Rupirana cardosoi* as externally indicated by lateral skin folds, after examination of specimens we coded this character as externally indistinct for this species.

(8) Vomerine odontophores: (0) absent (Fig. 11B); (1) present (Fig. 11A).

(9) Tubercle on upper eyelid: (0) absent; (1) present.

(10) Shape of tubercle on upper eyelid: (0) rounded; (1) acuminate, resembling a small dermal horn.

(11) Meniscus in the upper iris: (0) absent; (1) present.

(12) Mandibular tubercle: (0) absent; (1) present.

(13) Nuptial pads: (0) numerous (more than 20) small spicules (Fig. 3B); (1) few (less than 20) well developed spines (Fig. 3A).

(14) Dorsolateral fold: (0) absent (Fig. 14B); (1) present (Fig. 14A). This fold can be poorly or well-developed (see character 15).

(15) Dorsolateral fold development: (0) weakly developed; (1) well developed. Pombal and Haddad (1999) used this character to distinguish between species of *Paratelmatobius*. To avoid subjectivity in the states assignments, we considered only the quite distinct fold of *Scythrophrys sawayae* as well developed.

(16) Relative lengths of fingers I and II: (0) Finger I as long as or shorter than Finger II; (1) Finger I longer than Finger II.

(17) Disc of Finger I: (0) acute, i.e., with no apparent disc (Fig. 12E); (1) rounded (Figs. 12A–D).

(18) Discs of fingers II–IV: (0) narrow, i.e., same width or less dilated than the base of finger (Figs. 3D–F); (1) expanded, i.e., more dilated than the base of finger (Fig. 3C).

(19) Tubercle on outer margin of heel: (0) absent; (1) present.

(20) Tarsal fold: (0) absent (Figs. 3G–I); (1) present (Figs. 3J, K).

(21) Toes II–V webbing: (0) absent (Fig. 3G); (1) present (Figs. 3H–K).

(22) Type of toes II–V webbing: (0) weak lateral ridges (Figs. 3J, K); (1) well developed, flexible fringes (Fig. 3H).

(23) Cloacal flap: (0) inconspicuous (short free distal portion; Figs. 4B, C); (1) conspicuous (long free distal portion; Fig. 4A).

(24) Numerous white tubercles on males' dorsum: (0) absent (Figs. 5A–C); (1) present (Fig. 5D).

(25) Skin texture of males' dorsum: (0) shagreen; (1) coarsely granular.

(26) Bright and contrasting coloration (in life) on ventral surfaces of belly: (0) absent; (1) present.

(27) Bright and contrasting coloration (in life) on ventral surface of arm: (0) absent; (1) present.

(28) Iris coloration in life: (0) coppery or reddish with dark brown reticulations; (1) upper half gray and lower half dark brown; (2) uniformly black or brownish black; (3) yellowish with dark brown reticulations, interrupted by a brown horizontal bar at the pupil level.

(29) Reproductive mode (sensu Haddad and Prado 2005): (0) mode 1; (1) mode 6; (2) mode 18.

(30) Number and arrangement of eggs: (0) 50–200 eggs in a single group; (1) 10–40 eggs positioned in haphazard groups, or in groups of 2–20; (2) single eggs, positioned isolated from other eggs. Data available in: Garcia (1996); Pombal and Haddad (1999); Juncá and Lugli (2009); Santos et al. (2017); and Ferreira et al. (2019a).

(31) Foot length (in mm). This continuous character was optimized as minimum and maximum values of the ratio foot length/SVL under the Squared Change Parsimony model (Fig. 7).

Appendix IV.—Character matrix for 13 taxa of Paratelmatobiinae (see Appendix III for a description of characters and character states). Polymorphic characters are coded as such. Nonapplicable characters are indicated with (–), and unknown character states are indicated with (?).

	Characters and character states																													
Taxon	1	2	3	4	5	6	7	8	9	10	11	12	13	14	15	16	17	18	19	20	21	22	23	24	25	26	27	28	29	30	31
Rupirana cardosoi	0	1	1	1	?	1	0	1	0	–	0	0	0	1	–	0	0	0	0	1	1	0	0	1	0	0	0	0	0	0	(0.5–0.55)
Scythrophrys sawayae	0	1	0	0	?	1	1	1	1	1	1	0	0	1	1	0	0	0	1	1	1	0	0	0	0	0	1	1	0	1	(0.4–0.48)
Paratelmatobius poecilogaster	0	1	0	0	?	0	0	1	1	0	0	0	0	1	0	0	0	0	0	0	1	1	0	0	0	1	1	0	2	1	(0.4–0.49)
Paratelmatobius gaigeae	0	1	0	0	?	0	0	1	0	–	0	0	0	1	0	0	0	0	0	0	1	1	0	0	0	1	1	0	0	1	(0.44–0.48)
Paratelmatobius cardosoi	0	1	0	1	?	1	0	1	0	–	0	1	0	1	0	1	0	0	0	0	1	1	0	0	0	1	1	0	0	1	(0.41–0.44)
Crossodactylodes bokermanni Lin. A	0	0	–	–	0	1	0	1	1	0	0	0	1	1	0	0	0	1	0	0	0	–	1	0	0	0	0	0	1	2	(0.38–0.4)
Crossodactylodes bokermanni Lin. B	0	0	–	–	0	1	0	1	1	0	0	0	1	1	0	0	0	1	0	0	0	–	1	0	0	0	0	0	1	2	(0.37–0.41)
Crossodactylodes bokermanni Lin. C	0	0	–	–	0	1	0	1	1	0	0	0	1	1	0	0	0	1	0	0	0	–	1	0	0	0	0	0	1	2	(0.34–0.41)
Crossodactylodes itambe	1	0	–	–	1	0	–	0	0/1	–	0	0	1	0	–	0	0	1	0	0	0	–	1	0	1	0	0	2	1	2	(0.31–0.4)
Crossodactylodes septentrionalis	0	0	–	–	1	0	–	1	0/1	0	0	0	1	0	–	0	1	1	0	0	0	–	1	0	1	0	0	0	1	?	(0.36–0.4)
Crossodactylodes izecksohni Lin. A	0	0	–	–	0	0	–	0	0/1	0	0	0	1	0	–	0	0	1	0	0	0	–	1	0	1	0	0	3	1	2	(0.32–0.4)
Crossodactylodes izecksohni Lin. B	0	0	–	–	0	0	–	0	0/1	0	0	0	1	0	–	0	0	1	0	0	0	–	1	0	1	0	0	3	1	2	(0.35–0.4)
Crossodactylodes pintoi	0	0	–	–	0	0	–	0	0	0	0	0	1	0	–	0	0	1	0	0	0	–	1	0	1	0	0	?	?	?	(0.31–0.35)

Appendix V

Additional Specimens examined. *Specimens for which we measured SVL and foot length.

Paratelmatobius cardosoi.—BRAZIL: São Paulo: municipality of Bertioga, Parque das Neblinas (CFBH 38980, 38982, 38989–90, UFMG 3237); municipality of Santo André, Parque Estadual Municipal Nascentes de Paranapiacaba (topotypes: CFBH 3263–66*, 3269*, 28957–58*, 28969*, 29001*, 29004*).

Paratelmatobius gaigeae.—BRAZIL: São Paulo: municipality of Bananal, Estação Ecológica do Bananal (CFBH 7156; MZUSP 138657*, 138659*, 138661); municipality of São José do Barreiro, Parque Nacional da Serra da Bocaina (topotypes: CFBH 36069–70*, 36079*, UFMG 15004–08*).

Paratelmatobius lutzii.—BRAZIL: Minas Gerais: Itamonte, Parque Nacional de Itatiaia (topotypes: CFBH 295, MZUSP 94629–94633).

Paratelmatobius mantiqueira.—BRAZIL: São Paulo: Campos do Jordão, Cidade Azul (paratypes: MZUSP 15128–15132).

Paratelmatobius poecilogaster.—BRAZIL: São Paulo: municipality of Bertioga, Parque das Neblinas (UFMG 3238–40); municipality of Santo André, Parque Estadual Municipal Nascentes de Paranapiacaba (topotypes: CFBH 866, 3253–54, CFBH 12004–05, 28959–60, 29983).

Rupirana cardosoi.—BRAZIL: Bahia: municipality of Ibicoara, Parque Nacional da Chapada Diamantina (UFMG 7954–55); municipality of Lençóis, Parque Nacional da Chapada Diamantina and surroundings (CFBH 6666–67*, 6669*); municipality of Mucugê, Parque Nacional da Chapada Diamantina and surroundings (topotypes: UFMG 4252–54*, 4272*, 7915–21, 7922–23*); municipality of Palmeiras, Parque Nacional da Chapada Diamantina (CFBH 6665*).

Scythrophrys sawayae.—BRAZIL: Paraná: municipality of Piraquara, Mananciais da Serra (topotypes: CFBH 3397–98, 3400–01). Santa Catarina: municipality of Blumenau, Parque Nacional da Serra do Itajaí (UFMG 3241–42, 7504–07); municipality of Joinville, Castelo dos Bugres (UFMG 13896, 14470); municipality of São Bento do Sul, Rio Vermelho (CFBH 2981, 3186, 3190–91).

Appendix VI.—Uncorrected *p*-distances (percentage) among species and lineages of *Crossodactylodes*. Distances for COI fragment (ca. 650 bp) are shown under the diagonal, and distances for cytb fragment (ca. 770 bp) are shown above the diagonal. Intraspecific or intralineage distances are shown as COI/cytb (along diagonal). NC = not calculated because there was only one individual.

	C. bokermanni Lineage A (*n* = 1)	*C. bokermanni* Lineage B (*n* = 7)	*C. bokermanni* Lineage C (*n* = 7)	*C. itambe* (*n* = 5)	*C. izecksohni* Lineage A (*n* = 14)	*C. izecksohni* Lineage B (*n* = 5)	*C. septentrionalis* (*n* = 3)
C. bokermanni Lineage A	NC / NC	4.6–4.7	6.2–6.8	13.1–13.4	13.1–14.2	12.5–12.6	13.8–14.1
C. bokermanni Lineage B	5.0–5.3	0.0–0.3 / 0.0–0.6	8.1–9.0	12.6–13.7	11.5–14.1	12.5–12.9	13.1–14.0
C. bokermanni Lineage C	7.9–8.2	8.5–9.3	0.0–0.3 / 0.0–0.2	14.0–14.7	14.2–16.0	13.3–13.9	14.7–15.2
C. itambe	15.2–15.5	15.2–15.7	14.1–14.6	0.0–0.5 / 0.0–0.3	11.3–13.4	11.2–11.6	11.5–12.2
C. izecksohni Lineage A	16.3–17.0	15.3–16.0	15.7–16.3	11.3–11.9	0.0–1.4 / 0.0–1.2	7.7–8.9	12.9–14.6
C. izecksohni Lineage B	16.7–17.1	15.7–16.1	16.4–16.7	13.3–13.8	6.0–6.8	0.0–0.2 / 0.0–0.1	13.6–14.0
C. septentrionalis	16.7–16.9	16.7–17.3	16.6–17.0	12.4–12.9	14.1–15.2	16.1–16.4	0.0–0.5 / 0.1–0.8

Appendix VII.—Uncorrected *p*-distances (percentage) of the entire H1 fragment (ca. 2300 bp) within (along diagonal) and among species and lineages of *Crossodactylodes*. NC = not calculated because there was only one individual.

	C. bokermanni Lineage A (*n* = 2)	*C. bokermanni* Lineage B (*n* = 8)	*C. bokermanni* Lineage C (*n* = 3)	*C. itambe* (*n* = 5)	*C. izecksohni* Lineage A (*n* = 7)	*C. izecksohni* Lineage B (*n* = 3)	*C. septentrionalis* (*n* = 1)
C. bokermanni Lineage A	0.0						
C. bokermanni Lineage B	1.3	0.0					
C. bokermanni Lineage C	3.4–3.5	3.1–3.3	0.0				
C. itambe	7.7–7.9	7.6–7.9	7.3–7.5	0.0–0.2			
C. izecksohni Lineage A	8.2–8.3	8.2–8.5	8.1–8.3	5.5–5.8	0.0–0.4		
C. izecksohni Lineage B	8.8–9.0	8.9–9.2	8.8–9.1	6.0–6.4	3.8–3.9	0.1	
C. septentrionalis	8.9	8.8–9.1	8.4	5.2–5.3	6.8–7.0	6.9–7.2	NC